UNCLASSIFIED

AD NUMBER
AD011585

CLASSIFICATION CHANGES
TO: **unclassified**
FROM: **secret**

LIMITATION CHANGES
TO: Approved for public release, distribution unlimited
FROM: Controlling Organization: British Embassy, 3100 Massachusetts Avenue, NW, Washington, DC 20008.

AUTHORITY
DSTL, AVIA 6/19385, 31 Jul 2008; DSTL, AVIA 6/19385, 31 Jul 2008

THIS PAGE IS UNCLASSIFIED

AD No. 11585

ASTIA FILE COPY

ROYAL AIRCRAFT ESTABLISHMENT

FARNBOROUGH, HANTS

REPORT No: G.W.15

THE PREVENTION OF EXCESSIVE LIFT FORCES ON GUIDED MISSILES

by

J.J. GAIT, M.A., B.Sc., A.Inst.P., A.M.I.E.E.

and D.W. ALLEN

53AA 897

U.D.C. No 623.451-519:621-526:533.691.15:533.6.013.13

ROYAL AIRCRAFT ESTABLISHMENT, FARNBOROUGH

The Prevention of Excessive Lift Forces on
Guided Missiles

by

J.J. Gait, M.A., B.Sc., A.Inst.P., A.M.I.E.E.
and
D.W. Allen

SUMMARY

In order to prevent the development of destructive or excessive
lift forces during the flight of a guided missile it is generally
necessary to limit the total lift on the missile by some form of auto-
matic control action. It may also be necessary or advantageous similarly
to limit the control surface lifts of the missile.

Methods of obtaining overriding limiting actions which, within
bounds, function independently of missile altitude, velocity and static
margin are proposed and critically examined. These methods depend on
feedback to the control surfaces, via suitable threshold circuits, of
the outputs of lateral and angular accelerometers suitably situated within
the missile.

It is concluded that such an approach to the limiting problem
gives a technique whereby the control surface lift force and the total
lift force on the missile may be separately or jointly constrained
within the given design limits for these forces.

LIST OF CONTENTS

(Sections marked * discuss applications to beam riding)

LIST OF CONTENTS (Contd)

LIST OF APPENDICES

by

Lt. Cdr.(E). D.G. Satow, R.N., A.M.I.Mech.E.

LIST OF ILLUSTRATIONS

SECRET

LIST OF ILLUSTRATIONS (Contd.)

SECRET

LIST OF ILLUSTRATIONS (Contd.)

LIST OF SYMBOLS

A_a, A_{a1}	(rad)	The control surface incidences corresponding to the control surface deflections ζ_L, $-\zeta_L$
A_{max}	(ft.sec^{-2})	The desired maximum lateral acceleration of the missile
a	(ft.sec^{-2})	The output from a lateral accelerometer situated a distance d ft ahead of the centre of gravity of the missile
a_1	(ft.sec^{-2})	A contraction for $x_{\zeta r}/y_\zeta$
B	(rad)	The control surface demand signal corresponding to the initial diode bias in the monitored diode system of acceleration limiting
B_b, B_{b1}	(rad)	The peak control surface incidence corresponding to the steady state values A_a, A_{a1}
b	(rad/rad/sec)	The gain in the rate-of-yaw feedback loop
b_1	(sec^{-2})	A contraction for $Ux_{v\zeta}/y_\zeta$
C	(slugs)	The moment of inertia of the missile (in pitch or yaw) about the missile centre of gravity
D		The operator $^d/_{dt}$
d	(ft)	The displacement of the lateral accelerometer ahead of the centre of gravity of the missile
F	(rad/ft/sec^2)	The gain in the lateral accelerometer feedback loop (Used when the feedback is discontinuous)
f	(rad/ft/sec^2)	The gain in the lateral accelerometer feedback loop (Used when the feedback is continuous)
f_o	(c.p.s)	The undamped and unmodified weathercock frequency of the missile
f_o'	(c.p.s)	The undamped and unmodified weathercock frequency of the missile when the centre of gravity is moved forward through H ft
$f_a(p)$		The missile transfer function for $\ddot{\psi}/\zeta$
$f_\beta(p)$		" " " " " $\beta r/\zeta$
$f_h(p)$		" " " " " $\ddot{h}_F/\zeta$
$f_r(p)$		" " " " " r/ζ
$f_v(p)$		" " " " " v/ζ
5	(rad/ft/sec^2)	The quantity used to define F in simulator work

LIST OF SYMBOLS (Contd.)

G	(rad ft^{-1})	The constant of the beam riding system which determines the stiffness of control
g	(ft sec^{-2})	The acceleration due to gravity
H	(ft)	The distance of the missile centre of gravity forward of the design position - or - the change in static margin
H_C, H_E	(ft)	$H_C < H < H_E$ defines the range of H over which control surface lift limiting is effective
h_B	(ft)	The displacement of the radar beam axis from the datum line
h_p	(ft)	The displacement of the centre of gravity of the missile from the datum line
h_{po}	(ft)	An initial value of h_p
h_{p1}	(ft)	A boundary value of h_p
$\ddot{h}_G$	(ft sec^{-2})	The steady state lateral acceleration resulting from steady state control surface demand ζ_G
K	(rad/rad/sec^2)	The gain in the angular acceleration feedback loop
K_1	(rad/rad/sec^2)	The gain in the angular acceleration feedback loop. Used to denote a discontinuity in K
k_r	(rad/sec/rad)	The steady state ratio of r/ζ
k_v	(ft/sec/rad)	" " " " " v/ζ
k_h	$(\text{ft/sec}^2/\text{rad})$	" " " " " $\ddot{h}_p/\zeta$
ℓ	(ft)	A distance measured rear of the nose of the missile
ℓ_G	(ft)	The distance of the centre of gravity of the missile rear of the nose of the missile
L	(ft sec^{-2})	The limiting lateral acceleration of the missile as defined by the simple diode limiting system
M	(rad sec^{-2})	The threshold level in the angular acceleration feedback loop
m	(slugs)	The mass of the missile
N		A constant of the beam riding system. (Defines the impurity of the phase advancing network)
N_v $(\text{slugs.ft.rad.sec}^{-1})$ N_r $(\text{slugs.ft}^2 \text{ sec}^{-1})$ N_ζ $(\text{slugs.ft}^2 \text{ sec}^{-2})$		The aerodynamic moment derivatives
N_v' $(\text{slugs.ft.rad.sec}^{-1})$		The value N_v assumes when the missile centre of gravity is moved forward H ft from the design position

- 8 -

LIST OF SYMBOLS (Contd.)

n_v	$(\text{rad sec}^{-1}\text{ft}^{-1})$	N_v/C
n_r	(sec^{-1})	Contractions for N_r/C
n_ζ	(sec^{-2})	N_ζ/C
n_v'	$(\text{rad sec}^{-1}\text{ ft}^{-1})$	N_v'/C

P (rad)   The maximum limited value of the control surface incidence

P_1 (rad)   The greatest permissible value of the control surface incidence as determined by structural considerations

p The complex variable of the Laplace Calculus

Q Contraction for $p^2+p(-y_v-n_r)+Un_v+x_{rv}$ or $p^2+2u\omega p+\omega^2$

Q_1 "   " $p^2+2u_1\omega_1 p+\omega_1^2$

Q_m "   " $(1-fy_\zeta)(p^2+2u_m\omega_m p+\omega_m^2)$

Q_c "   " $p^2(1-fy_\zeta - Kn_\zeta)+p(-y_v-n_r-bn_\zeta - fx_{\zeta r}+Kx_{\zeta v})$

$\qquad\qquad\qquad\qquad\qquad +Un_v+x_{rv}+b x_{\zeta v}+Ufx_{\zeta v}$

Q_K "   " $p^2(1-Kn_\zeta)+p(-y_v-n_r+Kx_{\zeta v})+Un_v+x_{rv}$

R (lbs)   The lift on the missile control surfaces

R_s (lbs)   The steady state lift on the missile control surfaces

$\mathcal{R}$ (lbs)   The lift on the missile due to rotational motion

$\mathcal{R}_s$ (lbs)   The steady state lift on the missile due to rotational motion

r (rad sec^{-1}) The missile rotational velocity in yaw (or pitch)

T (lbs)   The total lift on the missile

T_s (lbs)   The steady state total lift on the missile

T_o (sec)   A time constant of the beam riding system. (The phase advance time constant)

T_a (sec)   The time lag of the angular accelerometer

T_c (ft sec^{-2}) The threshold level in the feedback from the displaced accelerometer

T_x (sec)   The time lag of the control surface servo

t (sec)   Time

t_1 (sec)   The time interval during which the control surface incidence is limited

LIST OF SYMBOLS (Contd.)

U	(ft sec^{-1})	The design forward velocity of the missile
U'	(ft sec^{-1})	The actual forward velocity of the missile
u or u_o		The unmodified damping ratio of the missile weather-cock motion
u_o'		The value u (or u_o) assumes when the centre of gravity is moved forward through H ft from the design position
u_c		The damping ratio of the controlled or weaving mode of the beam rider
u_o		The damping ratio of the weathercock mode when this is modified by feedback from a displaced accelero-meter
u_K		The damping ratio of the weathercock mode when this is modified by feedback from an angular accelero-meter
u_{K1}		The damping ratio of the weathercock mode when this is modified by rate-of-yaw, lateral acceleration and angular acceleration feedbacks
u_m		The damping ratio of the weathercock mode when this is modified by rate-of-yaw and lateral acceleration feedbacks
u_w		The damping ratio of the "weathercock-like" mode of motion of the beam rider
u_x		The value u_D assumes when the control surface servo lag T_x is considered
v	(ft sec^{-1})	The missile sideslip velocity
W	(lbs)	The lift on the wings and body of the missile due to sideslip
W_s	(lbs)	The steady state lift on the wings and body of the missile due to sideslip
$x_{v\zeta}$	(sec^{-3})	Contraction for $n_v y_\zeta - n_\zeta y_v$
x_{vr}	(sec^{-2})	" " $n_v y_r - n_r y_v$
$x_{r\zeta}$	(ft sec^{-3})	" " $n_r y_\zeta - n_\zeta y_r$
Y_v (slugs sec^{-1})		
Y_r (slugs ft rad^{-1}sec^{-1})		The aerodynamic force derivatives
Y_ζ (slugs ft rad^{-1}sec^{-2})		
y_v	(sec^{-1})	Contraction for Y_v/m
y_r	(ft rad^{-1} sec^{-1})	" " Y_r/m
y_ζ	(ft rad^{-1}sec^{-2})	" " Y_ζ/m

LIST OF SYMBOLS (Contd.)

y		A function of time approximating to $\zeta/\zeta_{\dot{a}}$ for a step function of ζ_d
α or β_w	(rad)	The incidence of the airstream on the missile body in the regions of the nose, wings and tail
α_R	(rad)	The incidence of the airstream on the missile body in the region of the control surfaces
$\alpha_{1,2,3,4}$	$(\sec^{-1})$	Roots of the characteristic equation for the missile weathercock motion when it is modified by rate-of-yaw and acceleration feedback and the damping ratio u_m is greater than unity
α_x	$(\sec^{-1})$	A root of the characteristic equation for the missile weathercock motion when the lag T_x of the control surface servo is considered
β_r	(rad)	The control surface incidence
β_r'	(rad)	The peak control surface incidence
β_{ro}	(rad)	The value of β_r at time $t = 0+$ in response to a step in control surface demand ζ_2
β_{r1}	(rad)	An initial or boundary value of β_r
γ	(rad sec^{-1})	The undamped angular frequency of response of the missile to control surface incidence inputs
δ		The damping ratio of the response of the missile to control surface incidence inputs
ε	(rad)	The airstream downwash angle
$\partial\varepsilon/\partial\alpha$		The downwash factor
ζ	(rad)	The control surface deflection with respect to the missile longitudinal axis
ζ_1	(rad)	The component of control surface deflection demanded by angular acceleration feedback
ζ_2 or ζ_d	(rad)	Arbitrary input demands for control surface deflections
ζ_D	(rad)	The total control surface deflection demand
ζ_f	(rad)	The component of control surface deflection demanded by feedback from an angular accelerometer with time lag T_x secs
ζ_G	(rad)	The component of control surface deflection demanded by the missile guidance system
ζ_{G1}	(rad)	An initial or boundary value of ζ_G
ζ_G'	(rad)	The hypothetical value of ζ_G which gives a constant control surface incidence

LIST OF SYMBOLS (Contd.)

$\pm\zeta_L$	(rad)	The limiting values of ζ_G in the simple diode limiting system
ζ_m	(rad)	The component of control surface deflection demanded by feedback controls
θ	(rad)	The maximum control surface traverse angle
λ		A constant used in determining the effect of time lags in the angular accelerometer and control surface servo
μ		The ratio of actual missile velocity to the value assumed in the standard design condition (i.e. U'/U)
ρ		A constant used in conjunction with λ
σ		The ratio of actual air pressure to the value assumed in the standard design condition
τ	(secs)	Contraction for $t + t_1$
ϕ	(rad)	The steady state value of ζ corresponding to 10g lateral acceleration of the missile
ϕ_{max}	(rad)	The maximum value of ϕ
ψ	(rad)	The heading angle of the missile relative to a fixed datum
$\ddot{\psi}_0$	(rad sec^{-2})	The value of $\ddot{\psi}$ at the time $t = 0+$ in response to a step in the control surface demand ζ_2
ω	(rad sec^{-1})	The undamped and unmodified angular frequency of the missile weathercock motion
ω_c	(rad sec^{-1})	The undamped angular frequency of the controlled or weaving mode of the beam rider
ω_D	(rad sec^{-1})	The undamped angular frequency of the weathercock mode when this is modified by feedback from a displaced accelerometer
ω_K	(rad sec^{-1})	The undamped angular frequency of the weathercock mode when this is modified by feedback from an angular accelerometer
ω_{K1}	(rad sec^{-1})	The undamped angular frequency of the weathercock mode when this is modified by rate-of-yaw, lateral acceleration and angular acceleration feedbacks
ω_m	(rad sec^{-1})	The undamped angular frequency of the weathercock mode when this is modified by rate-of-yaw and lateral acceleration feedbacks
ω_W	(rad sec^{-1})	The undamped angular frequency of the "weathercock-like" mode of motion of the beam rider
ω_X	(rad sec^{-1})	The value ω_D assumes when the control surface servo lag T_X is considered

1 Introduction

1.1 The lift problem

It is essential that the method of control adopted for a guided weapon should not make excessive demands on the structural strength of the missile. In general terms we assume that the structural strength of the missile may be defined in terms of the maximum tolerable values of wing lift, control surface lift and total lift. The control system should therefore be such that at no time does it call for excessive values of these quantities. One approach to this problem is to design the control system to function effectively on the assumption that the system is unhindered by structural strength considerations and then to impose overriding constraints or limits such that the safe lift values cannot be exceeded. These limits must be independent of missile altitude, missile velocity etc. and they should be such that the fullest use can be made of the lifts or accelerations available, that is, there should be a sharp cut-off action whenever the lift or acceleration concerned reaches the specified safe maximum.

The primary object of this report is to develop and discuss certain methods whereby the desired limiting may be obtained for a particular type of missile. A secondary objective has been to investigate certain of the penalties of such limiting action on the performance of the missile.

1.2 The type of missile considered

The majority of guided missiles at present being developed for ground or ship-to-air and air-to-air operation have fixed cruciform wings and rear cruciform control surfaces in line with the wings. The usual design is such that the body-wing combination in the absence of the rear control surfaces is neutrally stable. Some of the essential steps in the design of such a missile are as follows.[1]. The lift due to unit sideslip velocity (Y_v) is first fixed from considerations of the maximum lateral acceleration required and the permissible maximum wing incidence. The yawing moment due to sideslip (N_v), which determines the frequency of the weathercock motion of the missile is chosen by the selection of the manoeuvre margin; this choice usually being made at the expected average altitude of the missile. The yawing moment due to unit control surface deflection (N_ζ) determines the surface deflection necessary to produce a given angular acceleration and steady state lateral acceleration. It is desirable that the demands on the control surface actuators should be kept small. By designing for a body-wing combination which is neutrally stable the control surface incidence in a steady turn is very small and the average value is therefore small. As a consequence of the neutrally stable body wing design we have

$$- U N_v = N_\zeta \left(1 - \frac{\partial \varepsilon}{\partial \alpha}\right)$$

where U is the forward velocity of the missile and $\frac{\partial \varepsilon}{\partial \alpha}$ is the downwash factor (frequently assumed to be $\frac{1}{2}$).

In the steady state the lateral acceleration of such a missile is a function of the control surface deflection – being proportional to the deflection if nonlinear downwash effects on the control surfaces are ignored. If the demand for control surface deflection is limited and the weathercock mode of motion is critically damped by suitable control action

(e.g. feedback of rate of yaw) then the maximum achieved acceleration is proportional to the maximum control surface deflection[2]. This however does not provide a good method of limiting the acceleration to a predetermined value since the proportionality factor between control surface deflection and acceleration is a function of altitude, velocity, centre of gravity and centre of pressure positions etc. so that changes in these quantities may either cause the final acceleration to be in excess of the design limit or less than the design limit - the first leading to self destruction and the second to inefficient use of the missile. The problem to be tackled here is as follows. Can the control surface motion be modified by control action so as to limit the acceleration and hence the lift to a level which is independent of the aerodynamic parameters?

Also, while the average and steady state control surface lifts with the above missile design are small, the peak control surface lifts (especially at low altitudes) are liable to be so large that they present structural design difficulties. Two of the issues discussed in this report are (1) Can these peak control surface lifts be reduced by suitable control action without deterioration of the overall performance of the system? and (2) If so does this indicate that a smaller control surface can be used?

1.3 The general scheme of attack

In order to develop methods of limiting which are independent of the aerodynamic parameters etc. it seems essential that the methods hinge upon some direct measurement of the quantity to be limited. While strain guage methods etc. may be used it is felt that at present the difficulties of applying such techniques in guided weapons is very great and for the present attention should be concentrated on the use of such instruments as lateral accelerometers, angular accelerometers and gyros which are either already developed or should be available in the near future. It is assumed here that measures of lateral acceleration and angular acceleration can be obtained within the missile. The actual measuring instruments are not discussed although the general effects of instrument time lags are studied.

Lateral accelerometers situated at the C of G of the missile provide measures of the components of the total lift force acting on the missile while lateral accelerometers situated at a certain point ahead of the C of G provide measures of the components of the body and wing lift forces only. Also for a missile with a neutrally stable body-wing combination angular accelerometers provide measures of the control surface moments. We may assume constant moment arms and control surface areas so that the angular acceleration components are proportional to the control surface moments, lifts and incidences.

Given that the lift forces to be limited can be measured in this way the obvious attack on the problem is to feed signals proportional to these quantities back to the control surfaces in such a way as to prevent the occurrence of excessive lift forces. Since we wish the missile to be unhindered unless it is at or near a condition of dangerous lift we arrange that the feedbacks are only effective if and when the measures of the lifts reach predetermined levels. It should be noted at this point that there is no attempt to produce a system in which the lift forces are proportional to the input demand signal but an attempt is made to override the method of control (whatever it may be, linear or otherwise) whenever dangerous lift forces are approached. It is believed that the quality of measurement of the accelerations or lifts would have to be an order better in any "lift force demand system" than it has to be for pure "overriding control" as used here. For example, the measuring instruments need only

be accurate at the critical feedback level and questions of good linearity
of response do not arise. Also the quantities to be measured for over-
riding control are large, e.g. 10g.

There are a number of possible alternative techniques by which the
feedback loops may operate and the bulk of this report is concerned with
detailed analysis of such feedback loops. For example the feedback signals,
after passing through threshold systems which will only permit the feed-
backs to take place if the signals are in excess of specified values,
may either be added into the normal control channels or may be used to
monitor diodes which are clipping signals in the normal control channels.
Studies of such nonlinear feedback systems are greatly assisted by the
use of simulators or analogue computors and at all stages of the work
such use has been made freely to extend, verify and illustrate the theoreti-
cal approaches. The simulator used for this work has been described in
detail elsewhere (Refs. (2) and (3)) and no account of it is given in
this report. The real value of a simulator lies in the fact that it can
be used for analysis of nonlinear systems in cases where theoretical
solutions to the problems are not practical. It is good practice to
obtain simulator solutions for a number of cases where the theoretical
solutions are readily obtained since in this way the operation of the
simulator may be checked and confidence increased in those simulator
results for which no direct theoretical check is possible. Throughout
the report a number of such cross checks between theory and simulator are
given.

When nonlinear feedback systems, such as those proposed, are
applied to a missile a host of problems arise. Do the feedbacks achieve
their desired objective? What are the stability conditions? How do the
feedbacks affect the aerodynamic response i.e. the weathercock motion of
the missile? How sensitive is the system to parameter variations? Can
total lift and control surface lift limits be successfully applied at
one and the same time? What are the relative advantages and disadvantages
of different feedback techniques etc. etc.? An attempt is made to present
the methods and the answers to the major problems, such as those above, in
logical sequence.

1.4   Illustrations, Examples, etc.

In all the numerical and simulator work, the values of the aero-
dynamic derivatives etc. appropriate to a particular typical missile have
been assumed.

Since the simulator used was specifically designed for beam riding
investigations it was possible to check at many stages just how the limit-
ing systems (designed on the basic of arbitrary input control signals)
were affecting the performance of a typical beam riding system. All sec-
tions in which beam riding is being specifically discussed are marked *
so that the reader not interested in this particular application may omit
such sections.

If the methods of limiting discussed here are adopted for any
existing missile control system then it may well be that they will have
repercussions on the design of that control system. The impact of the
limiting methods on the design of beam riding system tested is not dis-
cussed and the work is restricted to discussions on how the limiting
methods affect the performance of the beam rider with its existing control
system.

2   The Basic Equations and Properties of the Missile

Before proceeding to a study of the proposed limiting systems the relevant equations for and the characteristics of the type of missile to which the limiting is to be applied are first discussed.

Since the missile is symmetrical and may be assumed to be roll stabilised its motion may be analysed in terms of its motion in one plane only; consider this plane to be the yaw plane.

2.1   The equations of motion

The basic equations of motion of the missile, as normally assumed Refs. (1), (2), (3) are

$$m\ddot{h}_p = Y_v.v + Y_r.r + Y_\zeta.\zeta \quad \text{(Force Equation)}$$

$$C\dot{r} = N_v.v + N_r\ r + N_\zeta\ \zeta \quad \text{(Moment Equation)} \qquad (1)$$

together with the relationship

$$\dot{h} = \dot{v} + Ur$$

In these equations the variables are

ζ, the control surface angle w.r.t. the missile longitudinal axis

r, the rotational velocity ($= \dot{\psi}$, where ψ is the heading angle)

v, the sideslip velocity

h_p, the displacement of the C of G of the missile from a datum line

while   m, C and U are the mass, moment of inertia and forward velocity respectively.

Y_v, Y_r, Y_ζ and N_v, N_r, N_ζ are the aerodynamic force and moment derivatives, assumed constant.

Throughout the report Y_v/m, Y_r/m, Y_ζ/m and N_v/C, N_r/C, N_ζ/C are contracted to y_v, y_r, y_ζ and n_v, n_r and n_ζ.

Terms of the form $(n_v y_\zeta - y_v n_\zeta)$ are of frequent occurrence and these terms have been contracted as follows

$$x_{v\zeta} = n_v y_\zeta - y_v n_\zeta$$

$$x_{vr} = n_v y_r - y_v n_r$$

$$x_{\zeta r} = n_\zeta y_r - n_r y_\zeta$$

2.2   The test missile

For the purposes of numerical and simulator work a test missile is assumed.   This missile may be broadly classed as of the R.T.V.2 type and considered to have the aerodynamic parameters of Table I when operating at its maximum altitude.

TABLE I

Test Missile

$$
\begin{aligned}
y_v &= -1 && \text{sec}^{-1} \\
y_r &= 2.4 && \text{ft sec}^{-1} \\
y_\zeta &= 800 && \text{ft sec}^{-2} \\
n_v &= 1/15 && \text{ft}^{-1}\ \text{sec}^{-1} \\
n_r &= -1 && \text{sec}^{-1} \\
n_\zeta &= -200 && \text{sec}^{-2} \\
U &= 1500 && \text{ft sec}^{-1} \\
C/m &= 25 && \text{ft}^2 \\
&\quad\ \text{giving} \\
x_{\zeta r} &= 320 && \text{ft sec}^{-3} \\
x_{v\zeta} &= -146.6 && \text{sec}^{-3} \\
x_{vr} &= -0.64 && \text{sec}^{-2}
\end{aligned}
$$

2.3   The response of the missile to its control surfaces

If equations (1) are solved for the transfer functions r/ζ, v/ζ and $p^2 h_p/\zeta$ we obtain

$$
\begin{aligned}
\frac{r}{\zeta} &= \frac{pn_\zeta + x_{v\zeta}}{Q} &&= f_r(p) \quad \text{say} \\[2mm]
\frac{v}{\zeta} &= \frac{py_\zeta - Un_\zeta + x_{\zeta r}}{Q} &&= f_v(p) \quad " \\[2mm]
\frac{p^2 h_p}{\zeta} &= \frac{p^2 y_\zeta + px_{\zeta r} + Ux_{v\zeta}}{Q} &&= f_h(p) \quad "
\end{aligned}
\qquad (2)
$$

where

$$
Q = p^2 + p(-y_v - n_r) + Un_v + x_{rv} \qquad (3)
$$

and

$$
Q \begin{bmatrix} \dfrac{r}{v} \\ \text{or} \\ p^2 h \end{bmatrix} = 0 \text{ is the characteristic equation} \qquad (4)
$$

of the weathercock motion of the missile.

In the steady state equations (2) give

$$\frac{r}{\zeta} = \frac{x_{v\zeta}}{Un_v + x_{rv}} = k_r \quad \text{say}$$

$$\frac{v}{\zeta} = \frac{-Un_\zeta + x_{\zeta r}}{Un_v + x_{rv}} = k_v \quad " \qquad (5)$$

$$\frac{r^2 h_p}{\zeta} = \frac{Ux_{v\zeta}}{Un_v + x_{rv}} = k_h \quad "$$

The expression for Q given in equation (3) may be written in the form

$$Q = p^2 + 2u\omega p + \omega^2 \qquad (6)$$

where $\omega/2\pi$ is the undamped weathercock frequency and u is the damping ratio.

2.4   The control surface incidence

The control surface incidence is denoted by β_r where β_r is determined by the following consideration[1].

The wind incidence will vary along the length of the missile because of the rotation of the longitudinal axis. If the incidence at the C of G, which is situated at a distance ℓ_G rear of the nose, is taken as $-v/U$ then the incidence at any point at a distance ℓ rear of the nose is

$$-\frac{v}{U} - (\ell - \ell_G) \frac{r}{U} \qquad (7)$$

This variation of incidence with rate of yaw is small and may be neglected. The local incidence is however changed by the presence of the body and lifting surfaces upstream. The downwash effect from the nose is negligible, that from the wings onto the control surfaces is appreciable and that from the wings and control surfaces onto the tail cone can be neglected in view of the unimportance of lift on this cone. It is assumed that the change in incidence at the control surface is proportional to the incidence on the wing surface. This assumption ignores the time lapse between the deflection of the airstream by the wings and the downwash reaching the control surfaces. Thus if the incidence in the regions of nose, wings and tail is denoted by α and the incidence on the control surface is denoted by α_R we have

$$\alpha = -v/U \qquad (8)$$

$$\alpha_R = \alpha - \frac{\partial \epsilon}{\partial \alpha} \cdot \alpha \qquad (9)$$

- 18 -

where $\frac{\partial \varepsilon}{\partial \alpha}$ is the downwash factor, assumed to be equal to 0.5.

If the control surface is deflected through an angle ζ with respect to the body then the incidence on the control surface is

$$\beta_r = \zeta + \alpha_R$$

or $$\beta_r = \zeta + \alpha \left(1 - \frac{\partial \varepsilon}{\partial \alpha} \right) \tag{10}$$

2.5 The equations of motion in terms of control surface incidence

(a) Force Equation.

If we substitute from (10) in the force equation (1) we get

$$m\ddot{h} = \left[Y_v + \frac{Y_\zeta}{U} \left(1 - \frac{\partial \varepsilon}{\partial \alpha} \right) \right] v + Y_r\, r + Y_\zeta\, \beta_r \tag{11}$$

This equation enables the various components of the total lift to be identified

$m\ddot{h}$ is the total lift, identified by T

$\left[Y_v + \frac{Y_\zeta}{U} \left(1 - \frac{\partial \varepsilon}{\partial \alpha} \right) \right] v$ is the lift on the wings and body due to sideslip, identified by W

$Y_r.r$ is the lift on the missile due to its rotational motion, identified by ζ

$Y_\zeta\,\beta_r$ is the lift on the control surface, identified by R

Thus

$$T = W + R + \zeta \tag{12}$$

Now ζ is normally a small fraction of W and may be neglected so that

$$T \doteq W + R \tag{13}$$

(b) Moment Equation.

If we substitute from (10) in the moment equation (1) we get

$$C\dot{r} = \left[N_v + \frac{N_\zeta}{U} \left(1 - \frac{\partial \varepsilon}{\partial \alpha} \right) \right] v + N_r.r + N_\zeta\, \beta_r \tag{14}$$

This equation shows the moments corresponding to the lifts defined above.

The basic missile design is such that the body-wing combination is neutrally stable (in the sense that there is no moment on the body-wing combination due to sideslip). Thus the basic design is such that

$$N_v + \frac{N_\zeta}{U} \left(1 - \frac{\partial \varepsilon}{\partial \alpha} \right) = 0 \tag{15}$$

- 19 -

2.6 The relationship between control surface incidence and angular acceleration

The control surface incidence β_r is given by

$$\beta_r = \zeta - \frac{v}{U}\left(1 - \frac{\partial \varepsilon}{\partial \alpha}\right) \qquad \text{cf. eqn.(10)}$$

but

$$\frac{v}{\zeta} = \frac{py_\zeta - Un_\zeta + x_{\zeta r}}{Q} \qquad \text{cf. eqn.(5)}$$

so that

$$\left.\begin{aligned}
\frac{\beta_r}{\zeta} &= \frac{p^2 + p\,(-y_v - n_r) + Un_v + x_{rv} - \left(1 - \frac{\partial \varepsilon}{\partial \alpha}\right)\left(p\,\frac{y_\zeta}{U} + \frac{x_{\zeta r}}{U} - n_\zeta\right)}{Q} \\
&= f_\beta(p) \text{ say}
\end{aligned}\right\} \quad (16)$$

Now

$$\frac{p^2 \psi}{\zeta} = \frac{p^2 n_\zeta + x_{v\zeta}\,p}{Q} = pf_r(p) = F_1(p) \text{ say} \qquad \text{cf. eqn.(2)}$$

Thus

$$\frac{\beta_r}{p^2 \psi} = \frac{p^2 + p\,(-y_v - n_r) + Un_v + x_{rv} - \left(1 - \frac{\partial \varepsilon}{\partial \alpha}\right)\left(p\,\frac{y_\zeta}{U} + \frac{x_{\zeta r}}{U} - n_\zeta\right)}{p^2 n_\zeta + x_{v\zeta}\,p} \qquad (17)$$

This relationship between control surface incidence and angular acceleration will hold irrespective of any local feedbacks (of angular rate, lateral acceleration etc.) used to modify the missile weathercock characteristics. It forms the basis of the control surface lift limiting system to be discussed.

If the body-wing combination is neutrally stable then from equation (15) we have

$$N_v + \frac{N_\zeta}{U}\left(1 - \frac{\partial \varepsilon}{\partial \alpha}\right) = 0$$

or

$$n_v + \frac{n_\zeta}{U}\left(1 - \frac{\partial \varepsilon}{\partial \alpha}\right) = 0 \qquad (18)$$

so that

$$\frac{\beta_r}{p^2 \psi} = \frac{p^2 + p\,(-y_v - n_r) - p\left(1 - \frac{\partial \varepsilon}{\partial \alpha}\right)\frac{y_\zeta}{U} + x_{rv} - \left(1 - \frac{\partial \varepsilon}{\partial \alpha}\right)\frac{x_{\zeta r}}{U}}{p^2 n_\zeta + x_{v\zeta}\,p} \qquad (19)$$

2.7   Departures from the neutral stability condition

The condition for neutral stability of the body-wing combination defined in equation (15) is a critical relationship and departures from it give rise to difficulties in the limiting methods to be discussed. Such departures will arise as the result of changes in the lift coefficients or as a result of changes in the moment arms. The centre of pressure of the body-wing combination is believed to be fixed in position. The centre of pressure of the control surfaces may vary, and while this will change the static margin of the complete missile it will not disturb the neutral stability of the body-wing combination. If the centre of gravity of the missile moves (due to fuel consumption) then the moment arms for both the wing lift and control surface lift will change. Since the percentage change in wing arm will be much greater than that for the control surface arm the centre of gravity shift may be interpreted as a change in N_v with no corresponding change in N_χ. In order to study the effects of departures from the neutral stability condition it is therefore assumed that the force coefficients are constant but that N_v is changing and this is physically attributed to a shift in the centre of gravity due to fuel consumption.

Taking N_v as given by $N_v = - Y_v$ (static margin) we see that if the centre of gravity of the missile moves forward through a distance H ft then the new value of N_v say N_v' is given by

$$N_v' = N_v - Y_v H \tag{20}$$

The limiting systems discussed are tested for sensitivity to departures from the neutral stability condition by determining what departure of H from zero can be tolerated.

It is convenient to note at this point the direct effects of a varying centre of gravity position on the general missile characteristics. Such variations will result in variations in the weathercock frequency and damping, the aerodynamic stiffness and the steady state control surface incidence.

(a)   The Effect of centre of gravity shifts on the Weathercock Mode

Interpreting the C of G shift as a change from N_v to N_v' we have from equation (3) the following approximate relationships for the corresponding frequencies (f_0 and f_0') and damping ratios (u_0 and u_0').

$$\left.\begin{aligned}
\frac{f_0'}{f_0} &= \sqrt{\frac{N_v'}{N_v}} \\[2ex]
\text{and} \\[2ex]
\frac{u_0'}{u_0} &= \sqrt{\frac{N_v}{N_v'}}
\end{aligned}\right\} \tag{21}$$

Table II shows the order of these changes for the test missile.

TABLE II

H inches	+9	+6	+3	0	-3	-6	-9
f_o'/f_o	1.20	1.14	1.07	1	0.92	0.84	0.74
u_o'/u_o	0.83	0.88	0.93	1	1.08	1.20	1.35

(b)   **The Effect of centre of gravity shifts on the Aerodynamic Stiffness**

From equation (5) the steady state lateral acceleration per unit control surface angle (the aerodynamic stiffness) is given by

$$\frac{p^2 h_r}{\zeta} = \frac{Ux_{v\zeta}}{Un_\zeta + x_{rv}} = k_h$$

Table III shows the variations in $\dfrac{p^2 h_p}{\zeta}$ as a function of H for the test missile.

TABLE III

H inches	+12	+9	+6	+3	0	-3	-6	-9	-12
$-\dfrac{p^2 h_r}{\zeta}\dfrac{g}{\text{deg}}$	0.59	0.70	0.82	1.00	1.21	1.50	1.92	2.55	3.68

(c)   **The Effect of C of G Shifts on the Steady State Control Surface Lifts**

From equation (16) the control surface incidence β_r as a function of control surface deflection ζ is given by

$$\frac{\beta_r}{\zeta} = \frac{p^2 + p(-y_v - n_r) + Un_v + x_{rv} - \left(1 - \frac{\partial \varepsilon}{\partial a}\right)\left(p\frac{y_\zeta}{U} + \frac{x_{\zeta r}}{U} - n_\zeta\right)}{p^2 + p(-y_v - n_r) + Un_v + x_{rv}}$$

and in the steady state this becomes

$$\frac{\beta_r}{\zeta} = \frac{Un_v + x_{rv} - \left(1 - \frac{\partial \varepsilon}{\partial a}\right)\left(\frac{x_{\zeta r}}{U} - n_\zeta\right)}{Un_v + x_{rv}} \qquad (22a)$$

- 22 -

$$\dot{=} \frac{Un_v + n_r\, y_v + \left(1 - \frac{\partial \varepsilon}{\partial \alpha}\right) n_\zeta}{Un_v + n_r\, y_v} \qquad (22b)$$

Table IV shows how the steady state value of $^\beta r/\zeta$ varies with H for the test missile.

TABLE IV

H inches	+9	+6	+3	0	−3	−6	−9
β_r/ζ	0.315	0.237	0.138	0.010	−0.163	−0.408	−0.785

Thus for a constant control surface deflection the missile executes a steady turn in which the steady state control surface incidence is determined by the C of G position.

2.8   The effects of altitude and velocity variations

In assessing the effects of air pressure variation with altitude and the effects of varying velocity on the performance of the missile we let μ and σ denote the ratio of actual velocity and air pressure to the values at the standard design condition. If dashed symbols are used to denote the values of parameters at other than the standard design condition then as an approximate guide to the gross variation of the parameters with μ and σ we may use

$$U' = \mu\, U$$

and

$$
\begin{aligned}
&y_\zeta' = \sigma\, \mu\, y_\zeta \qquad\quad n_\zeta' = \sigma\, \mu\, n_\zeta \\
&y_v' = \sigma\, y_v \qquad\qquad n_v' = \sigma\, n_v \\
&y_r' = \sigma\, y_r \qquad\qquad n_r' = \sigma\, n_r
\end{aligned}
\qquad (23)
$$

These approximations, while not being of wide general application, are realistic for the type of missile considered here, (i.e. missiles with static margins large compared with any shifts in the centre of pressure).

The effects of altitude and velocity variations on the steady state lift forces are of interest.

If the steady state values of T, W, R and R are denoted by T_s, W_s, R_s and R_s respectively then equations (11) and (12) show that

$$\frac{W_s}{T_s} = \left[y_v + \frac{y_\zeta}{U}\left(1 - \frac{\partial \varepsilon}{\partial \alpha}\right)\right]\left[\frac{\sigma}{\mu}\frac{x_{\zeta r}}{Ux_{v\zeta}} - \frac{n_\zeta}{x_{v\zeta}}\right]$$

$$\left.\frac{R_s}{T_s} = \left[\frac{y_\zeta}{Ux_{v\zeta}}\left\{Un_v + \left(1 - \frac{\partial \varepsilon}{\partial \alpha}\right)n_\zeta\right\}\right] + \frac{\sigma}{\mu}\left[x_{rv} - \left(1 - \frac{\partial \varepsilon}{\partial \alpha}\right)\frac{x_{\zeta r}}{U}\right]\ \right\} \quad (24)$$

$$\frac{R_s}{T_s} = \frac{\sigma}{\mu}\frac{y_r}{U}$$

Inspection of the order of magnitudes of the above terms for the test missile shows that

(1) Neglecting the term $\sigma/\mu\ ^x\zeta r/Ux_{v_\zeta}$ in the expression for $^W s/T_s$ introduces at most a 1/3 error. Thus $^W s/T_s$ is constant (to within 1%) irrespective of altitude and missile velocity.

(2) If the body-wing combination is neutrally stable then $^R s/T_s$ is at most 2% of $^W s/T_s$. If the body-wing combination is not neutrally stable then $^R s/T_s$ when it can no longer be neglected in comparison with $^W s/T_s$ is such that it is independent of missile altitude and velocity.

(3) $^\Lambda s/T_s$ is at most 2% of $^W s/T_s$.

Thus we assume that $^W s/T_s$ and $^R s/T_s$ are independent of missile altitude and velocity and that

$$T_s = {^W}_s + R_s \qquad\qquad (25)$$

$^W s/T_s$ and $^R s/T_s$ are however dependent on the degree of stability of the body-wing combination, e.g. they are dependent on H, the shift in the C of G position of the missile.

2.9 Modification of the weathercock characteristics of the missile

There are a number of reasons for modifying the natural weathercock motion of the missile. For example, the natural damping ratio of the missile is low (usually of the order of 0.1 to 0.2) and for the purpose of imposing some restraint on the maximum lateral acceleration of the missile it is desirable that the damping ratio be near to unity. (This point is discussed in detail later.) The damping is normally controlled by negative feedback of angular velocity from a rate gyro. Also it may be desirable to have some control over the weathercock frequency — in general to increase it by negative feedback of lateral acceleration from an accelerometer, although in certain circumstances it may be advantageous to decrease it by positive feedback of lateral acceleration. Negative feedback from either gyro or accelerometer or both tends to reduce the effects of non-linearities in the response of the missile.

If the component of control surface deflection demanded by the local control feedbacks is denoted by ζ_m then

$$\zeta_m = b_r + f\ \ddot{h}_p \qquad\qquad (26)$$

where b and f determine the feedback gains of the angular velocity and lateral acceleration respectively.

If ζ_G denotes the component of control surface deflection demanded by the missile guidance system and ζ_D denotes the total control surface deflection demand then

$$\zeta_D = \zeta_G + \zeta_m \qquad\qquad (27)$$

If the lag of the control surface actuator is neglected we may put

$$\zeta = \zeta_D \qquad\qquad (28)$$

In section 2.3 the transfer functions r/ζ, v/ζ and $p^2 h_p/\zeta$ were obtained. Using equations (26) and (27) the transfer functions r/ζ_G, v/ζ_G, $p^2 h_p/\zeta_G$ may now be determined. These are identical with those given by equations (2) except that the expression

$$Q = p^2 + p\,(-y_v - n_r) + U n_v + x_{rv} \qquad \text{cf. eqn. (3)}$$

$$\text{or} \qquad p^2 + 2u\,\omega\,p + \omega^2$$

becomes

$$Q_m = p^2\,(1 - y_\zeta f) + p\,(-y_v - n_r - bn_\zeta + fx_{\zeta r}) + U n_v + x_{rv} + bx_{\zeta v} + Ufx_{\zeta v}$$

$$\text{or} \qquad (1 - y_\zeta f)\,[p^2 + 2\,u_m\,\omega_m\,p + \omega_m^2] \qquad (29)$$

so that in response to the guidance system the weathercock characteristics of the missile ω and u have been changed to ω_m and u_m by the angular velocity and lateral acceleration feedbacks.

For the test missile $\omega = 10$ rad/sec (i.e. undamped frequency = 1.59 c.p.s.) and $u = 0.1$. When we wish to consider a typical modified missile we assume the modifications are those suitable for a beam riding system. For example in Refs. (2) and (3) the response of the test missile (used as a beam rider) has been modified so as to increase the damping ratio to unity while holding the undamped frequency constant, i.e. $u_m = 1$, $\omega_m = \omega = 10$. The feedback constants required for this are

$$\left. \begin{array}{l} b = 0.09 \text{ rad per rad/sec} \\ f = -6.3 \times 10^{-5} \text{ rad per ft/sec}^2 \end{array} \right\} \qquad (30)$$

In this case the required acceleration feedback is very small but it has been retained in all the work for the sake of completeness.

In the presence of such feedbacks the steady state values of $\ddot{h}_p$, r, v etc. per unit of ζ_G depend on the feedback gains. If negative feedback is employed then the greater the feedback gain the smaller the steady state values of $\ddot{h}$, r, v etc. per unit of ζ_G. It should be noted however that the order of feedback gains required to modify the test missile to the desired characteristics are small and the change in steady state values per unit of ζ_G differ by only a few percent from those per unit of ζ. This may be established by noting that the transfer function

$$\frac{\zeta_G}{\zeta} = 1 - \frac{b\,(x_{v\zeta} + n_\zeta p) - f\,(p^2 y_\zeta + px_{\zeta r} + Ux_{v\zeta})}{p^2 + p\,(-y_v - n_r) + Un_v + x_{rv}} \qquad (31)$$

becomes

$$\frac{\zeta_G}{\zeta} = 1 - \frac{x_{v\zeta}\,(b + fU)}{Un_v + x_{rv}} \qquad (32)$$

in the steady state and this is approximately unity for the test missile and the specified feedback gains. This fact leads to a useful simplification. For the purposes of approximate calculations the steady state values of $\ddot{h}_p$, r, v etc. for the test missile may be taken as those given by the unmodified and not the modified missile.

- 25 -

It is convenient at this point to note the general form that the weathercock characteristic expression Q assumes for certain other feedback combinations considered later.

If the control equation is

$$\zeta_D = \zeta_G + br + f\ddot{h}_p + K\ddot{\psi} \qquad (33)$$

where $K\ddot{\psi}$ represents feedback from an angular accelerometer then Q becomes

$$Q_c = p^2 (1-fy_\zeta-Kn_\zeta) + p (-y_v-n_r-bn_\zeta-fx_{\zeta r}+Kx_{\zeta v})+Un_v+x_{rv}+bx_{\zeta v}+U f x_{\zeta v} \qquad (34)$$

2.10* The test beam rider

At various stages in the analysis of the limiting methods the application of these methods to a typical beam riding system is discussed. (In paragraphs marked *). This beam riding system is of a type which has received much study in Guided Weapons Department.[1],[2],[3]. The weathercock motion of the missile is modified by the process outlined above so that the weathercock motion is critically damped and its frequency is intermediate between the other major frequencies of the missile motion, namely, the frequency of the roll stabilisation system and the frequency of the weave motion resulting from the beam riding control. The choice of modified weathercock frequency is also influenced by the fact that other things being equal the higher this frequency the greater the ease of stabilising the beam riding control loop.

Ideally the guidance component of control surface motion ζ_G consists of the beam riding error distance plus the rate of change of this error distance, i.e. in operational form

$$\zeta_G = G (1 + p T_o)(h_p - h_B) \qquad (35)$$

where

$\quad h_p$ is the missile position relative to a fixed datum

$\quad h_B$ " " radar beam " " " the same datum

$\quad T_o$ is a time constant

and $\quad$ G is a constant determining the stiffness of control.

The rate of change of error is however normally derived in an approximate manner by an electrical network so that

$$\zeta_G = G \frac{(1 + p T_o)}{(1 + pN T_o)} (p_p - h_B) \qquad (36)$$

where N is a constant of the order of $1/20$.

The complete equation for the control surface deflection demand is therefore

$$\zeta_D = G \frac{(1 + p T_o)}{(1 + pN T_o)} (h_p - h_B) + br + f \ddot{h}_p \qquad (37)$$

If we consider the test missile as the beam rider then typical values of the parameters in this equation are:-

$b = 0.09$ rad per rad/sec

$f = -6.3 \times 10^{-5}$ rad per ft/sec^2

giving as in Section 2.9 a modified undamped weathercock frequency of 1.59 c.p s. with a damping ratio of unity.

$$G = 0.746 \ 10^{-3} \ \text{rad ft}^{-1}$$
$$T_o = 0.91 \ \text{sec} \tag{38}$$
$$N = 1/20$$

The effects of the various limiting systems on this test beam rider are studied mainly in terms of the characteristics of the various modes of motion and on the beam riding response to step displacements of the radar beam.

If the radar beam, which the missile is attempting to ride, is auto-following a target then for various reasons there is a pronounced noise or "jitter" motion superimposed on the steady motion of the radar beam. This in turn means that the guidance information passed to the missile control system has a pronounced noise component. If the control system were linear then this noise would simply result in a dispersion in the miss distance against the target. Any nonlinearities in the control system, such as the limiting systems to be discussed, may result in rectification of the noise and consequently introduce a bias as well as a dispersion into the miss distance against the target. It is important therefore that the limiting systems be tested in the presence of radar beam jitter to ensure that they are not unduly affecting the overall performance of the missile regarded as a weapon.

"Jitter" is discussed in Ref.1, and in Ref.2 a method of simulating it and measuring the miss distances obtained with the test missile is given. For a representative radar set the radar beam jitter at 30,000 yds range is of the order of 60 ft R.M.S. Jitter of this order of magnitude and with a frequency spectrum appropriate to the typical radar set (the Naval 901 Radar Set) has been used in tests on the limiting systems.

3   Limitation of Total Lift

3.1   Failings of the present method

One method at present in use for the limitation of the total lift on the missile is simply that of limiting the guidance component (ζ_G) of the control surface demand signal.

If the lateral acceleration and rate of yaw feedbacks are arranged to give critical damping at a desired frequency then there is no overshoot of acceleration beyond the steady state value. Thus if the aerodynamic derivatives are constant and the weathercock mode is critically damped then limitation of the control surface demand signal (ζ_G) effectively limits the acceleration; the limiting acceleration (and hence the total limiting lift force) being proportional to the limiting value of the control surface demand signal (ζ_G).

This condition cannot be attained in flight because the aerodynamic derivatives are not constant. Consequently for a fixed control surface demand limit the limiting acceleration can vary over a wide range - leading either to destruction or inefficient use of the missile.

Consider for example changes in the static margin of the missile due to fuel consumption. Table III on page 22 shows that for the test missile a static margin change of +9" will cause a 58% reduction in the maximum acceleration and a static margin change of -9" a 210% increase in maximum acceleration.

3.2 Proposals for the limitation of the total lift

In order to develop a method of limiting the total lift to a value which is independent of aerodynamic parameters it seems essential that the method be based on some measurement of the lift occurring, followed by appropriate feedback of the lift signal to control the maximum lift. The lift forces are readily measured by an accelerometer and the immediately following sections consist of a study of various techniques of acceleration feedback aimed at obtaining an effective total lift limiting system.

Simple acceleration feedback is first discussed and then the advantages of using an accelerometer displaced from the centre of gravity of the missile are brought out. The attenuating action of direct feedback on the lift is then converted into a limiting action by passing the feedback signals through a threshold system. An improved system has been developed in which the acceleration is fedback through a threshold system and then used to monitor the level at which diode limiters limit the control surface demand signal. These systems have been tested over a range of values of H, the change in static margin.

3.3 Feedback from a lateral accelerometer

3.31 The effect of direct acceleration feedback on the response of the missile

The general effects of direct acceleration feedback may be derived from a study of the behaviour of the modified missile when the acceleration feedback gain is varied.

From equation (29) we have for the modified missile the characteristic expression for the weathercock motion

$$Q_m = p^2 (1 - y_\zeta f) + p (-y_v - n_r - bn_\zeta + fx_{\zeta r}) + Un_v + x_{rv} + bx_{\zeta v} + U fx_{\zeta v}$$

Clearly the effect of the acceleration is critically dependent on the value of y_ζ if $fy_\zeta > 1$.

It is of interest to consider two cases:-

(a)   the test missile with the normal values of y_ζ and n_ζ and

(b)   the test missile with $y_\zeta = 0$ but n_ζ unaltered. This is a hypothetical case but provides an interesting comparison with cases (considered later) of feedback from accelerometers situated away from the C of G of the missile.

We assume a fixed value for the angular velocity feedback constant b, say the value 0.09 sec as used earlier to give critical damping with a lateral acceleration feedback constant $f = -6.3$, 10^{-5} rad ft^{-1} sec^2.

Q_m may be written as $(1 - y_\zeta f)[p^2 + 2 u_m \omega_m p + \omega_m^2]$ indicating an undamped modified weathercock frequency of $\omega_m/2\pi$ and a damping ratio u_m. If $u_m > 1$, Q_m may be written as $(1 - y_\zeta f)[p+a_1][p+a_2]$ indicating an exponential

weathercock response with time constant $1/a_1$, and $1/a_2$. ($a_1 = a_2$ if $u_m = 1$). Regarding the pair a_1 and a_2 as functions of the acceleration feedback constant f we may indicate any change of branch in these functions by further subscripts e.g. a_3 and a_4.

Table V gives the values of ω_m, u_m or the pairs (a_1, a_2) or (a_3, a_4) as functions of f for case (a) above.

TABLE V

Case (a). y_ζ and n_ζ normal

f rads ft^{-1} sec^{+2}	ω_m sec^{-1}	u_m	a_1 sec^{-1}	a_2 sec^{-1}	a_3 sec^{-1}	a_4 sec^{-1}
-0.000515			0			
-0.0005			0.20	14.2		
-0.0002			4.70	12.5		
-0.0001			8.25	10.3		
0	10.6	0.941				
0.0001	12.1	0.896				
0.0002	13.7	0.843				
0.0005	19.3	0.859				
0.00066	21.8	0.875				
0.001					22	76.0
0.0011					20.5	156
0.00125					Change of mode	
0.00143					20.75	-147

Table VI gives the corresponding data for Case (b).

TABLE VI

Case (b). Hypothetical Case, $y_\zeta = 0$, n_ζ normal

f rads ft^{-1} sec^{-2}	ω_m sec^{-1}	u_m	a_1 sec^{-1}	a_2 sec^{-1}
-0.0002			3.60	16.3
-0.0001			6.72	13.2
0	10.9	0.918		
0.0005	16.4	0.620		
0.001	17.8	0.575		
0.002	26.8	0.391		
0.004	36.0	0.306		
0.01	55.7	0.222		
0.02	78.2	0.189		

Figure 1 shows the root pattern of Table V in graphical form. From this diagram it is clear that there is a limited range of f (0 to 0.0008 rads ft^{-1} sec^{+2}) for which u_m is approximately unity while ω_m

increases from 10 to 25 sec^{-1}, i.e. in this range f is a frequency control
and it is as such that it is normally used in modifying the weathercock
characteristics of missiles. Outside this range of f however the system
rapidly goes unstable developing negative real roots for f< -0.000515
and f> 0.00125 rads ft^{-1} sec^2.

Figure 2 shows the corresponding root pattern for Table VI . Here
the pattern is very much simpler and for positive values of f (i.e.
negative feedback, ω_m increases indefinitely but u_m tends to zero as f
increases).

The acceleration response of the missile to a step in ζ_G, the
control surface demand signal, is of the form shown in Figure 3(a).
There is an initial "kick" due to the suddenly applied control surface
lift (the y_ζ-effect) followed ultimately by a steady state acceleration
which is opposite in sign to the initial kick of acceleration.

The magnitude of the initial acceleration kick is given by

$$\frac{\ddot{h}_r}{\zeta_G} = \frac{y_\zeta}{1 - y_\zeta f} \qquad (39)$$

and therefore it increases as f is increased from zero.

The magnitude of the steady state acceleration is given by

$$\frac{\ddot{h}_r}{\zeta_G} = \frac{Ux_{v\zeta}}{Un_v - x_{vr} - (b + f U) x_{v\zeta}} \qquad (40)$$

and this decreases as f is increased from zero.

Using the test missile as an example Figure 3(b) shows the magni-
tude of the kick, Figure 4 the steady state acceleration and Figure 5
the ratio of (kick)/(steady state) acceleration. Also shown on Figure 4
are some simulator results which indicate the degree of agreement between
theory and simulator and act as a check on the operation of the simulator.

In the case of the hypothetical missile of Case (b) with y_ζ = 0,
n_ζ normal, there is no acceleration kick.

3.32 Feedback from a displaced accelerometer

In the previous section the effects of lateral acceleration feed-
back on the response of the missile were considered. Since the accelera-
tion kick and the steady state acceleration are of opposite signs any
system using a high level of acceleration feedback in order to attenuate
(or limit) the steady state acceleration will result in accentuated accele-
ration kicks and this is very undesirable.

The difficulties over the acceleration kick and the stability of
the system may be overcome as follows. The results of the previous
section are based on feedback of lateral acceleration i.e. feedback from
an accelerometer situated at the centre of gravity of the missile. If
however the accelerometer is not at the C of G but is suitably displaced
from it then the undesirable y_ζ-effects may be removed. In effect the
accelerometer is situated so that it does not register the acceleration

due to the control surface lift. The feedback is then as though $y_\zeta = 0$ although the forward channel still has the normal y_ζ terms. Since the control surface lift occurs at a point at a fixed distance behind the C of G there is a corresponding point ahead of the C of G at which the angular acceleration of the missile contributes a lateral acceleration component which is equal and opposite to the lateral acceleration due to the control surface lift. Thus the output of a lateral accelerometer at this point ahead of the C of G corresponds to that measured at the C of G of a hypothetical missile in which $y_\zeta = 0$ but n_ζ is unaltered (i.e. Case (b) of previous section).

For an accelerometer situated d feet ahead of the C of G of the missile the accelerometer output is

$$a = \ddot{h}_p + d\dot{r} \quad \text{or} \quad h''_p + d\ddot{\psi} \tag{41}$$

Now from equations (2) and (3) we have the transfer functions

$$\frac{p^2 h_p}{\zeta} = \frac{p^2 y_\zeta + x_{\zeta r} p - U x_{\zeta v}}{Q}$$

$$\frac{pr}{\zeta} = \frac{p^2 \psi}{\zeta} = \frac{n_\zeta p^2 - x_{\zeta v} p}{Q}$$

where $Q = p^2 + p (-y_v - n_r) + U x_{v\zeta}$.

Thus the transfer function for the accelerometer output is

$$\frac{a}{\zeta} = \frac{p^2 (y_\zeta + d n_\zeta) + p (x_{\zeta r} - d x_{\zeta v}) - U x_{\zeta v}}{Q} \tag{42}$$

and the troublesome coefficient of p^2 in the numerator may be removed by having

$$d = -\frac{y_\zeta}{n_\zeta} = -\frac{\frac{Y_\zeta}{m}}{\frac{N_\zeta}{C}} \quad (= 4 \text{ ft for the test missile}) \tag{43}$$

This gives

$$\frac{a}{\zeta} = \frac{p \left(x_{\zeta r} + \frac{y_\zeta}{n_\zeta} x_{\zeta v}\right) + U x_{v\zeta}}{Q} \tag{44}$$

so that providing

$$x_{\zeta r} + \frac{y_\zeta}{n_\zeta} x_{\zeta v} \quad \text{and} \quad U x_{v\zeta}$$

are of the same sign as will be the case with missiles of the type considered, then the output of the accelerometer is always of the sign appropriate to the steady state value and if used in a feedback loop it can consistently give negative feedback.

Figure 6 shows simulator records for the output of an accelerometer as a function of its distance ahead of the C of G of the missile. The acceleration kick is seen to decrease in amplitude and then change sign as the distance ahead of the C of G increases.

For $d = - y_\zeta/n_\zeta$, the initial acceleration kick of the missile is given by

$$\frac{p^2 h_r}{\zeta_G} = \frac{y_\zeta}{1 - y_\zeta f - dfn_\zeta} = y_\zeta \qquad (45)$$

which is independent of the amount of feedback (f), while the steady state acceleration is given by

$$\frac{p^2 h_r}{\zeta_G} = \frac{Ux_{v\zeta}}{Un_v - x_{vr} - (b + fU) x_{v\zeta}} \qquad (46)$$

which is independent of the position (d) of the accelerometer.

With a displaced accelerometer the control equation becomes

$$\zeta_D = \zeta_G + br + f (\ddot{h}_p + d\ddot{v}) \qquad (47)$$

Reference to the weathercock characteristic expression Q_C given in equation (34) of Section 2.9 shows that in this case the weathercock characteristic expression may be written as

$$Q_C = p^2(1 - fy_\zeta - dfn_\zeta) + p(-y_v - n_r - bn_\zeta - fx_{\zeta r} + dfx_{\zeta v}) + Un_v + x_{rv} + bx_{\zeta v} + Ufx_{\zeta v} \qquad (48)$$

For $d = - y_\zeta/n_\zeta$ and b = 0.09 sec in the test missile this gives

$$Q_C = (p^2 + 2u_D \omega_D p + \omega_D^2) \times (\text{Constant}) \qquad (49)$$

where $\omega_D/2\pi$ the modified weathercock frequency and u_D its damping ratio are as given in Table VII.

- 32 -

TABLE VII

f rad ft^{-1} sec^2	ω_D sec^{-1}	u_D -
-5.2×10^{-4}	Change of mode	
-5.0×10^{-4}	2.01	4.96
-10^{-4}	9.60	1.04
-10^{-5}	10.6	0.95
0	10.7	0.94
10^{-5}	10.8	0.92
10^{-4}	11.7	0.86
10^{-3}	18.3	0.56
10^{-2}	48.0	0.24
10^{-1}	149	0.16

These results are plotted in Figure 7 where they are compared with the results for pure acceleration feedback ($\ddot{m}_p$) but for $y_\zeta = 0$, n_ζ normal. There is close correspondence between the two sets of curves and in fact, within the plotting accuracy the damping curves coincide. This illustrates the point that by suitably displacing the accelerometer the advantages of a hypothetical missile in which $y_\zeta = 0$ but n_ζ is normal may be attained.

In all the work which follows it is assumed that the accelerometer is situated at a distance $d = - y_\zeta/n_\zeta$ ahead of the C of G of the missile. In practice the exact distance would not be critical since a small increase or decrease in the acceleration kick when the acceleration is fedback would not be important.

3.33 The effects of time lags

An indication of the effects of instruments and control surface servo time lags on the operation of a limiting system based on acceleration feedback may be obtained as follows:

If the total control surface demand signal (ζ_D) consists of a guidance demand (ζ_G), a rate-of-yaw feedback demand (br) and an accelerometer feedback demand $f(\ddot{h} + d\ddot{\psi})$ then the control surface angle is defined by

$$\zeta = \frac{\zeta_G + br + f\,(p^2 h + dp^2 \psi)}{1 + pT_x} \qquad (50)$$

where T_x is the time lag of the control surface servo.

The same relationship exists if the servo time lag is zero but each of the component demands has a time lag of T_x seconds.

This control relationship leads to the following characteristic equation for the missile motion.

- 33 -

$$(A_1 p^3 + B_1 p^2 + C_1 p + D_1) \begin{bmatrix} p^2 h \\ v \\ \text{or} \\ r \end{bmatrix} = 0 \qquad (51)$$

where $A_1 = T_x$

$B_1 = 1 - T_x (y_v + n_r)$

$C_1 = -y_v - n_r - bn_\zeta - fx_{\zeta r} + afx_{\zeta v} + T_x (Un_v + x_{rv})$

$D_1 = Un_v + x_{rv} + bx_{\zeta r} + fUx_{\zeta v}$

for $d = - y_\zeta/n_\zeta$.

Writing this equation in the form

$$(p + \alpha_x)(p^2 + 2u_x \omega_x p + \omega_x^2) \begin{bmatrix} p^2 h \\ v \\ \text{or} \\ r \end{bmatrix} = 0 \qquad (52)$$

and evaluating ω_x, u_x and α_x for the test missile we obtain the results of Table VIII when $b = 0.09$ seconds and $f = 10^{-3}$ rad ft^{-1} sec^2.

TABLE VIII

T_x sec	ω_x rad sec^{-1}	u_x -	α_x sec^{-1}
0	18.3	0.56	-
10^{-3}	18.5	0.55	98.0
10^{-2}	20.3	0.52	80.8
510^{-2}	20.3	0.14	16.2
710^{-2}	18.8	0.074	13.5
10^{-1}	17.2	0.02	11.3

The system remains stable as T_x increases, the frequency remaining approximately constant but the damping ratio tending to zero. The damping ratio does not fall appreciably until the time lag T_x exceeds 10 milliseconds. This loss in damping may be partly regained by an increase in the amount of rate-of-yaw feedback - i.e. an increase in b. Thus the general impression is that if the rate-of-yaw feedback is chosen to give adequate damping in the presence of the time lags then these lags should not be a serious handicap in applying the method.

The general trend of Table VIII is borne out by the simulator records of Figure 8. These records show the responses of the missile to step demands of ζ_C for various values of T_x (inserted on the simulator as a control surface time lag). The feedback gain of the acceleration terms (f) happened to be greater in these records than that assumed in Table VIII being 0.0055 rad ft^{-1} sec^2 instead of 0.001 rad ft^{-1} sec^2. The decreasing negative kick in the records of Figure 8 is a direct consequence of the increasing time lag in the control surface servo.

3.34 Multiple acceleration feedbacks

Up to this point the acceleration feedback gain has been denoted by f (in rads ft^{-1} sec^2 or degrees per g). In the acceleration limiting systems there are several possible types of acceleration feedback which may be used in different ways for different purposes, e.g. feedback of pure acceleration or feedback of the output from a displaced accelerometer for the purpose of weathercock frequency modification or feedback from a displaced accelerometer for the purposes of limiting. To distinguish between such feedbacks the feedback gain in a system using <u>continuous</u> acceleration feedback for weathercock modifications is denoted by f (in rads ft^{-1} sec^2 or degrees per g) whereas the feedback gain in a system using <u>discontinuous</u> acceleration feedback for the purposes of limiting is denoted by F (in rads ft^{-1} sec^2 or degrees per g). Both types of feedback may occur in the same system.

3.4 Threshold feedback from a displaced accelerometer

Negative feedback to the control surfaces from a forward displaced accelerometer produces an attenuation of the steady state acceleration without accentuating the y_ζ-kick of acceleration and gives a system with a range of stability approximating to that of a missile with $y_\zeta = 0$. If the feedback is only operative if and when the acceleration exceeds a specified value then the attenuation effect becomes a limiting effect. Figure 9 shows in schematic form a limiting system based on this approach.

Whenever the output from the displaced accelerometer $(\ddot{h}_p + d\ddot{\psi})$ becomes more positive than a fixed positive level T_c then the threshold circuit (1) feeds back to the control surfaces a demand proportional to the excess $[\ddot{h}_p + d\ddot{\psi} - T_c]$. System (2) operates in a similar manner to feed back a demand proportional to $[T_c - \ddot{h}_p - d\ddot{\psi}]$ whenever the accelerometer output is more negative than $-T_c$. Only one of these feedback loops can be in operation at any one time. In operation the missile will respond to the input demands ζ_G until the accelerometer output indicates excessively large accelerations (defined by $+T_c$ and $-T_c$) when the appropriate feedback loop comes into operation to reduce the demanded control surface deflection ζ and so attenuate the acceleration response beyond the $\pm T_c$ levels.

Figure 10 shows simulator records for this type of limiting system as applied to the test missile with the weathercock modification to give critical damping, (i.e. $b = 0.09$ sec. $f = -6.3 \cdot 10^{-5}$ rad ft^{-1} sec^2). The limiter accelerometer was situated $-y_\zeta/n_\zeta = 4$ ft ahead of the missile C of G. The threshold levels $\pm T_c$ were set to correspond to steady state accelerations of $\pm 10g$. In response to step control surface demands (ζ_G) the missile acceleration $(\ddot{h}_p)$ and the wing incidence (β_W) were recorded for various values of the feedback gain (F). The wing plus body lift $(W,$ measured in g's) is given by $-0.57 \beta_W$. It will be noted that in all the records the steady state values of $\ddot{h}_p$ and W are the same, as is to be expected for a neutrally stable body-wing combination. The control surface lift $(R,$ measured in g's) is the difference between $\ddot{h}_p$ and W and is therefore clearly in the form of an impulsive response when the demand (ζ_G) is applied followed later by another impulsive response when the feedback suddenly comes into operation.

Figure 11 shows the steady state value of $\ddot{h}_p$ or W (deduced from the simulator records) as a function of the magnitude of the control surface demand and the feedback gain. There is no absolute bound to the acceleration, only an attenuation of the excess of acceleration over the $\pm 10g$ level, this attenuation increasing as the feedback gain is increased.

If the control surface has a fixed traverse, say ±20°, then the
steady state acceleration reaches an absolute bound, which is dependent
on altitude, velocity etc, when the input control surface demand exceeds
±20°. This effect is indicated on Figure 11.

The rather indefinite limiting obtained with this system may be
greatly improved by the method discussed in later sections.

3.5 The monitored diode system of acceleration limiting

The feedback from the displaced accelerometer can be used more
effectively than as described in the previous section. A system is
proposed which is a combination of the two systems mentioned so far.

(a) The current method of using diode clippers on the input demands
for control surface deflection which gives sharp limiting but to a
level dependent on the aerodynamic parameters, and

(b) The feedback system of the previous section which does not give a
sharp limit but is less dependent on the aerodynamic parameters.

If the output from the displaced accelerometer is fedback and used
to monitor the level at which the diode clippers work then a system which
gives sharp limiting and is less dependent on the aerodynamic parameters
is obtained. If the sense of the feedback is such as to decrease the
magnitudes of the biassing voltages on the diodes then, as and when the
accelerometer output tends to overshoot the values set by the threshold,
the magnitudes of the diode voltages decrease to the value at which the
ultimate acceleration is very nearly equal to the value defined by the
threshold circuit. In this way the maximum lateral acceleration does
not increase appreciably even if the aerodynamic stiffness of the missile
increases. It is an important requirement that if the aerodynamic
stiffness decreases then the ultimate acceleration should not be appreci-
ably less than the design limit or the missile is being used inefficiently.
The effects of decreasing aerodynamic stiffness may be countered in the
above system of limiting by making the original diode biassing voltages
such that, at the least aerodynamic stiffness expected, the full design
acceleration is achieved and the feedback system will keep the accelera-
tion down to this figure as the aerodynamic stiffness increases. The
smaller the margin that has to be allowed for this purpose the better since
the amount of correction to be applied by the feedback system increases
as the original biasses are increased in magnitude.

Figure 12 shows the system in block schematic form. The two thres-
hold blocks of Figure 9 have now been drawn as one block since in a practi-
cal application the threshold levels $+T_0$ and $-T_0$ could be defined by a
pair of diodes as on Figure 13. The usual diode clipping or limiting
arrangement is shown but in place of the usual D.C. biassing voltages on
these diodes we have the output voltages of a pair of summing amplifiers.
One input to each amplifier is a constant D.C. voltage so that the critical
bias on the diodes may be set to give the designed acceleration for the
lowest aerodynamic stiffness to be expected. The voltage output from
the displaced accelerometer passes through the threshold system and is
then applied to the input of the biassing amplifiers so that the output
voltages from these amplifiers decrease when the accelerometer output
breaks through the threshold system. Figure 13 gives a detailed circuit
diagram of the arrangement used in the simulation. It is probable that
this could be simplified for a missile application.

3.51 Analysis of the monitored diode system

This analysis is directed towards the determination of appropriate
values of the initial diode bias expressed in terms of the equivalent

control surface demand angle (B degrees), the threshold levels ($\pm T_c$ in g's) and the gain (F degrees per g) in the feedback loop from the displaced accelerometer.

Since this is a steady state analysis we may make use of the approximation that the weathercock modifying feedbacks (br and f$\ddot{h}_p$) have a negligible effect on the steady state response of the tests missile. (See Section 2.9).

The twin feedback loops, one for excessive positive accelerations and one for excessive negative accelerations, see Figure 14(a) may be analysed as one feedback loop if the correct sign convention is adopted.

Let B, T_c and F be positive quantities. In the steady state relationship

$$\frac{p^2 h_p}{\zeta} = k_h \qquad \text{cf. eqn.} \quad (5)$$

k_h is a negative number. Thus if the input control surface demand $\zeta_G > B$ we have

$$\zeta = B + F (\ddot{h}_p + T_c)$$

while if $\zeta_G < - B$ we have

$$\zeta = - B + F (\ddot{h}_p - T_c)$$

Both of these relationships conform to the expression

$$|\zeta| = B - F (|\ddot{h}_p| - T_c) \qquad (53)$$

which may be represented diagramatically as in Figure 14(b).

(a)   <u>The choice of diode bias B</u>

The value of B is given by the value of ζ which gives the required acceleration under the conditions of least aerodynamic stiffness. This is given by

$$|\ddot{h}_p| = |k_h| \zeta$$

where $|\ddot{h}_p| = T_c$ and $|k_h|$ has its lowest possible value.

Now $k_h \doteq \dfrac{x_v \zeta}{n_v}$

$$= (146.6)(15) \text{ ft sec}^{-2} \text{ rad}^{-1} \text{ for the test missile.}$$

These figures are for maximum altitude where $|k_h|$ has its lowest value. If in addition we allow a (0.75) times reduction in $|k_h|$ to allow for a possible fall in the expected velocity we have

$$|k_h|_{min} = (0.75)(146.6)(15) \text{ ft sec}^{-2} \text{ rad}^{-1}$$

$$= 0.86 \text{ g per degree.}$$

- 37 -

Thus if the design acceleration limit is given by $T_c = 10g$ the largest value of ζ ever required is $10/0.86 = 11.6$ degrees. Therefore the diode bias B should be such that

$$B > 11.6 \text{ degrees} \tag{54}$$

(b) The feedback loop

When the acceleration exceeds T_c we have from equations (5) and (53)

$$|\ddot{h}_p| = \frac{B + FT_c}{F + \frac{1}{|k_h|}} \quad \text{(in g's)} \tag{55}$$

The limiting acceleration therefore tends to T_c as F tends to infinity.

The monitored bias on the clipping diodes is

$$B - F\left(|\ddot{h}_p| - T_c\right) \quad \text{(in degrees)}$$

or

$$\frac{B + FT_c}{1 + F|k_h|} \quad \text{(in degrees)} \tag{56}$$

and this tends to $\dfrac{T_c}{|k_h|}$ degrees as F tends to infinity.

Equations (55) and (56) show that the monitored bias on the diodes is multiplied by $|k_h|$ we get the effective acceleration to which the system is limiting.

The difference between the effective acceleration limit $|\ddot{h}_p|$ and the desired limit viz. the threshold level T_c is given by

$$T_c - \frac{B + FT_c}{\left|\frac{1}{k_h}\right| + F} \quad \text{(in g's)} \tag{57}$$

or

$$\frac{T_c - B|k_h|}{1 + F|k_h|} \quad \text{(in g's)} \tag{58}$$

Now this difference in the absence of feedback is $(T_c - B|k_h|)$ in g's, so that the feedback reduces the difference between the effective acceleration limit and the desired limit by a factor $1 + F|k_h|$.

Figure 15 shows the form of the steady state acceleration as a function of the input control surface demand ζ_G and the system constants T_c, B, F and k_h. This figure differs from Figure 11, for the direct feedback case in that for a given feedback gain F there is now an absolute bound to the acceleration.

(c)   **The choice of feedback gain F**

Assume as the design criterion that the limiting acceleration has to be within 10% of the design value over the expected altitude and speed range.

We have for the limiting acceleration

$$|\ddot{h}_p| = \frac{B + F T_c}{F + \frac{1}{|k_h|}} \qquad \text{cf. eqn. (55)}$$

Now

$$\frac{1}{k_h} = \frac{Un_v + x_{rv}}{Ux_{v\zeta}} \qquad \text{cf. eqn. (5)}$$

at the design altitude and velocity.

If μ and σ denote the ratio of actual velocity and air pressure to the values under the design conditions then using equations (23) we have

$$\frac{1}{k_h} = \frac{\mu Un_v + \sigma x_{rv}}{\mu^2 \sigma Ux_{v\zeta}}$$

$$\doteq \frac{n_v}{x_{v\zeta}} \cdot \frac{1}{\mu\sigma}$$

for the test missile since x_{rv}/μ^2 is at most 10% of $Un_v/\mu\sigma$. This approximation is justified for as will be seen below we require $F > 0.005$ rads ft^{-1} sec^2 whereas the maximum value of $|1/k_h|$ over the range of variables considered is of the order of 0.0005 rads ft^{-1} sec^2. Thus a 10% approximation in $1/k_h$ gives at most a 1% error in the calculated limiting acceleration.

Therefore

$$|\ddot{h}_p| = \frac{B + F T_c}{F + \left| \frac{n_v}{x_{v\zeta}} \cdot \frac{1}{\mu\sigma} \right|}$$

giving

$$\frac{|\ddot{h}_p|_{min}}{|\ddot{h}_p|_{max}} = \frac{F + \left| \frac{n_v}{x_{v\zeta}} \frac{1}{(\mu\sigma)} \right|_{max}}{F + \left| \frac{n_v}{x_{v\zeta}} \frac{1}{(\mu\sigma)} \right|_{min}}$$

$$= x, \quad \text{say}$$

Hence

$$F = \frac{\dfrac{x|n_v|}{(\mu\sigma)_{min}} - \dfrac{|n_v|}{(\mu\sigma)_{max}}}{(1-x)|x_{v\zeta}|} \qquad (59)$$

and for the altitude and speed range defined by

$$1 < \sigma < 10$$

$$0.75 < \mu < 1.33$$

this gives the results of Table IX

<div align="center">TABLE IX</div>

F	x
rad ft^{-1} sec^2	
∞	1
0.011	0.95
0.005	0.9
0.0023	0.8

Therefore to hold the limiting acceleration within 10% of the design value we require $F > 0.005$ rads ft^{-1} sec^2.

(d) <u>The overall performance of the monitored diode system</u>

We consider the problem of limiting the acceleration of the test missile to within 10% of a 10g limit.

From Para.(a) above the diode bias B should be $\geqslant 11.6$ degrees to ensure that 10g is reached under all expected flight conditions.

From Para.(c) above the feedback gain F should be>0.005 rad ft^{-1} sec^2 to ensure that the acceleration limit does not vary by more than $\pm10\%$ from 10g.

Suppose then that

$$T_0 = 10g \text{ i.e. } 320 \text{ ft/sec}^2$$
$$B = 15 \text{ degrees}$$
$$F = 0.006 \text{ rad } ft^{-1} \text{ sec}^2$$

equation (55) gives the limiting acceleration for the design condition as 10.5g. For exactly 10g equation (55) shows that for the design conditions T_0 would have to be 303 ft/sec^2.

As a fuller illustration consider the application of this limiting system to the test missile under the following conditions:-

$$\text{Design altitude} = 30,000 \text{ ft}$$

$$\text{Design velocity} = 1,500 \text{ ft/sec}$$

$$\text{Design value of } n_v = {}^1/15 \text{ ft}^{-1} \text{ sec}^{-1}$$

$$F = 0.006 \text{ rad ft}^{-1} \text{ sec}^2$$

$$T_c = 303 \text{ ft sec}^{-2}$$

$$B = 15 \text{ degrees}$$

Possible departures from these design conditions may be defined by

$1 < \sigma < 10$, where σ is the ratio of actual air pressure to the pressure at the design altitude

$0.75 < \mu < 1.33$, where μ is the ratio of actual velocity to the design velocity

$0.5 < \lambda < 2$, where λ is the ratio of actual n_v to the design n_v.

The limiting accelerations as given by equation (55) are as quoted in Table X.

TABLE X

	$\sigma = 1$		$\sigma = 10$	
	$\mu = 0.75$	$\mu = 1.33$	$\mu = 0.75$	$\mu = 1.33$
$\lambda = 0.5$	10.3g	10.5g	10.7g	10.7g
$\lambda = 1.0$	9.8g	10.2g	10.7g	10.8g
$\lambda = 2.0$	8.2g	9.1g	10.4g	10.6g

It will be noted that for the design value of n_v (i.e. $\lambda = 1$) the limiting accelerations over the operating altitude and velocity range, are all within the desired 10% of the design value of 10g. The departures from the desired 10g limit are not great even when the value of the design n_v is changed by 2:1 (i.e. $\lambda = 0.5$ or $\lambda = 2$). The limiting acceleration is therefore effectively independent of the aerodynamics and flight conditions over their probable range of variation.

(e) **Limitation of wing lift**

The feedback systems discussed in the previous sections are such that limits are set to the total lift T. In later sections methods of limiting the control surface lift R are described. Ideally what is required are individual limits to the wing lift and the control surface lift. Unless the departure from neutral stability is very great $W \doteqdot T$ and the limitation of W rather than T is in the nature of a refinement. For completeness however we now consider the possibility of modifying the total lift limiting system so that we get a wing lift limiting system, i.e. we consider the problem of limiting W directly and in the presence of a changing missile stability (e.g. changing H or n_v) by using feedback from a displaced accelerometer.

In the steady state we have

$$\left. \begin{aligned} \frac{\ddot{h}_p}{\zeta} &= k_h \\ \frac{v}{\zeta} &= k_v \end{aligned} \right\} \qquad \text{cf. eqn. (5)}$$

But the feedback system limits h_p'' so that

$$\text{Lim } |\ddot{h}_p| = \frac{B + F\,T_c}{F + |^1/k_h|} \qquad \text{cf. eqn. (55)}$$

Thus

$$\text{Lim } |v| = \left| \frac{k_v}{k_h} \cdot \frac{B + F\,T_c}{F + |^1/k_h|} \right|$$

But k_h is negative, therefore

$$\text{Lim } |v| = \left| k_v \cdot \frac{B + F\,T_c}{F k_h + 1} \right|$$

on substituting for k_v from equation (5) this gives

$$\text{Lim } |v| = \left| \frac{(B + F\,T_c)(x_{\zeta_r} - U n_\zeta)}{F\,U x_{v\,\zeta} - U n_v - x_{rv}} \right| \qquad (60)$$

Lim $|v|$ is independent of n_v, i.e. independent of H, if

$$\frac{\partial}{\partial n_v}\left[F\,U x_{v\zeta} - U n_v - x_{rv} \right] = 0$$

$$\text{i.e. if } \quad F = \frac{1}{y_\zeta}\left(1 - \frac{y_r}{U}\right) \cdot \frac{1}{y_\zeta} \qquad (61)$$

with this value of F

$$\text{Lim } |v| = \left| \frac{y_\zeta}{y_v}\left(B + \frac{T_c}{y_\zeta}\right) \right| \qquad (62)$$

Now $\quad W = \left[y_v + \frac{y_\zeta}{U}\left(1 - \frac{\partial \varepsilon}{\partial \alpha}\right) \right] v \qquad$ cf. eqns. (11) and (12)

Therefore

$$\text{Lim } |W| = \left| \left[y_v + \frac{y_\zeta}{U} \left(1 - \frac{\partial \varepsilon}{\partial \alpha}\right)\right]\left[\frac{y_\zeta}{y_v}\left(B + \frac{T_o}{y_\zeta}\right)\right]\right|$$

$$\doteqdot |B y_\zeta + T_o| \quad \text{since } y_v \gg \frac{y_\zeta}{u}\left(1 - \frac{\partial \varepsilon}{\partial \alpha}\right) \quad (63)$$

Thus Lim $|W|$ can be made independent of n_v provided F can be programmed so that over the altitude and velocity variations expected $F = {}^1/y_\zeta$ of. eqn. (61) or more generally $F = {}^1/y_\zeta' = {}^1/\sigma \mu y_\zeta$. The limit achieved, $|B y_{\zeta + } T_o|$, is a function of y_ζ and so will vary greatly over the altitude and velocity range, being $|B \sigma \mu y_\zeta + T_o|$ at anything other than the design altitude and velocity. Consequently B and/or T_C would also have to be programmed with altitude and velocity and the system becomes very involved.

3.52 Simulator results for the monitored diode system of limiting

Figure 16 shows the input-output relationship for the threshold system used on the simulator. This figure shows the voltage developed at the monitored diodes as a function of the voltage output from the accelerometer. $\mathcal{B}$ is defined as the slope of the linear portion of the curves in degrees per ft/sec^2. In operation the system is such that the operating point on these curves is on the knee of the curves since the accelerometer output is only slightly greater than the threshold level. Thus the effective feedback gain (F) is less than that given by the linear slope of the curves ($\mathcal{B}$). In a practical application of this, or a similar system for the threshold system, a calibration would have to be prepared giving the effective feedback gain as a function of the system parameters. In the present simulator work $\mathcal{B}$ (which is closely related to F and has the same dimensions) has been used as the parameter descriptive of the feedback gain of the system.

The responses of the test missile with the monitored diode system of limiting have been detained on the simulator. A large step demand for control surface angle was used as input and the resulting responses in total lift T and wing lift W were obtained for a feedback gain range of $^1/730 < \mathcal{B} < {}^{10}/730$, and a static margin shift range of $-9" < H < + 9"$. The T-records are given in Figure 17 and the W-records in Figure 18. The difference between T and W in any given case is the control surface lift R. It will be noted that W is limited with negligible overshoot so that the overshoots on the T-records are the transient control surface lifts R

The steady state ratio W_s/T_s (see Section 2.8) is independent of altitude, velocity and feedback gain but is dependent on the static margin change H. We have

$$\frac{W_s}{T_s} = \left[y_v + \frac{y_\zeta}{U}\left(1 - \frac{\partial \varepsilon}{\partial \alpha}\right)\right]\left[\frac{x_{y_r} - U n_\zeta}{U x_{v\zeta}}\right] \quad \text{of. eqn. (24)}$$

and for the test missile this is approximately

$$\frac{W_s}{T_s} \doteqdot \left(1 - \frac{H}{55}\right)^{-1} \quad \text{where H is in inches} \quad (64)$$

- 43 -

Figure 19 compares this approximate theoretical evaluation of W_S/T_S with the simulator results of Figures 17 and 18 and the agreement is reasonably good.

The steady state values T_S and W_S given by the records of Figures 17 and 18 are plotted as function of β and H in Figures 20 and 21. It will be noted that T_S tends to become less dependent on H for large values of β. For W_S however Figure 21 indicates that W_S is independent of H for $\beta = 0.0055$ rad ft^{-1} sec^2. Now in Section 3.52 (e) it was shown that W_S should be independent of H if the feedback gain $F = 1/y_\gamma = 1/800$ rad ft^{-1} sec^2. A very approximate indication of the inter-relationship between F and β is therefore $\beta = 4.4$ F and this is consistent with the concept of the system operating on the knee of the threshold curves.

Figure 22 shows the absolute bound to T_S given by the monitored diode system. For various values of β the system was set by T_Θ to give a nominal 10g limit and the actual limit obtained was plotted as a function of the input demand signal. Comparison with Figure 11 which gives the corresponding results for direct feedback of acceleration shows the advantages of the monitored diode technique. Figure 23, which shows various limiting systems applied under identical conditions, further illustrates the superiority of the monitored diode system.

3.6 A comparison of the limiting systems

The maximum acceleration or lift of the missile must be limited but we should not compare limiting systems solely on the efficiency of their limiting action since an important consideration relating to the overall performance of the missile system (e.g. estimates of miss distances) is the "effective point" in the system at which the limit occurs. In general terms a non-linear element is being introduced into the system and the overall performance of the system is dependent on where in the system this non-linearity occurs.

An important example of this is provided by the case of a beam riding missile. As a result of radar beam jitter (cf. Section 2.10 and Refs. 1 and 2) the legitimate guidance and control signals have pronounced noise or jitter components. Non-linearities in the missile control system such as the acceleration limiting system, may result in rectification of the "legitimate control signal plus noise" and give as a consequence an effective distortion of the legitimate signal. For example, if the legitimate signal is a steady demand for 7g acceleration and the noise component superimposed on the legitimate signal has peaks greater than that corresponding to 3g, then lateral acceleration limits set at 10g will, because of the asymmetrical clipping of the noise peaks, result in a mean acceleration of less than 7g.

The higher the signal/noise ratio at the stage when limiting is applied the smaller the distortion of the signal. Thus it is preferable to apply the limiting after rather than before any noise filtering that may be present. The response of the missile to its control surfaces is such that it provides a filter against the higher frequencies so that ideally we would like to have the missile develope acceleration as though there were no limits and then by some means only accept those values less than a specified amount. With such a system we would have limiting but other than that no distortion of the legitimate signals. "Acceleration clipping" may be used to describe such a system. In practice we cannot limit the acceleration in this way since the only method of manoeuvring the missile is by moving its control surfaces and accepting the subsequent acceleration.

Although the different limiting systems discussed here have been applied to the same physical point in the system, namely that point in the system at which the control surface demand signal appears, they are dependent to different degrees on feedback of the missile acceleration and thus will give results intermediate between simple limiting of the control surface demand signal and ideal acceleration clipping. Figure 24 illustrates, in an approximate fashion (i.e. neglecting the closed loop nature of the missile guidance system) the limiting action of various systems. We assume Curve (a) to represent the acceleration developed by the missile during the course of some manoeuvre. If $\pm A_{max}$ represents the desired maximum accelerations then Curve (b) illustrates the ideal case of "acceleration clipping" - being simply Curve (a) between the values $\pm A_{max}$. Curve (c) shows the type of acceleration response to be expected with simple limiting of the input demand signals and rate-of-yaw feedback to achieve critical damping. The acceleration builds up in a critically damped fashion to the limits $\pm A_{max}$. Curve (c) is clearly less desirable than Curve (b) since the acceleration build up to the limits is slower. The acceleration feedback systems of limiting give acceleration responses which are intermediate in type between those shown in Figure 24 Curves (b) and (c). The build up of acceleration is still exponential as in (c) but now builds up to a value greater than A_{max} and is only arrested in its build up when the threshold system is operated at or near A_{max}. The build up rate of acceleration is still less however than in case (c).

It is of interest to determine which of the limiting methods discussed in this report most nearly approaches the ideal acceleration clipping concept. From Figure 24 it would seem reasonable to assume that a measure of the R.M.S. acceleration would give a criterion by which the different systems may be compared. The best system will have a larger R.M.S. value than any of the other systems, tending in the limit to the R.M.S. value given by an ideal acceleration clipping system.

This problem has been studied on the simulator using the test beam rider with a typical radar jitter signal (cf. Section 2.9 and Refs.2 and 3). For each of the limiting methods discussed earlier the R.M.S. wing lift has been determined when the nominal limiting lift corresponds to +10g. In each case a range of values of n_v, or centre of gravity positions, has been explored by assuming H, the change in static margin from the design static margin, to be -9", 0 or +9".

Case (a)

The test beam rider with typical jitter signals.
No acceleration limiting.

Case (b)

As for (a) but with ideal "acceleration clipping" at $\pm 10g$.

Case (c)

As for (a) but with the input control surface demand signals limited. For each value of H the limits were adjusted to give a $\pm 10g$ limit to the acceleration.

Case (d)

As for (a) but with the monitored diode system of limiting. System set up to give a limit of $\pm 10g$ with a feedback gain of $F = 0.0055$ rad ft^{-1} sec^2 for H = 0.

- 45 -

Case (e)

As for (a) but with simple threshold feedback of acceleration.
Gains, thresholds etc. as for (D) but with the feedback signals fed
directly to the control surface demand signal instead of onto the
diode clippers.

Case (f)

As for (e) but with a prelimiter e.g. mechanical stops on control
surface set to give the desired limiting acceleration under the condi-
tion of least aerodynamic stiffness in the range $-9'' < H < +9''$.

Figure 25 compares in graphical form the results obtained for cases
(a) to (f). From this figure it is clear that the monitored diode system
of limiting is the nearest approach to the ideal case of acceleration
clipping.

3.7 Conclusions on total lift limiting

The monitored diode system, employing threshold feedback from an
accelerometer situated a distance approximately equal to $-y_\zeta/n_\gamma$ ahead of
the centre of gravity of the missile, gives a method by which the total
lift of the missile may be limited.

By a suitable choice of feedback gains etc. the total lift may be
constrained within a specified percentage of a given value over a given range
of variations in altitude, velocity and missile static margin. For example
consider a typical medium-range fog missile operating over a 10:1 air
density range and a 0.75:1:1.33 velocity range. The results of Table X on
page 41 indicate that a feedback gain of the order of 0.006 rads ft^{-1} sec^2
together with appropriate biases and thresholds gives at most an 8% variation
in the lift limit over this density and velocity range. Further, a 2:1
change in the N_γ derivative produces, in conjunction with the same density
and velocity variations, a change of at most 20% in the lift limit.

This system of limiting has advantages over all the other systems
assessed and most nearly approximates to the ideal case in which limiting
occurs as the final event in the development of the missile lift.

4 The Limitation of Control Surface Lift

It is first shown that if a missile has a neutrally stable body wing
combination then the angular acceleration of the missile provides a good
measure of the peak control surface incidence and hence of the peak
control surface lift. This leads to proposals for limiting the peak
control surface lift by suitable feedback of angular acceleration. The
proposed system is then studied in detail. Further sections discuss the
performance of this system when the neutral stability condition is not
satisfied.

4.1 Angular acceleration as a measure of peak control surface lift

In Section 2.6 it was shown that the relationship between the control
surface incidence (β_r) and the missile angular acceleration ($\ddot\psi$) <u>for a</u>
<u>neutrally stable body-wing combination</u> was given by

$$\frac{\beta_r}{p^2\psi} \approx \frac{p^2 + p\,(-y_v - n_r) - p\left(1 - \frac{\partial\varepsilon}{\partial\alpha}\right)\frac{y_\zeta}{U} + x_{rv} - \left(1 - \frac{\partial\varepsilon}{\partial\alpha}\right)\frac{x_{\zeta r}}{U}}{p^2 n_\zeta + x_v \zeta\, p} \qquad \text{cf. eqn.(17)}$$

- 46 -

In order to estimate the conditions under which the angular accelera-
tion $p^2\psi$ may be used as a measure of control surface incidence β_r we
consider the above transfer function as it applies in the different
frequency ranges $\omega^2 < 1$; $\omega^2 > 1$; $\omega^2 \gg 1$.

For frequencies such that $\omega^2 < 1$ the constant term in the numerator
is important and the angular acceleration is not a good measure of the
control surface incidence. However for such low frequencies the control
surface incidence is small, β_r/ζ being of the order of $1/100$ for the test
missile.

For frequencies such that $\omega^2 > 1$ then

$$\frac{\beta_r}{p^2\psi} \doteq \frac{p + (-y_v - n_r) - \left(1 - \frac{\partial\epsilon}{\partial\alpha}\right)\frac{y_\zeta}{U}}{pn_\zeta + x_{v\zeta}}$$

so that if $[-y_v - n_r - (1 - \partial\epsilon/\partial\alpha)\, y_\zeta/U]$ and $x_{v\zeta}/n_\zeta$ are of the same order
of magnitude then the angular acceleration gives an approximate estimate
of the control surface incidence. The weathercock frequency of the test
missile is such that it lies in this frequency region so that the values
of the control surface incidence will be appreciable in this frequency
region.

For frequencies such that $\omega^2 \gg 1$ then

$$\frac{\beta_r}{p^2\psi} \doteq \frac{1}{n_\zeta}$$

so that the angular acceleration is proportional to $\beta_r\, n_\zeta$ i.e. the control
moment. Assuming a constant moment arm we have angular acceleration
proportional to control surface lift. It is in this high frequency region
that peak values of control surface incidence and control surface lift
will occur since the frequency of control surface motion for $\omega \gg 1$ is
greater than the weathercock frequency of the missile and consequently the
control surface incidence is not reduced by a rotation of the missile as
a whole.

It follows that the missile angular acceleration may be used as a
measure of the control surface lift (or incidence) when this lift becomes
very large.

The similarity in the responses of the control surface incidence
and the angular acceleration to a step in the control surface deflection
for the test missile is shown by the following approximate solutions.

$$\frac{\beta_r}{\zeta} \doteq e^{-t} \sin (10t + 85^\circ)$$

and

$$-151\,\frac{\ddot\psi}{\zeta} \doteq e^{-t} \sin (10t + 105^\circ)$$

If the body-wing combination is not neutrally stable then the close relationship between control surface incidence and angular acceleration breaks down. This circumstance is discussed later in Section 4.5.

4.2 Proposals for the limitation of control surface lift

The main proposal is to use an angular accelerometer to measure the large control surface lifts and by feeding the output of this accelerometer back through a threshold circuit and injecting it into the control surface demand signal so limit the peak values of the control surface lift. Figure 26 shows the basic arrangement. In effect this is a twin loop arrangement similar to that used for lateral acceleration limiting. The threshold system is such that if $\ddot{\psi} > + M$ then $\ddot{\psi} - M$ is fedback while if $\ddot{\psi} < - M$ then $\ddot{\psi} + M$ is fedback, where M defines the threshold level. There are a number of parameters which determine the performance of such a system chief among which are the threshold level (M deg/sec²), the loop gain (K deg per deg/sec² or sec⁻²) and the level to which the lateral acceleration of the missile is being limited. We are interested however not only in the limiting action of such a system but also in the effect it has on the modes of motion of the missile.

In the following sections the attenuating action and the effect on the modes of motion of angular acceleration feedback without any threshold system is first discussed. The stability of the system and the limiting action when the threshold is inserted are then examined. Finally the application of the system under different combinations of circumstances is investigated.

In discussing the effects of this form of limiting on the performance of missiles it is essential that the method of obtaining the limiting be underlined since the method by which it is obtained determines to a large degree the effect on the performance of the missile. Thus we study the effect of "threshold feedback of angular acceleration" rather than simply "rudder lift limiting".

4.3 Feedback of angular acceleration

4.31 The attenuating action of angular acceleration feedback on control surface incidence

From equation (16) we have

$$\frac{\beta_r}{\zeta} = f_\beta(p)$$

and $$\frac{p^2\psi}{\zeta} = f_a(p)$$

From Figure 26 we have (ignoring the threshold system)

$$\zeta_1 = - K p^2 \psi$$

and $$\zeta = \zeta_2 - \zeta_1$$

Thus

$$\frac{\beta_r}{\zeta_2} = \frac{f_\beta(p)}{1 - K\, f_a(p)} \tag{65}$$

and

$$\frac{p^2\psi}{\zeta_2} = \frac{f_a(p)}{1 - K\, f_a(p)} \tag{66}$$

If we denote the values of $\ddot{\psi}$ and β_r at time $t = 0+$ by $\ddot{\psi}_0$ and β_{ro} then these values in response to a step in control surface demand ζ_2 are given by

$$\frac{\beta_{ro}}{\zeta_2} = \underset{p \to \infty}{\mathcal{L}} \frac{f_\beta(p)}{1 - K\, f_a(p)} = \frac{1}{1 - Kn_\zeta} \tag{67}$$

and

$$\frac{\ddot{\psi}_0}{\zeta_2} = \underset{p \to \infty}{\mathcal{L}} \frac{f_a(p)}{1 - K\, f_a(p)} = \frac{n_\zeta}{1 - Kn_\zeta} \tag{68}$$

whilst the final steady state values are given by

$$\frac{\text{final } \beta_r}{\zeta_2} = \underset{p \to 0}{\mathcal{L}} \frac{f_\beta(p)}{1 - K\, f_a(p)}$$

$$= \frac{(Un_v + x_{rv}) - \left(1 - \frac{\partial \varepsilon}{\partial a}\right)\left(x_{\zeta r} - n_\zeta\right)}{Un_v + x_{rv}} \tag{69}$$

and

$$\frac{\text{final } \ddot{\psi}}{\zeta_2} = \underset{p \to 0}{\mathcal{L}} \frac{f_a(p)}{1 - K\, f_a(p)} = 0 \tag{70}$$

The initial peak values of β_r and $p^2\psi$ (at $t = 0+$) are thus attenuated by a factor $(1 - Kn_\zeta)$ but the final steady state values are independent of the feedback.

- 49 -

For example if a 10 degree step in ζ_2 is considered then with no feedback and for $n_\zeta = -200 \ sec^{-2}$ we have

$$\beta_{ro} = 10^\circ, \qquad \ddot{\psi}_o = -2000^\circ/sec^2$$

while for $K = 0.2 \ sec^2$ we have

$$\beta_{ro} = 0.25^\circ, \qquad \ddot{\psi}_o = -52^\circ/sec^2$$

4.32 The effect of angular acceleration feedback on the weather-cock mode

The influence of angular acceleration feedback on the weather-cock motion of the missile may be assessed by a study of the appropriate weathercock characteristic expression.

In Section 2.9, equations (33) and (34), it is shown that if the control equation is

$$\zeta_D = \zeta_G + br + f\,\ddot{h}_r + K\ddot{\psi} \qquad \qquad cf.(33)$$

then the weathercock characteristic expression is

$$Q_c = p^2\,(1 - fy_\zeta - Kn_\zeta) + p\,(-y_v - n_r - bn_\zeta - fx_{\zeta r} + Kx_{\zeta v})$$
$$+ Un_v + x_{rv} + bx_{\zeta v} + Ufx_{\zeta v} \qquad cf.(34)$$

We consider two cases:- Case (a). Angular acceleration feedback only, i.e. $K \neq 0$, $b = f = 0$ and Case (b) normal weathercock modifying feed-backs br and $f\ddot{h}_p$ (see Section 2.9) and an additional angular acceleration feedback $K\ddot{\psi}$.

Case (a) Angular acceleration feedback only.

In this case Q_c becomes Q_K where

$$Q_K = p^2\,(1 - Kn_\zeta) + p(-y_v - n_r + Kx_{\zeta v}) + Un_v + x_{rv} \qquad (71)$$

and this may be written in the form

$$Q_K = (1 - Kn_\zeta)\,[p^2 + 2\,u_K\,\omega_K\,p + \omega_K^2] \qquad (72)$$

where ω_K denotes the undamped angular frequency and u_K the damping ratio.

Table XI shows how ω_K and u_K vary with positive values of K (i.e. negative feedback of angular acceleration) for the test missile.

TABLE XI

K sec^2	ω_K rad/sec	u_K
0	10.0	0.10
0.1	2.1?	0.24
0.5	0.99	0.51
1	0.70	0.71
∞	0	∞

With increasing angular acceleration feedback (K +^{ve}) the weather-cock frequency therefore decreases whilst the damping ratio increases.

Case (b) Angular acceleration feedback in addition to normal rate and lateral acceleration feedbacks.

In this case the expression for Q_c above is directly applicable. We consider the test missile. As shown in Section 2.9 the weathercock characteristics of this missile may be modified to give an angular frequency of 10 rads/sec and a damping ratio of unity by angular velocity and lateral acceleration feedbacks such that b = 0.09 sec and f = -6.3 10^{-5} rad ft^{-1} sec^2. Consider now the effect on this modified missile of angular acceleration feedback.

Q_c may be written as

$$(1 - fy_\zeta - Kn_\zeta)\ [p^2 + 2\ u_{K1}\ \omega_{K1}\ p + \omega_{K1}^2] \tag{73}$$

where ω_{K1} is the undamped angular frequency and u_{K1} the damping ratio.

Table XII shows how ω_{K1} and u_{K1} vary with positive values of K for the test missile and the above values of b and f.

TABLE XII

K sec^2	ω_{K1} rad/sec	u_{K1}
0	10.0	1.0
0.005	7.1	0.74
0.010	5.8	0.70
0.025	4.3	0.51
0.050	3.0	0.45
0.10	2.2	0.44
0.25	1.4	0.50
0.50	1.0	0.60
1.00	0.71	0.78

Figure 27 shows in graphical form the contents of Tables XI and XII. For $K = 0$, the effect of the rate and lateral acceleration feedbacks is to increase the damping ratio to unity while maintaining an undamped angular frequency of 10 rads/sec. The addition of angular acceleration feedback has the effect of destroying the synthetic damping due to the rate feedback. For large values of K the angular acceleration feedback completely dominates the others giving $\omega_K \doteq \omega_{K1}$ and $u_K \doteq u_{K1}$.

The operation of the simulator in respect to the weathercock motion has been checked by applying an input a step in the demand signal ζ_G and recording the response of the test missile under the conditions of Case (b) above. Sample records are shown in Figure 28. Measurements of frequency and damping from such records give the results of Figure 29 in which a comparison is made with the theoretical results of Table XII. The agreement obtained indicates that the simulator is functioning correctly.

4.33* The effect of angular acceleration feedback on the weave mode of a beam rider

For the "test beam rider" outlined in Section 2.10 the control equation is

$$\zeta_D = G \cdot \frac{1 + p\,T_o}{1 + N p\,T_o}\,(h_p - h_B) + br + f\ddot{h}_p \qquad \text{cf. (37)}$$

where G, T_o, N, b, f are constants and h_B is the radar beam position relative to the space datum.

If we now add to this system a component of angular acceleration feedback $(K\,\ddot{\psi})$ then the control equation becomes

$$\zeta_D = G\,\frac{1 + p\,T_o}{1 + N p\,T_o}\,(h_p - h_B) + br + f\ddot{h}_p + K\ddot{\psi} \qquad (74)$$

Neglecting the control surface servo delays we may put

$$\zeta_D = \zeta. \qquad (75)$$

This control equation in conjunction with the aerodynamic equation (1) gives the following characteristic equation for the motion of the beam rider

$$[A'\,p^5 + B'\,p^4 + C'\,p^3 + D'\,p^2 + E'\,p + F]\begin{bmatrix} p^2 h_p \\ v \\ \text{or} \\ r \end{bmatrix} = 0 \qquad (76)$$

where

$$A' = (1 - y_\zeta f - n_\zeta K) N T_o$$

$$B' = (1 - y_\zeta f - n_\zeta K) + (-y_v - n_r - bn_\zeta - fx_{\zeta r} + Kx_{\zeta v}) N T_o$$

$$C' = (-y_v - n_r - bn_\zeta - fx_{\zeta r} + Kx_{\zeta v}) + (Un_v + x_{rv} + bx_{\zeta v} + Uf x_{\zeta v}) N T_o$$

$$D' = Un_v + x_{rv} + bx_{\zeta v} + Uf x_{\zeta v} + G T_o x_{r\zeta} - G y_\zeta$$

$$E' = G T_o Ux_{\zeta v} + G x_{r\zeta}$$

$$F' = G Ux_{\zeta v}$$

If this equation is written in the form

$$(p + \alpha)(p^2 + 2 u_W \omega_W p + \omega_W^2)(p^2 + 2 u_c \omega_c p + \omega_c^2) \begin{bmatrix} p^2 h_p \\ v \\ or \\ r \end{bmatrix} = 0 \qquad (77)$$

then the modes of motion may be identified as a controlled (or weaving) mode with frequency $\omega_c/2\pi$ and damping ratio u_c and a weathercook-like mode with frequency $\omega_W/2\pi$ and damping ratio u_W.

For the test beam rider the control constants are

$$G = 0.746 \times 10^{-3} \text{ rad ft}^{-1}$$

$$T_o = 0.91 \text{ sec}$$

$$N = 1/20$$

$$b = 0.09 \text{ sec}$$

$$f = -6.3 \times 10^{-5} \text{ rad ft}^{-1} \text{ sec}^2$$

Approximate evaluation of α, ω_c, u_c, ω_W, u_W for these parameters and for various values of K gives the data of Table XIII.

TABLE XIII

K sec^2	α sec^{-1}	ω_W rads/sec	u_W	ω_c rads/sec	u_c
0	2.92	18.5	1.00	2.24	0.51
0.005	23.7	4.47	0.66	2.32	0.62
0.02	21.9	2.98	0.20	2.23	0.83
0.05	21.9	2.46	-0.07	1.84	0.85
0.10	21.9	2.03	-0.21	1.61	0.86
1.0	21.9	1.00	-0.43	1.06	0.86

Figure 30 shows these quantities plotted against K. It will be noted that the "weathercook like" motion (ω_W, u_W) is very similar to the weathercook motion in the absence of the main beam riding control loop (ω_{K1}, u_{K1}) (see Figure 27) with the exception that the decrease in damping

- 53 -

with increasing K is now such that u_r becomes negative for $K > 0.04$ sec^2 approximately and the system is consequently unstable. The weave frequency ($\omega_b/2\pi$) decreases slightly and the weave damping (u_o) increases towards critical damping as K increases. For K greater than 0.02 sec^2 the weave and weathercock like frequencies merge to the same value so that these descriptive terms for the two modes have no physical signifi-cance for $K > 0.02$ sec^2. As a result of the crossover of the damping curves it will be seen, for low values of K (i.e. $K < 0.005$ sec^2), that the weave mode is dominant but at large values of K (i.e. $K > 0.01$ sec^2) it is the weathercock-like mode which is dominant. Observation of the system will apparently show it as a system with a constant frequency dominant mode whose damping decreases as K increases. There may however be a region in which both modes are equally weighted and something like a "beat effect" will occur between the two modes. For this effect to show up K would have to be large so as to render the two modes close in frequency and yet not so large that one of them is unstable or the other too heavily damped.

Figure 31 gives a set of simulator results demonstrating the above effects. It shows, for various values of K, the responses in $\ddot{h}_p$ as the missile recovers from an initial lateral displacement of 375 ft. As K increases these acceleration records show a dominant mode of motion with decreasing damping. For K in the region 0.03 to 0.04 sec^2 there is evidence of the "beat effect" as the amplitudes of the peaks on the tran-sient recoveries firstly increase and then decrease.

The frequency and damping ratio of the dominant mode as measured from the records of Figure 31 are shown compared with the theoretical results on Figure 30. As is to be expected the experimental points coin-cide with the theoretical mode of least damping.

Figure 32 shows the complete beam riding response of the missile for $K = 0.021$ sec^2 and for $\pm10g$ lateral acceleration limits (simple diode limiting) in response to a step displacement of the radar beam.

4.4　Threshold feedback of angular acceleration

The immediately preceding sections have indicated how the modes of motion of the missile are affected when the angular acceleration feedback comes into operation. We have now to study the behaviour of the system when threshold feedback of angular acceleration is incorporated i.e. as a system with two zones, one in which there is feedback and one in which there is no feedback of angular acceleration.

The nonlinear control equation is of the form

$$\zeta_D = \zeta_G + br + f\,\ddot{h}_r + K_1\,\ddot{\psi} \tag{78}$$

where
$$K_1 = K,\ \text{if}\ |\ddot{\psi}| > M, \quad (M\ \text{being the threshold level})$$
$$K_1 = 0,\ \text{if}\ |\ddot{\psi}| < M$$

In the beam riding applications $\zeta_G = G\,\dfrac{1 + p\,T_o}{1 + N\,p\,T_o}\,(h_p - h_B)$ as before.

If the control surface servo lag is neglected $\zeta_D = \zeta$.

4.41 The limiting action of threshold feedback of angular acceleration

It has been shown in Section 4.31 that linear feedback of angular acceleration produces an attenuating action on the peak angular acceleration and control surface lifts. If the feedback is only applied when the angular acceleration exceeds a specified level then this attenuating action becomes a limiting action, the limit being defined by the threshold level. The greater the feedback gain the better the limiting action.

From Section 4.31 we have that the attenuating factor is $(1 - Kn_\zeta)$. If the angular acceleration threshold level is $|M|$ $^\circ/\mathrm{sec}^2$ the corresponding level for the control surface incidence (β_r) is $|M/n_\zeta|$ degrees. Thus if an input step control surface demand of ζ_G degrees is applied and if $|\zeta_G| > |M/n_\zeta|$ then the threshold system is operated and the peak values of angular acceleration and control surface incidence (at $t = 0+$) are given by

$$\mathrm{Peak}\ \ddot{\psi} = |M| + \frac{|n_\zeta\,\zeta_G| - |M|}{|1 - Kn_\zeta|}\ \ ^\circ/\mathrm{sec}^2 \rightarrow |M| \quad \mathrm{as}\ K \rightarrow \infty \qquad (79)$$

$$\mathrm{Peak}\ \beta_r = \left|\frac{M}{n_\zeta}\right| + \frac{|\zeta_G| - |M/n_\zeta|}{|1 - Kn_\zeta|}\ \ \mathrm{degrees} \rightarrow \left|\frac{M}{n_\zeta}\right| \mathrm{as}\ K \rightarrow \infty \qquad (80)$$

Table XIV shows some typical results for a step input control surface demand ζ_G of 10 degrees applied to the test missile.

<u>TABLE XIV</u>

Peak β_r (degrees)		β_r threshold level $\left\|\dfrac{M}{n_\zeta}\right\|$			
		∞	6°	3°	1.5°
Feedback gain $K\ \mathrm{sec}^2$	0	10	10	10	10
	0.04	10	6.57	4.0	2.7
	0.20	10	6.13	3.18	1.72
	∞	10	6.0	3.0	1.5

Figure 32 shows in graphical form a more extensive set of results. This figure also compares simulator results with the theoretical results and indicates a good measure of agreement. Figure 34 illustrates the responses of the test system with threshold feedback. It gives typical simulator records for the test missile and the test beam rider.

4.42 The integral of control surface lift

There is some indication from the simulator records (e.g. Figure 34) that when the peak responses are limited then the width of the peak increases so that the integral of the peak tends to remain constant.

This has been checked on the simulator by directly recording the integrals and the results of Table XV were obtained for a feedback gain of $K = 0.418$ sec^2.

TABLE XV

Threshold Level Angular Acceleration $^o/sec^2$	Control Surface Incidence Degrees	Integral of Angular Acceleration (Arbitrary Units)	Integral of Control Surface Incidence (Arbitrary Units)
150	0.75	8	8
300	1.5	10	10
600	3	13	13.5
900	4.5	14.5	15
1200	6	15	14.5
2000 or ∞	10 or ∞	17	16.5

These results indicate that the integrals are only approximately constant when the limiting is not severe.

4.43* The limiting action of threshold feedback of angular acceleration (Beam riding example)

The limiting action which takes place when a step of control surface demand is applied has been discussed. The same limiting action occurs when the input is a more complicated function as is shown by the following example for the case of the test beam rider.

Simulator responses for the test beam rider were obtained for various values of angular acceleration feedback gain (K) and threshold level (M). In each case there were no lateral acceleration limits and the initial disturbance was a 375 ft step displacement of the radar beam. The large step of 375 ft was chosen so that a pronounced limiting action was obtained. Samples of these responses are given in Figure 34. From such responses the peak values of angular acceleration and control surface incidence were obtained and these are as shown in Figure 35. The overall behaviour of the beam rider is very little affected over the range of K variations studied (provided the threshold level is not too low) but the peak values of angular acceleration and control surface incidence are more and more efficiently limited as K increases.

4.44* The stability of the test beam rider with threshold feed-back of angular acceleration and with lateral acceleration limits

The non-linear control equation for threshold feedback of angular acceleration is given by equation (78). The system has however, in general, a further major non-linearity in that the lateral acceleration of the missile is limited to a specified value. It is sufficient, for the purpose of an initial study of threshold feedback of angular accelera-tion, to assume that the lateral acceleration limitation is obtained simply by limiting the input control surface demand signal (ζ_G).

i.e. $|\zeta_G| < \zeta_L$ where ζ_L sets the lateral acceleration limit   (81)

This assumption can be made since the initial studies are confined to a missile operating at a fixed altitude, velocity etc. The use of feedback

types of limiting for both total lift and control surface lift is considered in a later section of the report.

The stability of such a system is of interest. This can only be determined in association with a particular form of guidance. The test beam rider is used as an example.

When the threshold level (M) is set at zero then in Section 4.33 it has been shown that the system becomes unstable when K is greater than approximately $0.04 \sec^2$. In the presence of a non-zero threshold level the gain (K) at which instability sets in is increased and as a consequence the use of higher gains leads to more effective limiting action. The onset of instability is also influenced by the presence of the lateral acceleration limits. In a very non-linear system of this type it is not possible to readily define the stability conditions but some idea can be obtained by exciting the system with a large initial displacement (say 300 ft) and plotting the values of feedback gain (K), threshold level (M) and lateral acceleration limits (L) at which instability starts. Such a plot is given in Figure 36 which shows rapidly increasing stability with increasing threshold level. An increase in the ratio of the exciting step displacement to the threshold level will give a decrease in the stability range but since the step displacement used in the test (300 ft) was very much greater than any likely beam motion that will occur in practice the results of Figure 35 should not be optimistic.

The general indications are that if the threshold level (M) is in excess of $100^\circ/\sec^2$ and the lateral acceleration limits (L) are of the order of 5 to 20g then feedback gains of the order of $K = 0.1 \sec^2$ may be used without rendering the system unstable.

4.45* The jitter response of the test beam rider with threshold feedback of angular acceleration and with lateral acceleration limits

A major disturbing influence on the performance of any beam riding system is the jitter component of the guidance information. The general properties of and a method of simulating this jitter, for a typical radar system (the 901 radar set) have been given elsewhere[2],[3].

The same method of simulation has been applied in this case under similar conditions to determine the effects of threshold feedback of angular acceleration on a system subjected to jitter signals. The test missile is operating at high altitude. If the range from radar set to target is assumed to be of the order of 30,000 yds then the jitter, as defined in Ref.2, is approximately scaled at 60 ft r.m.s. beam motion.

Figure 37 (a) gives a typical set of jitter results showing the responses of the test missile to a jittering beam when 10g lateral acceleration limits are in operation but there is no angular acceleration feedback.

Figure 37 (b) shows the same system but with threshold feedback of angular acceleration ($K = 0.042 \sec^2$, $M = 600^\circ/\sec^2$).

Comparison of these diagrams shows that the addition of the threshold feedback of angular acceleration produces a limiting action on the angular acceleration ($\ddot{\psi}$) and on the control surface incidence (β_r). In addition to this limiting action there is a filtering action on the high frequency components of the control surface motion but the consequent smoothing of the missile response is small as is shown by the lateral acceleration records and the lateral displacement of the missile is virtually unaffected by the feedback.

As a result of the loss of damping in the weathercock-like mode of motion when the angular acceleration feedback comes into operation (see Section 4.32) the lateral acceleration limiting is slightly less effective and acceleration overshoots of the order of a few percent beyond the desired limit occur.

A considerable number of such jitter runs have been made on the simulator under different conditions of the threshold feedback of angular acceleration. In all cases the lateral displacement of the missile was affected only to a negligible extent and in effect the only penalty paid for limiting the control surface lift in this way is a slight overshooting beyond the lateral acceleration limits which starts to appear when the control surface incidence is limited to less than two degrees.

4.46* The effect of threshold feedback of angular acceleration on the accuracy of attack of a beam rider

It is important that the influence of the proposed method of limiting the control surface lift on the accuracy of attack of a beam rider be determined.

A previous report[3] has studied the accuracy of attack of a beam rider of the type used as the test case here. The most stringent cases treated were attacks on accelerating targets at extreme range and in the presence of radar beam jitter and lateral acceleration limits. A number of the test runs of this previous report have been repeated with threshold feedback of angular acceleration in operation in order to determine the influence of this feedback on the miss distances.

A set of 150 records of missile displacement (h_p), lateral acceleration ($\ddot{h}$), control surface incidence (ξ_r) and angular acceleration ($\ddot{\psi}$) obtained for the following set of parameters:-

Lateral acceleration limit (L) = 10g. This acceleration limit was imposed by a simple diode limiter. The combined use of feedback limiting for both lateral acceleration and angular acceleration is considered in a later section.

Target accelerations = 0, $\pm 3g$, $\pm 6g$

Angular acceleration feedback gain (K) = 0.021, 0.042, 0.209 sec^2

Angular acceleration threshold (M) = 300, 600, ∞ $°/sec^2$

The general conclusion drawn from these records are that the angular acceleration feedbacks have negligible effect (for this range of parameters) on the mean miss distance and on the R.M.S. scatter about this mean. Apart from very occasional peaks of lateral acceleration which overshoot the 10g limits by about 20% during attacks on the 6g targets the acceleration remained reasonably bounded at $\pm 10g$.

Calculation of the acceleration lag of the complete system shows it to be independent of K and since the miss distance on an accelerating target is mainly influenced by the "effective acceleration lag" (defined as the acceleration lag plus the lag introduced by non-linear effects such as rectification of noise by the lateral acceleration limiting system) it is to be expected that K would, even in the presence of non-linearities, have little influence on the miss distance.

The peak values of the angular acceleration occurring in each of the test runs were obtained and are as plotted in Figure 38. These results are in good agreement with the theoretical peak values given by equation (79).

4.47 The effects of time lags

It is important that some estimate be formed of the quality of the angular accelerometer required for control surface lift limiting. Non-linearity in the instrument is not important as we are critically interested in only one value (that corresponding to the threshold level) but the effects of time lags in the instrument are very important as is shown by the following discussion.

Consider the closed loop system of Figure 39(a) which shows a missile, a control surface servo with time lag T_x seconds and an angular accelerometer feedback loop with time lag T_a seconds. For this system we have

$$
\left.
\begin{aligned}
\zeta &= \frac{\zeta_d - \zeta_f}{1 + p\, T_R} \\[2mm]
\zeta_f &= \frac{-K}{1 + p\, T_a}\, p^2 \psi \\[2mm]
p^2 \psi &= f_a(p)\, \zeta
\end{aligned}
\right\}
\qquad \text{cf. eqns. (16) and (2)}
\tag{82}
$$

which leads to the transfer function

$$
\frac{p^2 \psi}{\zeta_d} = \frac{(1 + p\, T_a)\, f_a(p)}{(1 + p\, T_a)(1 + p\, T_x) - K\, f_a(p)}
\tag{83}
$$

If the value of $\ddot{\psi}$ at time $t = 0+$ is defined as $\ddot{\psi}_0$ then the above expression enables $\ddot{\psi}_0$ to be determined in response to a step input of ζ_d for various combinations of K, T_a and T_x.

If $K = T_a = T_x = 0$ (i.e. direct missile response), $\ddot{\psi}_0 = n_\zeta\, \zeta_d$ and this value is also the peak value of $\ddot{\psi}$ in response to the step input of ζ_d.

If $K \neq 0$, $T_a = T_x = 0$, then $\ddot{\psi}_0 = \frac{n_\zeta}{1 - K n_\zeta} \cdot \zeta_d$ and the immediate and peak value of $\ddot{\psi}$ is attenuated by a factor $(1 - K n_\zeta)$ as described in Section 4.31.

If $K \neq 0$, $T_a \neq 0$, $T_x = 0$ then $\ddot{\psi}_0 = n_\zeta\, \zeta_d$, that is there is no attenuating action on the immediate and peak value of $\ddot{\psi}$.

From these cases it is clear that an instrument lag (T_a) in the absence of a control surface actuator lag (T_x) renders the limiting system ineffective for the immediate and peak response of $\ddot{\psi}$ to a step in ζ_d.

If however $T_x \neq 0$ then $\ddot{\psi}_0 = 0$ and $\ddot{\psi}_0$ is not the peak value of $\ddot{\psi}$ in response to the step input of ζ_d.

Figure 39(b) indicates the nature of the response in $\ddot{\psi}$ to the step in ζ_d.

An estimate of the combined effects of T_a and T_x may be obtained if the aerodynamic response of the missile is simplified to $p^2 \psi = n_\zeta\, \zeta$. This gives the high frequency response of the missile only.

The system is now such that

$$\zeta = (\zeta_d - \zeta_f)(1 - e^{-t/T_x}) \tag{84}$$

and

$$\zeta_f = -Kn_\zeta \zeta_d (1 - e^{-t/T_a}) \tag{85}$$

giving

$$\frac{\zeta}{\zeta_d} = \frac{(1 - e^{-t/T_x})}{1 - Kn_\zeta (1 - e^{-t/T_x})(1 - e^{-t/T_a})} \tag{86}$$

If ζ/ζ_d shows an appreciable overshoot beyond its final steady state value this will be indicative of an overshoot beyond the desired limit on the $\dot\psi$ response obtained when the full aerodynamics are considered.

Consider an expression of the form

$$y = \frac{1 - e^{-t/T_x}}{1 + \lambda (1 - e^{-\rho t/T_x})} \tag{87}$$

This will give an overshoot beyond its final steady state value $1/1+\lambda$ if

$$\frac{1 - e^{-t/T_x}}{1 + \lambda (1 - e^{-\rho t/T_x})} = \frac{1}{1 + \lambda}$$

is satisfied by a finite value of t.

This relationship may be written as

$$e^{(\rho-1)t/T_x} = \frac{\lambda}{1 + \lambda}$$

and this is satisfied by a finite value of t if $\rho < 1$ so that overshooting can only occur if $\rho < 1$.

Figure 40 gives y as a function of t/T_x for various values of λ and ρ.

The expression for ζ/ζ_d may be approximated by the expression y where $\rho = 1$ if $T_a < T_x$ and $\rho < 1$ if $T_a > T_x$ and $\lambda = -Kn_\zeta$. Appreciable overshooting will only occur therefore if $T_a > T_x$.

- 60 -

Thus as a first estimate of the effects of the time constants on the control surface lift limiting process it is to be expected that the system will in fact limit the control surface lift unless T_a is comparable with or greater than T_x. This has been verified on the simulator. With a 50 millisec lag in the control surface servo the limiting process functions correctly for angular accelerometer time lags up to 10 millisecs but for angular accelerometer time lags of 20 millisecs or more the limiting process becomes rapidly ineffective.

This time lag restriction is probably the severest restriction in the application of the limiting method. It may be necessary to deliberately lag the input commands if the instrument lag is comparable with the control surface servo lag.

4.5 Control surface lift limiting with non-neutrally stable body-wing combinations

We have now to study the operation of the control surface lift limiting system under non-ideal conditions, such that the basic assumption of a neutrally stable body-wing combination may not be valid, with a view to determining what departures from ideal conditions are tolerable.

As discussed in Section 2.7 departures from the neutral stability (or design) condition are most likely to arise from centre of gravity shifts due to fuel consumption and for the purpose of the present investigation we can regard centre of gravity shifts as resulting in changes in N_v with no corresponding changes in N_ζ. If the centre of gravity shift is H ft then the new value of N_v, denoted by N'_v is given by

$$N'_v = N_v - Y_v H \qquad \text{cf. eqn. (20)}$$

The effects of changes in H on the weathercock frequency and damping, the aerodynamic stiffness and the steady state control surface lifts have been discussed in Section 2.7.

We now proceed to study the proposed method of obtaining control surface lift limitation by threshold feedback of angular acceleration for a range of possible values of H, i.e. for a certain range of departure from the neutral stability condition.

There are really two cases to consider corresponding to major differences in the method of limiting the lateral acceleration of the missile. Case A considers the control surface lift limiting method as it is applied to a missile in which the control surface demand signals are limited to a constant level and as a consequence the limiting acceleration is a function of h and other aerodynamic parameters. Case B considers the control surface lift limiting method as it is applied to a missile in which the lateral acceleration is limited to a fixed value independently of the value of H and other aerodynamic parameters as for example by the use of the monitored diode system of limiting described earlier.

Case A

Consider the test missile with a nominal ±10g lateral acceleration limit. The control surface demand signal limit is determined from the design condition corresponding to H = 0. Table III shows the aerodynamic stiffness for H = 0 to be -1.21g/degree so that for ±10g limits the control surface demand signal has to be limited to ±8.25 degrees. (When H deviates from zero Table III indicates how the limiting acceleration varies with H, being 5.8g for H = +9 inches and 21g for H = -9 inches.).

The most stringent test we can apply to the control surface lift limiting system is to initiate a demand signal such that the control surface moves rapidly from one stop to the other (a step of 16.5 degrees). A convenient way of discussing the various conditions under which the stop-to-stop motion may be applied is to consider the control surface as moving in square wave fashion from stop-to-stop. Figure 41 shows the nature (as indicated by the simulator) of the control surface incidences developed in response to such a control surface motion. Each step in control surface angle produces an immediate change of 16.5 degrees in the control surface incidence and then, as the missile responds to the control surface lift developed the control surface incidence changes until the new steady state condition is obtained. If the body-wing combination is neutrally stable then $H = 0$, Case (b) of Figure 41, and the steady state control surface incidence is always zero so that the control surface incidences in response to the step motions consist of a series of "impulsive-like" responses – an instantaneous change of ± 16.5 degrees followed by a decay to zero (assuming the weathercock motion to be critically damped.). If $H \neq 0$, Cases (a) and (c) of Figure 41, then the steady state control surface incidences is not zero, being positive or negative, for a positive control surface angle, according to whether H is > 0 or < 0, i.e. according to whether the body-wing combination has positive or negative stability.

Let the value of the control surface incidence (β_r) at the instant immediately following a control surface angle step be β_r'. In Cases (a) and (b) of Figure 41 β_r' is the peak value of β_r. In Case (c) the peak value of β_r is either β_r' or the steady state value of β_r according to whichever is the greater of these two.

If the missile is originally flying straight and level when the control surface motion is commenced and the frequency of the square wave motion is high, so that the missile as a whole cannot respond to the control surface motion, then $\beta_r = \zeta$ and in particular the peak value of β_r = peak value of $\zeta = 8.25$ degrees.

Reference to the diagrams of Figure 41 shows that in general

$$|\beta_r'| = | \ |\text{Value } \beta_r \text{ has attained from past motion}| \pm 16.5^\circ | \qquad (88)$$

where the $+^{ve}$ sign is taken if $H < 0$ and the $-^{ve}$ sign if $H > 0$.

If the frequency of the square-wave motion of the control surface is slow enough the control surface incidence reaches a steady state after each step of the square wave. Under these conditions equation (88) becomes

$$|\beta_r'| = | \ |\text{Steady state value of } \beta_r \text{ corresponding to } 8.25^\circ \text{ control surface deflection}| \pm 16.5^\circ | \qquad (89)$$

where the $+^{ve}$ sign is taken if $H < 0$ and the $-^{ve}$ sign if $H > 0$.

We denote the magnitude of the control surface square wave motion by $\pm \zeta_L$ ($= \pm 8.25^\circ$ for the test missile.).

Figure 42 shows as functions of H the steady state values of control surface incidence for $\zeta = \pm \zeta_L$. (Curves (a) and (a₁)). Also shown in this figure are the peak values of control surface incidence incurred in moving from one of these steady states to the other (Curves (b) and (b₁)). The peak value curves are displaced by $2\zeta_L$ units from the corresponding steady state curves. For example if $H < 0$ and the missile is in the steady condition for which $\beta_r = A_a$ then when the control surface moves to

the other stop, a step of $2\zeta_L$ units, β_r increases to the value B_b and then tends to the steady state value A_{a1}. The same argument applies for $H = 0$ or $H > 0$, the points A_a B_b A_{a1} simply moving to new positions on their respective curves (a), (b) and (a_1). Considered as functions of time the motions A_a to B_b to A_{a1} generate the curves given in Figure 41 as Cases (a), (b) and (c) for $H < 0$, $= 0$, > 0.

All that can be achieved in the way of limiting the control surface incidence by the feedback process described earlier is a limitation of the "impulsive-like" part of the control surface incidence response. That is, all that can be achieved is a reduction in the spacing between curves (a) and (b) and between (a_1) and (b_1) or in words in attenuation of the "immediate response" of the control surface to input demand signals. Complete suppression of the "impulsive-like" part of the response would merge curve (a) with curve (b) and (a_1) with (b_1).

Since the curves are symmetrical about the H-axis the numerical values of the peak values of control surface incidence are given by the loci of the points B_b and A_{a1} assuming the control surface incidence to be positive and taking the peak value as being given by the locus of B_b if $B_b > A_{a1}$ or the locus of A_{a1} if $B_b < A_{a1}$. Interpreted in this way the the curves C_bD_b and D_bE_{a1} of Figure 42 define the peak values of control surface incidence as functions of H.

Limitation of the "impulsive-like" part of the response makes curve (b) tend to curve (a) (see Figure 41). For various degrees of limiting a family of curves CD exist.

Such a family of curves is shown in Figure 43(a). Depending on the degree of limiting the curves CD and DE or C_1D_1 and D_1E or C_2D_2 and D_2E define the peak value of the control surface incidence. This diagram enables that departure from neutral stability of the body-wing combination which renders the limiting system ineffective to be determined. Clearly if the limitation of the "impulsive-like" part of the β_r-response is only just adequate under the design conditions of neutral body-wing stability then it will be inadequate for values of $H < 0$ since the CD, C_1D_1, C_2D_2 ... family of curves give increasing peak values of β_r for H increasing negatively. If H increases positively then the limitation of β_r will be adequate until the point D_1, D_2, D_3 ... is reached. Thus if the system is to give adequate limitation over a range of H the limiting has to be more than adequate under the design conditions. Suppose the "impulsive-like" part of β_r to be reduced by feedback to P giving the peak locus C_pD_p, D_pE of Figure 43(b). If the tolerable peak β_r is P_1 $(P_1 > P)$ then the tolerable variations in H are given by

$$H_C < H < H_E \qquad (90)$$

where H_C and H_E are the values of H for which the ordinates on C_pD_p and D_pE are equal to P.

Figure 44 shows for the test missile the dimensional diagram corresponding to the general diagram of Figure 43(b). This diagram indicates that large positive values of H are tolerable. For example if the "impulsive-like" part of the β_r response is reduced from ±16.5 degrees to ±2 degrees (very tight limiting) then the positive H limit, namely H_E, is 6 inches. For a limitation to ±4 degrees, H_E is greater than 12 inches. A more severe limitation exists for the negative range of H. Table XVI indicates how, for a maximum tolerable β_r of ±10 degrees, the negative H limit, namely H_C, varies with the attenuation applied to the "impulsive-like" part of the β_r response.

TABLE XVI

H inches	0	-3	-6	-9	-12
Attenuation ratio of "impulsive-like" part of β_r response	0.61	0.52	0.39	0.21	0

Case B

Consider the test missile with a lateral acceleration limit of ±10g which functions independently of the value of H. We may for present purposes imagine this as being achieved by limits on the control surface demand signal which vary in the appropriate manner as H varies so that the limiting acceleration is always ±10g.

Table XVII indicates how, for the test missile, the limits on the control surface demand signal would have to vary with H in order to maintain an acceleration limit of ±10g for all values of H. Also shown are the steady state values of control surface incidence corresponding to 10g lateral acceleration.

TABLE XVII

H (inches)	+9	+6	+3	0	-3	-6	-9
Limits on control surface demand signal (Degrees)	14.3	12.2	10.0	8.25	6.67	5.20	3.92
Steady state control surface incidence corresponding to lateral acceleration of 10g (degrees)	4.5	2.89	1.38	0.825	-1.09	-2.12	-3.08

Assumption of the values given in the above table does not quite fit in with the lateral acceleration limiting system described earlier (in Section 3.5) as giving ±10g irrespective of the value of H since in this system the control surface demand signal is only so limited when the acceleration is at or near ±10g and may be greater than the value given in the above table when the acceleration is less than the limiting value. There are however further stops imposed on the control surface motion due to the limited control surface traverse. If we denote the maximum control surface traverse angle by θ and the limiting angle for 10g by ϕ then the peak value of control surface incidence is given by

$$|\text{Peak } \beta_r| = ||\text{Steady state value of } \beta_r \text{ corresponding to 10g}| \pm |\theta + \phi||$$

(91)

where the $+^{ve}$ sign is used if H < 0 and the $-^{ve}$ sign is used if H > 0.

Now θ is such that $\theta \geqslant \phi_{max}$ where ϕ_{max} is the largest value of ϕ to be expected, i.e. the ϕ corresponding to the largest positive value of H to be expected. Suppose we put $\theta = \phi_{max}$ then

$$|\text{Peak } \beta_r| = ||\text{Steady state value of } \beta_r \text{ corresponding to 10g}| \pm |\phi + \phi_{max}||$$

(92)

For the test missile we assume the largest positive value of H to be +6 inches, giving ϕ_{max} = 12.2 degrees from Table III. Equation (92) then gives, for example, using the data of Table XVII.

H = +3 inches | Peak β_r | = | 1.38 - (10 + 12.2) | = 20.82 degrees (93)

H = -3 inches | Peak β_r | = | 1.09 + (6.67 + 12.2) | = 19.96 degrees (94)

Figure 45 shows, for the test missile, how the peak control surface incidence, calculated as above, varies as a function of H for various degrees of limiting of the "impulsive-like" part of the β_r response (i.e. attenuation of the $\phi + \phi_{max}$ terms in equation (92).

Comparison of Figures 44 and 45 for the Cases (A) and (B) shows that in Case (B) the tolerable range in H is more evenly distributed about H = 0. The differences between the two cases is unlikely to be important as far as the control surface lift limiting is concerned since over the range -9" < H < +9" the difference between the two cases is small and it is considered unlikely that H will vary by more than this amount.

4.6   Conclusions on control surface lift limiting

For a missile of conventional design with a neutrally stable body-wing combination the results of Sections 4.1 to 4.4 indicate that the proposed method of limiting the peak control surface lifts can be successfully applied provided certain instrumentation difficulties can be overcome.

The major difficulty in applying the method would seem to lie in the development of an angular accelerometer whose time constant is less than the time constant of the control surface servo-mechanism. If a sufficiently fast angular accelerometer cannot be developed then for the method to apply the control surface servo time constant would have to be increased with possible complications in the overall control problem.

Neglecting the accelerometer time constant then the results indicate that, for the test missile assumed and for the associated test beam rider, the peak control surface lifts can be reduced to at least one-third of their present values without an appreciable loss in general performance of the missile.

The departure from the neutral stability condition which can be tolerated before the method breaks down has been evaluated in terms of the range of centre-of-gravity positions (i.e. static margins) over which limiting can be successfully applied. This range is such that it should adequately cover static margin changes due to fuel comsumption. For example static margin changes of ±9 inches are tolerable in the test missile.

In the Appendices to the report the fact that control surface limiting can be applied is used to indicate how a more efficient control surface system may be designed.

5   Combined Total Lift and Control Surface Lift Limiting

In Section 3 a method of limiting the total lift on the missile and in Section 4 a method of limiting the control surface lift have been discussed. There now remains the problem of combining the two limiting processes in the same missile.

5.1   Application to the test missile

We consider first the test missile with a total lift limit of ±10g imposed by the monitored diode system of limiting and observe the performance of the missile as the control surface lift is more and more stringently limited. This problem has been studied on the simulator in terms of the responses of the missile to step demands for control surface deflections. The conditions of the tests were such that the angular acceleration threshold level (M) was $300^\circ/sec^2$ and the feedback gain (K) was increased from zero to 0.418 sec^2. Two input demand signals for control surface deflections were used, the first a step demand for 10° deflection and the second a step demand for 20° deflection. With increasing feedback gain (K) the "impulsive-like" control surface incidence is therefore progressively reduced from 10° to 1.5° for the 10° input step and from 20° to 1.5° for the 20° input step.

Figure 46 shows the responses of the test missile when the input step demand is for 10°. As K is increased the peak control surface lift is limited as described in Section 4.4 and this is indicated on Figure 46 by the reduction in the peak values of the angular acceleration ($\ddot{\psi}$) and by the reduction in the y_ζ-kick on the lateral acceleration ($\ddot{h}$) records. However, as K increases, overshooting beyond the desired limits occurs to an increasing extent in both the total acceleration ($\ddot{h}$) and wing incidence (β_η) responses. This overshooting is to be expected since the rapid corrective action called for in preventing any overshooting beyond these limits is hindered by the now reduced control surface lift available. The severity of this overshooting is increased as the initial demand for control surface deflection is increased as is shown in Figure 47 which corresponds to Figure 46 except that the demands are for 20° rather than for 10° of control surface deflection. In effect, given the tolerable overshoot beyond the steady state limiting total lift, then the minimum control surface lift necessary is defined and it may not be more stringently limited without exceeding the tolerable total lift overshoot.

Figure 48, which is derived from Figures 46 and 47 shows the percentage overshoot in wing lift for several combinations of possible control surface demand signals and control surface lift limiting parameters If the feedback gain (K) is large enough, say K > 0.418, then the system is relatively insensitive to the value of K and Figure 48 shows that:-

(a)   If the threshold level is $300^\circ/sec^2$ then for a 10° step demand the percentage overshoot in wing lift is 7% while for a 20° step demand the percentage overshoot in wing lift is 18%.

(b)   If the threshold level is $600^\circ/sec^2$ then for a 20° step demand the percentage overshoot in wing lift is 9%.

A very rough guide as to the percentage overshoot is given by

Percentage overshoot =

$$= (250). \frac{\text{Magnitude of step demand for control surface deflection in degrees}}{\text{Threshold level in degrees/sec}^2}$$

(95)

5.2*   Application to the test beam rider

Figures 49 and 50 show the responses of interest during a recovery from a step displacement of the radar beam of the test beam rider with ±10g

acceleration limits and with various degrees of control surface lift
limiting.

The overshoots in lift slow up as in the previous section although
it will be noted that these are only large for very large beam displace-
ments of the order of 500 ft or more and this is a more stringent condi-
tion than any which is likely to occur in the flight of a beam riding
missile. Thus the proposed limiting methods should be directly applic-
able to the test beam rider for lateral acceleration limits of the order
of ±10g and control surface incidence limits of the order of 15 degrees.

6   General Conclusions

Some detailed conclusions have already been given on total lift
limiting in Section 3.7 and on control surface lift limiting in Section
4.6.

The broad conclusions are that for a missile whose design conforms
to the design criterion given in the Report of the R.A.E. Project Group
on Medium Range Anti-Aircraft Guided Missiles[1] then:-

(a)   The output of a lateral accelerometer may be fedback to the
control surface system and used in various ways to limit the total lift
on the missile. A method of limiting in which the clipping level of
clipping diodes on the input guidance signals are monitored by feedback
from an accelerometer, suitably situated ahead of the centre of gravity
of the missile, has been shown to have advantages over all the other
systems considered.

(b)   Curtailment of the peak control surface lifts is possible
without a marked deterioration in missile performance. This may be
achieved by suitable feedback from an angular accelerometer. The proposed
method may only be applied providing that any departure of the body-wing
combination from neutral stability is small. This condition will in
general be satisfied. The major difficulty foreseen at the moment lies
in producing an angular accelerometer whose time constant is less than
the time constant of the control surface servo-mechanism with which it
is to be associated.

The Appendices to the report indicate how limitation of the peak
control surface lift may be used to advantage in the design of the
control surface system.

(c)   Total lift and control surface lift limiting of the above
types can be simultaneously applied to a missile although the relative
degrees of limiting attainable are inter-dependent.

REFERENCES

No.	Author	Title, etc.
1		Report of R.A.E. Project Group on Medium Range Anti-Aircraft Guided Missiles. Part V. RAE Report GW 6, December, 1949
2	J.J. Gait and D.W. Allen	A Simulator Study of the Effects of Radar Beam Jitter on the Performance of Beam Riding Missiles. RAE Tech Note GW 44, August, 1949
3	J.J. Gait and D.W. Allen	A Simulator Assessment of the Minimum Miss Distance Attainable with a Beam Riding Missile in the Presence of Radar Beam Jitter. RAE Tech Note GW 72, May, 1950

Attached:

    Appendix I and II
    Drgs. Nos. GW/P/4282 to 4332
    Detachable Abstract Cards

Advance Distribution:

    M.O.S. Headquarters

        Chief Scientist
        CGWL
        PDGW   90
        DMARD (RAF)
        GWB (Dr. R.C. Knight)
        TPA3/TIB   90

    R.A.E.

        Director
        DD(E)
        DD(A)
        RPD   2
        Aero   4
        Structures
        IAP Dept
        GWTW   2
        NAE Library
        Library

APPENDIX I

Calculation of the Acceleration Response of a Missile when the Control Surface Incidence is Limited

by

Lt. Cdr.(E). D.C. Satow, R.N., A.M.I.Mech.E.

1   If the control surface incidence of a missile is limited, by a method of the type described in Section 4.4 or otherwise, then its response in lateral acceleration to input demands is a non-linear function of these input demands. This appendix gives a method of calculating the non-linear response. The method is used in Appendix II where the acceleration responses of various missiles incorporating control surface incidence limiting are compared.

2   It is assumed that the basic aerodynamic equations are as in Section 2.1 equations (1) and Section 2.4 equation (10), namely

$$\ddot{h}_r = y_v \cdot v + y_r \cdot r + y_\zeta \cdot \zeta$$

$$\dot{r} = n_v \cdot v + n_r \cdot r + n_\zeta \cdot \zeta$$

$$\ddot{h}_p = \dot{v} + Ur$$

and

$$\hat{\beta}_r = \zeta - {}^v/_u \left(1 - {}^{\partial \varepsilon}/_{\partial \alpha}\right)$$

(i)

For the purpose of modifying the weathercock frequency and damping, feedback to the control surface (ζ) of lateral acceleration ($\ddot{h}_p$) and rate of yaw (r) are assumed. The control equation is thus that given in Section 2.9 equation (26), namely

$$\zeta = \zeta_G + br + f\ddot{h}_p$$

(ii)

where b and f are constants.

The following relationships are derived from equations (i) and (ii)

$$\frac{\ddot{h}_p}{\beta_r} = y_\zeta \cdot \frac{D^2 + \dfrac{x_{\zeta r}}{y_\zeta} D + \dfrac{U x_{v\zeta}}{y_\zeta}}{D^2 + D\left[-y_v - n_r - \left(1 - \dfrac{\partial \varepsilon}{\partial \alpha}\right)\dfrac{y_\zeta}{U}\right] + \left[U n_v + x_{rv} - \left(1 - \dfrac{\partial \varepsilon}{\partial \alpha}\right)\left(\dfrac{x_{\zeta r}}{U} - n_\zeta\right)\right]}$$

(iii)

$$\frac{\zeta_G}{\beta_r} = \frac{(1 - fy_\zeta)\, D^2 + D\,(-y_v - n_r - bn_\zeta - fx_{\zeta r}) + (Un_v + x_{rv} - bx_{v\zeta} - fUx_{v\zeta})}{D^2 + D\left[-y_v - n_r - \left(1 - \frac{\partial \varepsilon}{\partial \alpha}\right)\frac{y_\zeta}{U}\right] + \left[Un_v + x_{rv} - \left(1 - \frac{\partial \varepsilon}{\partial \alpha}\right)\left(\frac{x_{\zeta r}}{U} - n_\zeta\right)\right]} \quad \text{(iv)}$$

$$\frac{\ddot{h}_E}{\zeta_G} = y_\zeta \cdot \frac{D^2 + \dfrac{x_{\zeta r}}{y_\zeta} D + \dfrac{Ux_{v\zeta}}{y_\zeta}}{(1 - fy_\zeta)\, D^2 + D\,(-y_v - n_r - bn_\zeta - fx_{\zeta r}) + (Un_v + x_{rv} - bx_{v\zeta} - fUx_{v\zeta})} \quad \text{(v)}$$

If $\quad D^2\,(1 - fy_\zeta) + D\,(-y_v - n_r - bn_\zeta - fx_{\zeta r}) + (Un_v + x_{rv} - bx_{v\zeta} - fUx_{v\zeta})$

is written as

$$(1 - fy_\zeta)(D^2 + 2\,u_m \omega_m\, D + \omega_m{}^2)$$

then

$\omega_m/2\pi$ is the modified weathercock frequency

and u_m is the modified weathercock damping ratio.

For the various missiles to be considered in Appendix II it is assumed that the feedback constants b and f are chosen to give

$$u_m = 1 \quad \text{and} \quad \omega_m = 10 \text{ rads/sec.} \quad \text{(vi)}$$

If

$$D^2 + D\left[-y_v - n_r - \left(1 - \frac{\partial \varepsilon}{\partial \alpha}\right)\frac{y_\zeta}{U}\right] + \left[Un_v + x_{rv} - \left(1 - \frac{\partial \varepsilon}{\partial \alpha}\right)\left(\frac{x_{\zeta r}}{U} - n_\zeta\right)\right]$$

is written as

$$D^2 + 2\,\delta\gamma D + \gamma^2$$

then

$$\gamma^2 = Un_v + x_{rv} - \left(1 - \frac{\partial \varepsilon}{\partial \alpha}\right)\left(\frac{x_{\zeta r}}{U} - n_\zeta\right)$$

- 70 -

and

$$2\,\delta\gamma = -\,y_v - n_r - \left(1 - \frac{\partial\varepsilon}{\partial a}\right)\frac{y_\zeta}{U}$$

For the various missiles to be considered in Appendix II, δ is approximately equal to unity and

$$\delta = 1 \tag{vii}$$

is assumed in all the following work.

If in addition to these reformulations of the quadratic expressions we put

$$a_1 = {}^x\zeta r/y_\zeta \Bigg\}$$

and $$b_1 = {}^Ux_v\zeta/y_\zeta \Bigg\} \tag{viii}$$

then equations (iii) to (viii) give

$$\frac{\ddot{h}_p}{\beta_r} = y_\zeta \cdot \frac{D^2 + a_1\,D + b_1}{(D + \gamma)^2} \tag{ix}$$

$$\frac{\zeta_G}{\beta_r} = (1 - fy_\zeta) \cdot \frac{(D + \omega_m)^2}{(D + \gamma)^2} \tag{x}$$

$$\frac{\ddot{h}_p}{\zeta_G} = y_\zeta \cdot \frac{D^2 + a_1\,D + b_1}{(D + \omega_m)^2} \tag{xi}$$

Equations (ix) to (xi) form the basis of the calculation of the missile response.

3   We consider the response of the missile to a step input demand ζ_G sufficiently large to cause an initial limitation of the control surface incidence. The complete acceleration response consists of two parts: the first part is the response to a constant control surface incidence, i.e. the value to which the control surface incidence is limited; the second part is the response to the constant control surface demand ζ_G. The constant control surface incidence may be regarded mathematically as the results of an input demand ζ_G' which varies with time in such a way as that the control surface incidence is constant. The change over between the two parts occurs at the time at which this input demand signal reaches the value ζ_G.

(a)   The first part of the acceleration response.

From equation (ix) we have

$$\frac{\ddot{h}_r}{\beta_r} = y_\zeta \cdot \frac{D^2 + a_1 D + b_1}{(D+\gamma)^2}$$

The Laplace Transform of this relationship gives

$$(p+\gamma)^2 \ddot{h}^* = y_\zeta (p^2 + a_1 p + b_1) \beta_r^*$$
$$+ \left[\ddot{h}_{r_0} + \ddot{h}_{r_0} (p+2\gamma) \right]$$
$$- y_\zeta [\dot{\beta}_{ro} + \beta_{ro} (p+a_1)]$$

where the suffixes o indicate the initial values and the stars denote the Laplace transform of the quantity so labelled.

Let the value to which the control surface incidence β_r is limited be P; as this is applied as a step input.

$$\beta_r^* = P/p$$
$$\beta_{ro} = P$$
$$\dot{\beta}_{ro} = 0$$
$$\ddot{h}_{p_0} = y_\zeta P$$
$$\dddot{h}_{p_0} = 0$$

so that

$$\ddot{h}_p^* = y_\zeta \frac{P}{p} \cdot \frac{p^2 + 2\gamma p + b_1}{(p+\gamma)^2}$$

The inverse transformation of this gives the solution

$$\ddot{h}_p = y_\zeta P \frac{b_1}{\gamma^2} \left[1 - \left(1 - \frac{\gamma^2}{b_1}\right)(1+\gamma t) e^{-\gamma t} \right] \qquad \text{(xii)}$$

which is the first part of the acceleration response.

(b)   The instant of change over from the first to the second part of response.

The demand signal ζ' required to give the constant control surface incidence P is less than the actual demand signal ζ_G.

From equation (x) we have writing ζ_G' for ζ_G

$$\frac{\zeta_G'}{P} = (1 - fy_\zeta)\frac{(D + \omega_m)^2}{(D + \gamma)^2}$$

The solution of this for a step input P of control surface incidence is similar to (xii); thus

$$\zeta_G' = (1 - fy_\zeta)\, P\, \frac{\omega_m^2}{\gamma^2}\left[1 - \left(1 - \frac{\gamma^2}{\omega_m^2}\right)(1 + \omega_m\, t)\, e^{-\gamma t}\right]$$

The change over between the two parts of the response occurs at time t_1 when $\zeta_G' = \zeta_G$ thus t_1 is given by

$$\zeta_G = (1 - fy_\zeta)\, P\, \frac{\omega_m^2}{\gamma^2}\left[1 - \left(1 - \frac{\gamma^2}{\omega_m^2}\right)(1 - \gamma t_1)\, e^{-\gamma t_1}\right]$$

or

$$(1 + \gamma t_1)\, e^{-\gamma t_1} = \left[1 - \frac{\zeta_G}{P}\cdot\frac{\gamma^2}{\omega_m^2}\cdot\frac{1}{1 - fy_\zeta}\right]\bigg/\left(1 - \frac{\gamma^2}{\omega_m^2}\right) \qquad \text{(xiii)}$$

(c)   The second part of the acceleration response.

From equation (xi) we have

$$\frac{\ddot{h}_p}{\zeta_G} = \frac{y_\zeta}{1 - fy_\zeta}\ \frac{D^2 + a_1\, D + b_1}{(D + \omega_m)^2}$$

The Laplace Transform of this relationship gives

$$(p + \omega_m)^2\, \ddot{h}_p^* = \frac{y_\zeta}{1 - fy_\zeta}\cdot(p^2 + a_1\, p + b)\, \zeta_G^*$$

$$+ [\dddot{h}_{p1} + \ddot{h}_{p1}(p + 2\,\omega_m)]$$

$$- \frac{y_{\zeta 1}}{1 - fy_\zeta}\,[\zeta_{G1}' + \zeta_{G1}(p + a_1)]$$

where the suffixes 1 indicate the boundary values at the commencement of the second part of the response.

We have for a constant control surface demand ζ_G

$$\zeta_G{}^* = \zeta_G/_p$$

$$\zeta_{G1} = \zeta_G$$

$$\zeta'_{G1} = 0$$

The boundary values $\ddot{h}_{p1}$ and $\dddot{h}_{p1}$ are obtained by substituting the value of t_1 given by (xiii) into (xii) and its derivative: thus

$$\ddot{h}_{p1} = y_\zeta \, P \, \frac{b_1}{\gamma^2} \left[1 - \left(1 - \frac{\gamma^2}{b_1} \right) (1 + \gamma t_1) \, e^{-\gamma t_1} \right] \qquad \text{(xiv)}$$

$$\dddot{h}_{p1} = y_\zeta \, P \, \frac{b_1}{\gamma^2} \left[\left(1 - \frac{\gamma^2}{b_1} \right) \gamma^2 \, t_1 \, e^{-\gamma t_1} \right] \qquad \text{(xv)}$$

Hence

$$\ddot{h}_p{}^* = \ddot{h}_{p1} \frac{p^2 + 2\,\omega_m\,p + (b_1 \, y_\zeta \, \zeta_G)/(1 - fy_\zeta)\,\ddot{h}_{p1}}{p\,(p + \omega_m)^2} + \frac{\dddot{h}_{p1}}{(p + \omega_m)^2}$$

which on inverse transformation gives

$$\ddot{h}_p = \frac{b_1 \, y_\zeta \, \zeta_G}{(1 - fy_\zeta)\,\omega_m^2} \left[1 - \left\{ 1 - \frac{(1 - fy_\zeta)\,\omega_m^2\,\ddot{h}_{p1}}{b_1 \, y_\zeta \, \zeta_G} \right\} (1 + \omega_m \tau) e^{-\omega_m \tau} \right] + \dddot{h}_{p1} \, \tau \, e^{-\omega_m \tau} \qquad \text{(xvi)}$$

where $\tau = t + t_1$.

If the steady state $\ddot{h}_p$ corresponding to the steady state ζ_G is denoted by $\ddot{h}_G$ then

$$\ddot{h}_G = \frac{b_1 \, y_\zeta \, \zeta_G}{(1 - fy_\zeta)\,\omega_m^2} \qquad \text{(xvii)}$$

and (xvi) may be written as

- 74 -

$$\frac{\ddot{h}_p}{h_G} = 1 - \left(1 - \frac{\ddot{h}_{p1}}{\ddot{h}_G}\right) (1 + \omega_m \tau) \ e^{-\omega_m \tau} + \frac{\dddot{h}_{p1}}{\omega_m \ h_G} \omega_m \tau \ e^{-\omega_m \tau} \qquad \text{(xviii)}$$

and this is the second part of the response.

4   The response of the missile in acceleration to a step input demand ζ_G sufficiently large to cause an initial limitation of the control surface incidence is thus given by equations (xii), (xiii) (xiv), (xv) and (xvi).   These equations are used in Appendix II to obtain such acceleration responses.

———

APPENDIX II

A New Design Criterion for Control Surface Size

by

Lt. Cdr.(E). D.G. Satow, R.N., A.M.I.Mech.E.

———

1   It has been demonstrated in this report that the control surface incidence or lift may be limited quite severely without introducing any significant deterioration in the lateral acceleration response of the missile.. The control surface size of the "test missile" used in the report, in common with many actual missile designs, has been based on a design criterion given in the Report of the R.A.E. Project Group on Medium Range Anti-Aircraft Guided Missiles[1]. The fact that control surface lift limiting can be applied without deterioration in the response of the missile suggests that it may be possible to reduce the control surface size below that derived from the above criterion. Although this appendix is only a superficial examination of this issue it indicates that a reduction in control surface size is possible provided some method of control surface incidence or lift limiting is used.

2   A number of different missile designs are considered, these having different sizes of control surfaces and varying degrees of control surface lift limiting. For each design the acceleration response to a step input demand has been computed, using the method developed in Appendix I, and the results compared.

We consider as a "datum design" the test missile of the main report i.e.a missile designed on the basis of the R.A.E. Project Group design criterion. Briefly this criterion is such that the body-wing combination is neutrally stable, Y_r is decided by the maximum lateral acceleration required and the maximum wing incidence allowable, N_v is decided by the desired weathercock frequency and N_ζ is determined from N_v.

One possible approach to a new design is to use the "datum design" as a basis but then reduce the control surface size (i.e. reduce Y_ζ and N_ζ). The reduction in N_ζ results in a reduction in N_v. The decrease in weathercock frequency associated with this reduction in N_v may be offset by using lateral acceleration feedback to restore the weathercock frequency to its original value. As the control surface size is decreased in this way the peak control surface incidence or lift, for a given step demand for lateral acceleration say, increases but if this incidence or lift is limited (by the method of the main report or otherwise) then the peak control surface incidence or lift may be kept within desired limits.

Consider now the following alternative designs for a 15g missile.

Missile Design No.1.   (The datum design)

This is the test missile of the main report. For 15g lateral acceleration the steady state control surface deflection is 12.5 degrees. In response to a step demand for 15g the peak control surface incidence is also 12.5 degrees.

Missile Design No.2

In this missile the control surface size is half of that for Missile Design No.1. i.e. Y_ζ and N_ζ are halved. Y_r is unaltered so that the same wing incidence gives the same lateral acceleration but N_v is halved since the body-wing combination remains neutrally stable. The weathercock frequency is restored to that for Missile Design No.1 by lateral acceleration feedback.

For 15g lateral acceleration the steady state control surface deflection is 18.7 degrees and the peak control surface incidence in response to a step demand for 15g is 21.3 degrees. The peak incidence is greater than the steady state deflection since the lateral acceleration feedback has no effect on the initial step of control surface motion.

Three cases are considered: the first with no control surface incidence limitation; the second with the control surface incidence limited to the peak value occurring for Missile Design No.1 i.e. 12.5 degrees; the third with the control surface incidence limited to 6 degrees.

Missile Design No.3

In this missile the control surface size is a quarter of that for Missile Design No.1. (i.e. Y_ζ, N_ζ and consequently N_v are reduced in the ratio 4:1 and then the weathercock frequency is restored to that for Missile Design No.1 by lateral acceleration feedback).

For 15g lateral acceleration the steady state control surface deflection is 32.9 degrees and the peak control surface incidence in response to a step demand for 15g is 39.5 degrees.

The case considered here is that in which the peak control surface incidence is limited to the peak value occurring for Missile Design No.1 i.e. 12.5 degrees.

Table A gives the aerodynamic derivatives and certain other data for the above missiles.

/TABLE A

TABLE A

			Missile Design Number		
			I	II	III
Control surface size relative to Design I			1	$\frac{1}{2}$	$\frac{1}{4}$
Body-wing stability			Neutral	Neutral	Neutral
U		ft sec^{-1}	1500	1500	1500
y_ζ		ft sec^{-2}	800	400	200
n_ζ		sec^{-2}	-200	-100	-50
y_v		ft sec^{-1}	-1	-1	-1
n_v		sec^{-1}	$1/15$	$1/30$	$1/60$
y_r		ft sec^{-1}	2.4	1.4	1.0
n_r		sec^{-1}	-1	-0.6	-0.45
Weathercock angular frequency (rad/sec) when modified by acceleration feedback			10	10	10
Aerodynamic stiffness (g/degree) when modified by acceleration feedback			1.2	0.8	0.456
Steady state control surface deflection to give 15g when modified by acceleration feedback (degrees)			12.5	18.75	32.9
Maximum unlimited control surface incidence corresponding to 15g demand (degrees)			12.5	21.25	39.5
Key to acceleration in response to a 15g acceleration demand (Fig.51)					
Control surface incidence unlimited			Curve (a)	Curve (b)	
" " " " to 12.5°			Curve (a)	Curve (c)	Curve (e)
" " " " " 6°				Curve (d)	

Figure 51 shows the acceleration in response to demands for 15g lateral acceleration for the various missiles. There is little change in the acceleration response if the control surface size is reduced to a half or a quarter of that given by the datum design and the peak control surface incidence is limited to the maximum value occurring in the datum design. (See Curves (a), (c) and (e)). That is the new designs give comparable missile responses but with smaller control surfaces and hence smaller peak control surface loads.

The limit to what can be achieved by this new design approach would seem to be set by considerations of the magnitude of the static margin. As the control surfaces are reduced in size so also is the static margin. For example in Missile Design No.3 the static margin is only 5 inches (i.e. 6.7% of the control surface moment arm). As a consequence of the small static margin variations in the centre of gravity and centre of pressure positions during flight will be of increasing importance.

It is emphasized that this appendix is only intended to indicate the possibilities of improving on the "datum design". A very much fuller study of this problem would be necessary before definite conclusions could be drawn.

CHARACTERISTIC EXPRESSION FOR WEATHERCOCK MOTION :-

$$Q_m = (1 - y_3 f)(p^2 + 2u_m\omega_m p + \omega_m^2)$$
$$= (1 - y_3 f)(p + \alpha_{1,3})(p + \alpha_{2,4})\{f u_m > 1$$

UNSTABLE ZONE
α_4 NEGATIVE FOR $f > 0.00125$.

UNSTABLE ZONE
α_2 NEGATIVE
FOR $f < -0.0005$!

ACCELERATION FEEDBACK GAIN f. RAD ft^{-1} sec^2

u_m AND $\alpha_1, \alpha_2, \alpha_3, \alpha_4$.

FIG. I. ROOTS OF THE CHARACTERISTIC EXPRESSION FOR THE TEST MISSILE WITH DIRECT ACCELERATION FEEDBACK.

CHARACTERISTIC EXPRESSION FOR
WEATHERCOCK MOTION :-

$$Q_m = (1 - y_s f)(p^2 + 2u_m \omega_m p + \omega_m^2)$$

ACCELERATION FEEDBACK GAIN f. RAD. ft.$^{-1}$ sec.^{2}

FIG. 2. ROOTS OF THE CHARACTERISTIC EXPRESSION FOR THE
HYPOTHETICAL TEST MISSILE WITH DIRECT ACCELERATION
FEEDBACK. ($y_s = 0$; $\eta_s \neq 0$.)
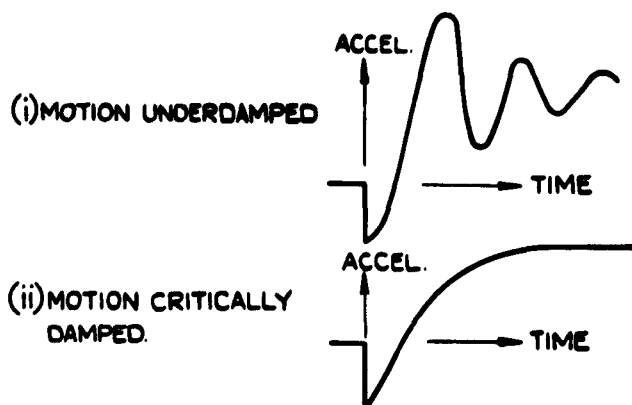
(a) THE FORM OF THE ACCELERATION RESPONSE OF THE MISSILE
TO A STEP MOTION OF THE CONTROL SURFACE SHOWING THE
REVERSE KICK.
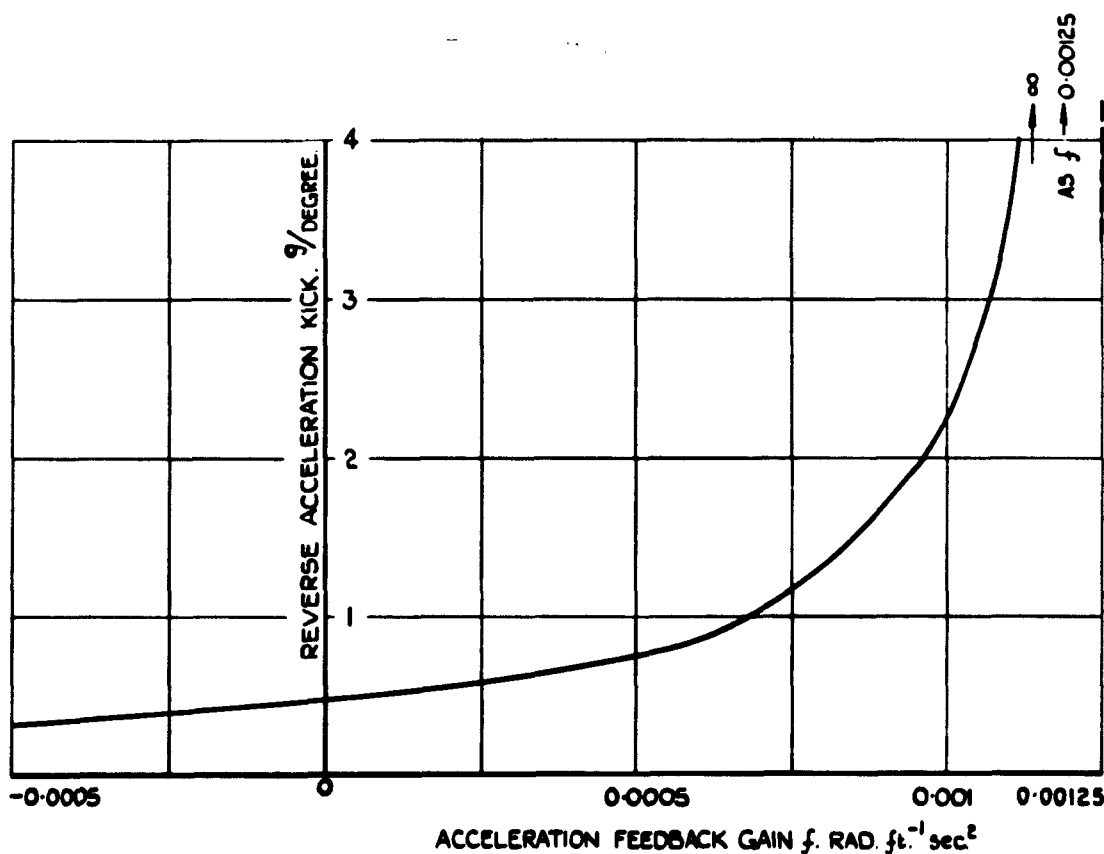
(b) THE REVERSE ACCELERATION KICK AS A FUNCTION OF THE
ACCELERATION FEEDBACK GAIN.

FIG. 3 (a&b) THE REVERSE ACCELERATION KICK
IN THE ACCELERATION RESPONSE OF THE MISSILE.

STEADY STATE
ACCELERATION PER.
UNIT CONTROL SURFACE
DEMAND SIGNAL.

$9/$DEGREE

————— THEORETICAL.
⊙ SIMULATOR RESULTS.

UNSTABLE
ZONE

-0·00025   0·0005   0·001   0·00125

ACCELERATION FEEDBACK GAIN F. RAD. ft.⁻¹ sec²
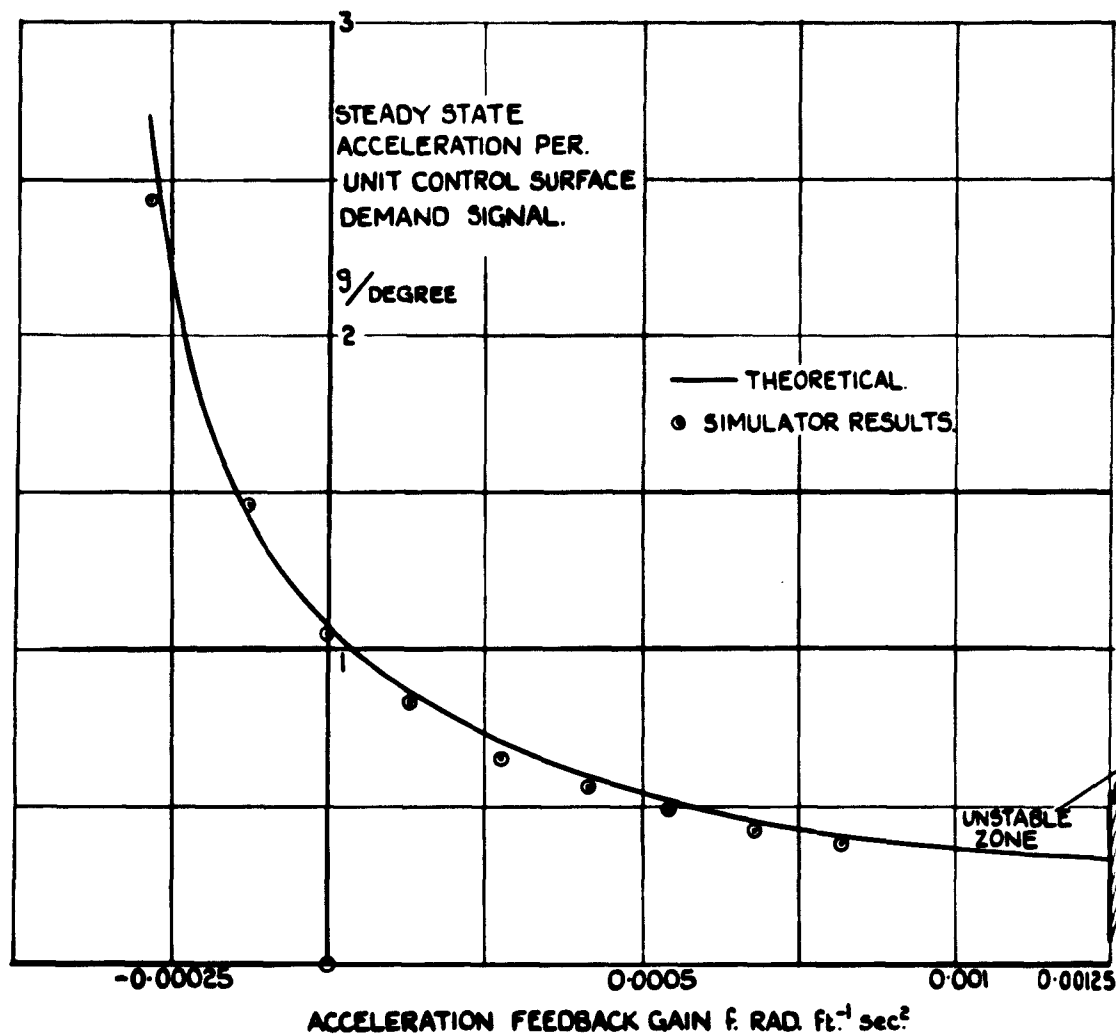
FIG. 4. THE STEADY STATE ACCELERATION
OF THE TEST MISSILE AS A FUNCTION
OF THE ACCELERATION FEEDBACK GAIN.
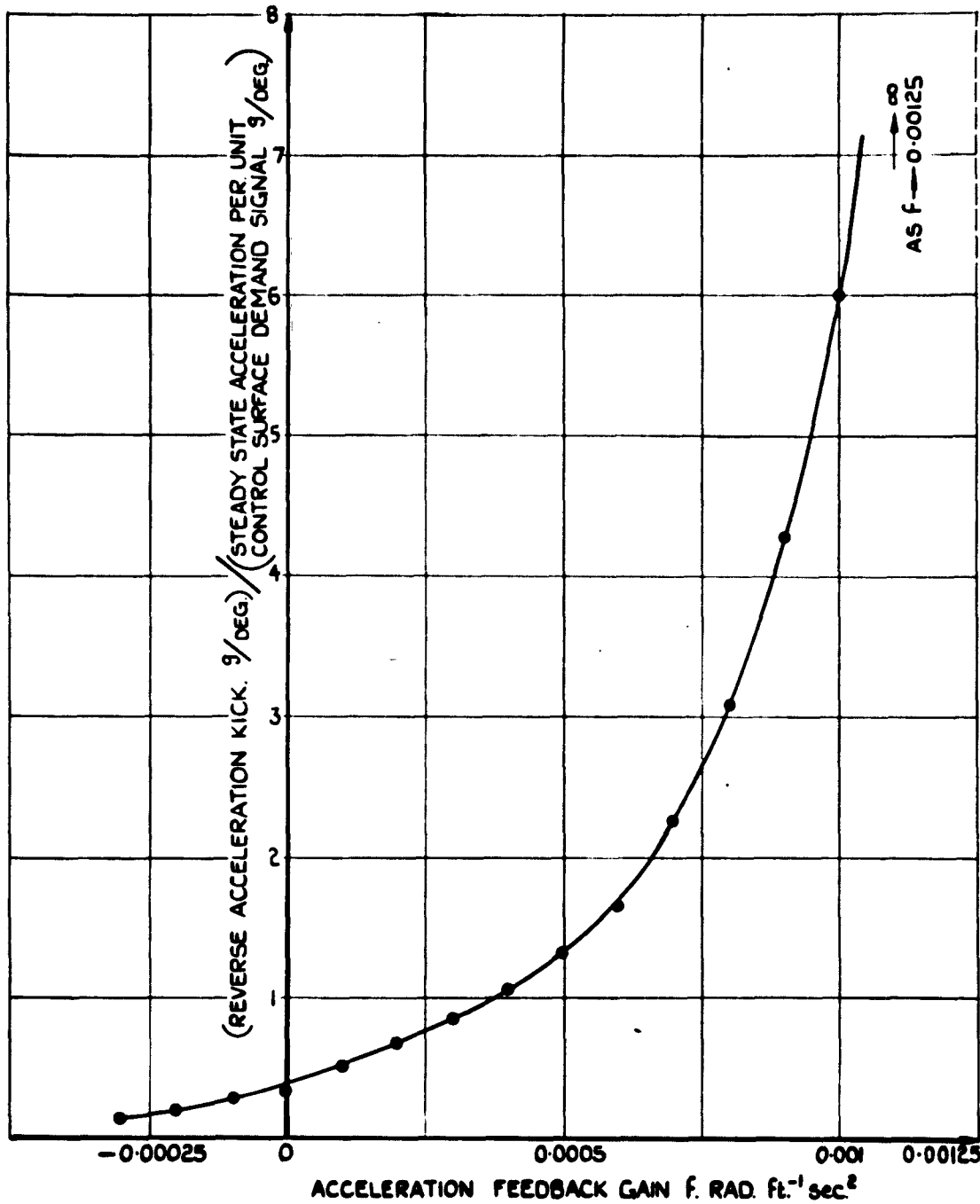
FIG. 5. RATIO OF REVERSE ACCELERATION
KICK TO STEADY STATE ACCELERATION.

ACCELEROMETER OUTPUT.

d = 21"

TIME

d = 33"

d = 45"

[CRITICAL DISTANCE FOR TEST MISSILE = $- \, {}^{ys}/_{n_s} = 48"$]

d = 57"

d = 63"
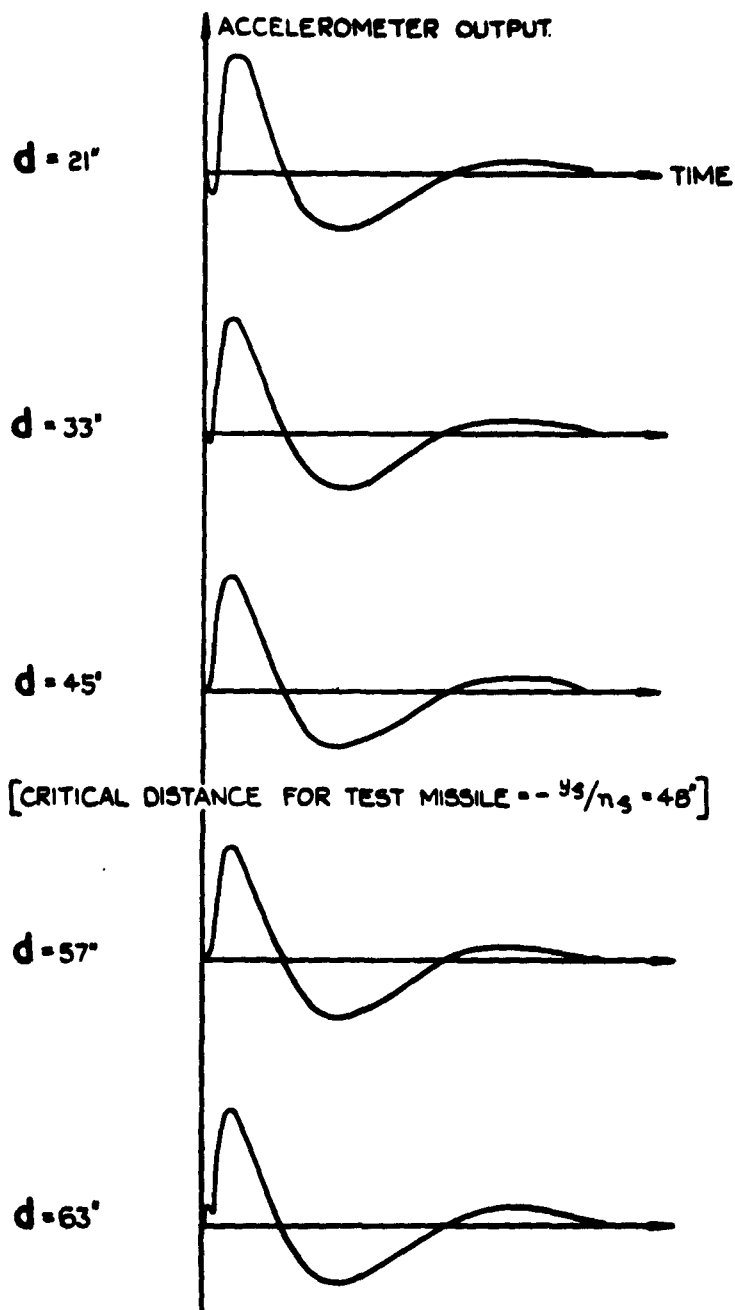
(THESE RESPONSES RELATE TO THE MANOEUVRES OF THE
TEST BEAM RIDER WHEN SUBJECTED TO A STEP DISPLACEMENT
OF THE RADAR BEAM.)

FIG.6. COMPARATIVE OUTPUTS FROM ACCELEROMETERS SITUATED DIFFERENT DISTANCES (d) AHEAD OF THE CENTRE OF GRAVITY OF THE TEST MISSILE.

CHARACTERISTIC EXPRESSIONS FOR

WEATHERCOCK MOTIONS:-

CASE(a) ACCELEROMETER AHEAD OF C OF G BY

$-y_o/n_o = 4$ ft.

$$Q_D = \lambda \left(p^2 + 2u_o \omega_D p + \omega_D^2 \right)$$

CASE(b) ACCELEROMETER AT C OF G BUT

$y_s = 0;\ n_3 \neq 0.$

$$Q_m = (1 - y_s f)(p^2 + 2u_m \omega_m p + \omega_m^2) \quad \text{[SEE FIG.2]}$$

u_m AND u_D

ω_m

ω_D

ω_m AND ω_D

u_m AND u_D

4·40

3·30

2·20

1·0

0·005   0·01   0·015   0·02

ACCELERATION FEEDBACK GAIN f RAD FT^{-1} SEC^2
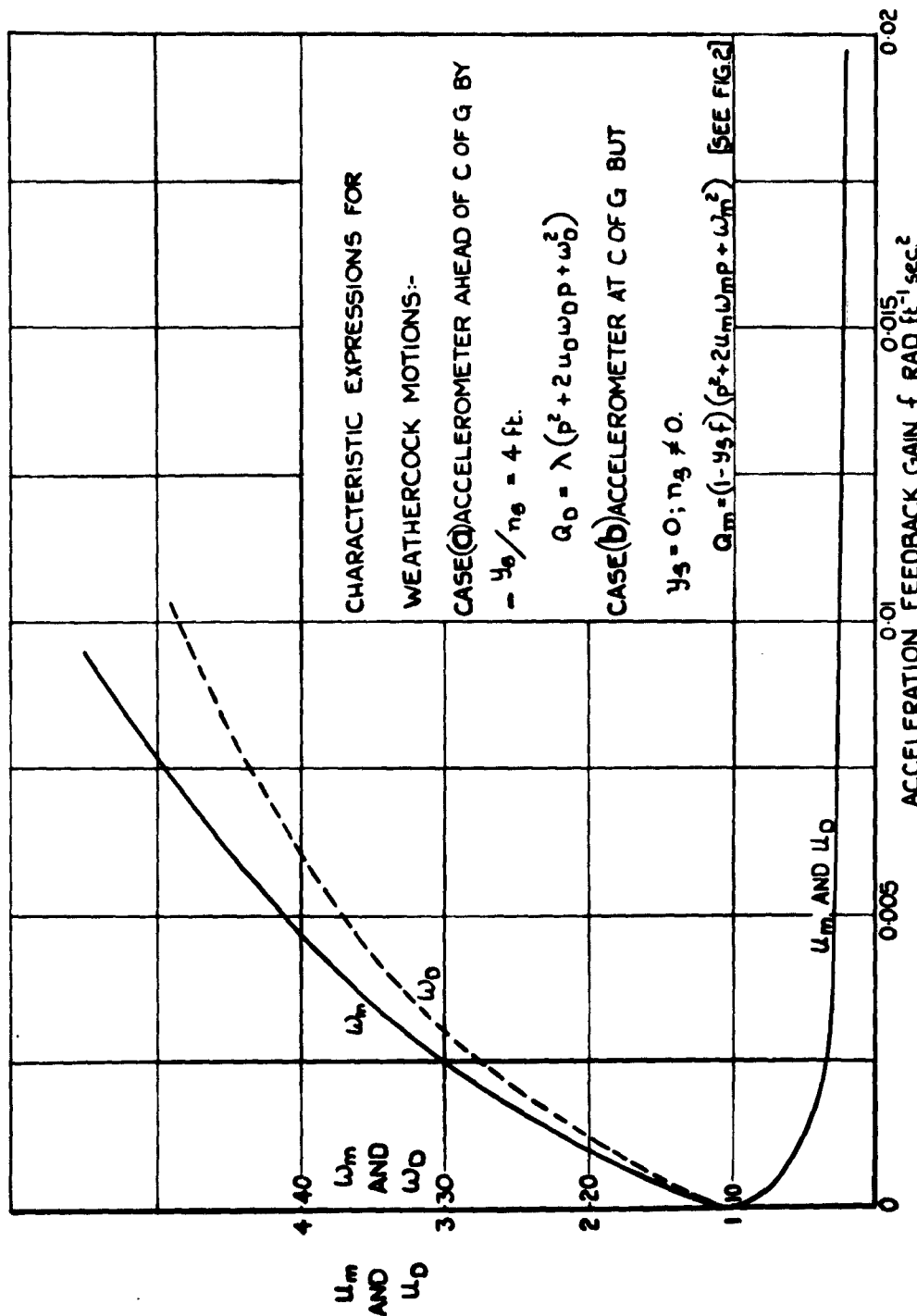
FIG. 7. ROOTS OF THE CHARACTERISTIC EXPRESSION FOR THE TEST MISSILE WITH DIRECT ACCELERATION FEEDBACK FROM A DISPLACED ACCELEROMETER.

FIG.8.

/4289
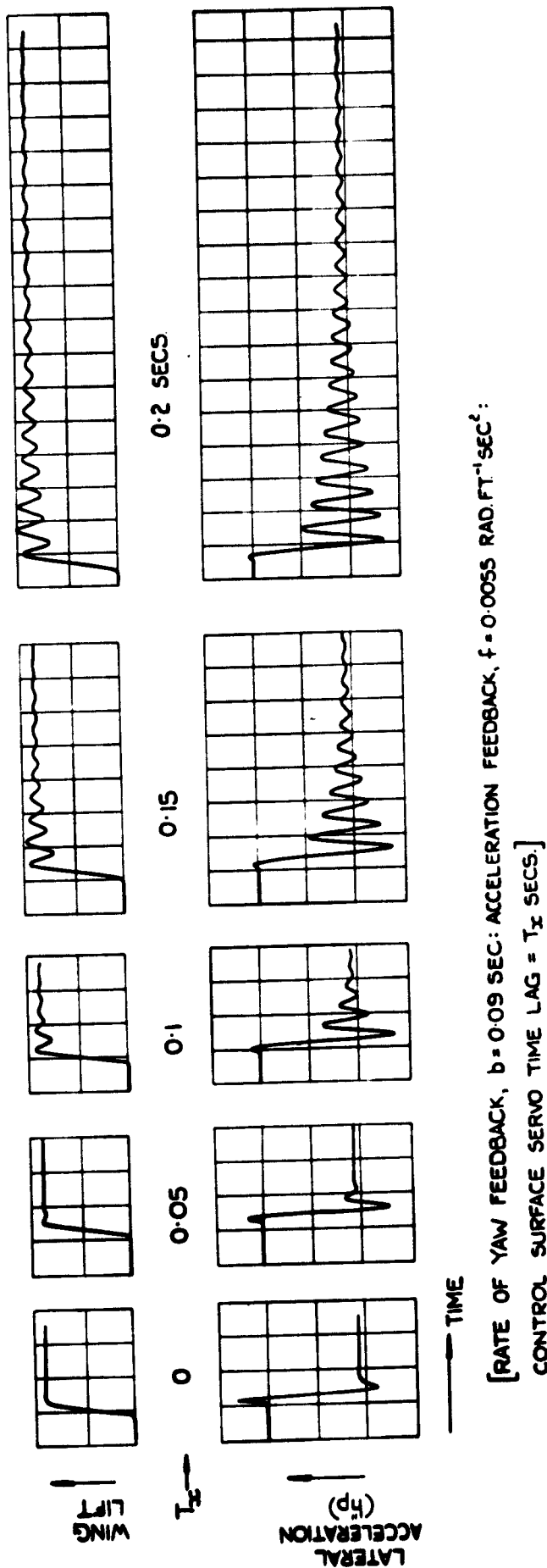
FIG.8. COMPARATIVE RESPONSES OF TEST MISSILE TO STEP DEMANDS FOR CONTROL SURFACE MOTION IN THE PRESENCE OF VARIOUS CONTROL SURFACE SERVO TIME LAGS.

[RATE OF YAW FEEDBACK, $b = 0.09$ SEC: ACCELERATION FEEDBACK, $f = 0.0055$ RAD.$FT^{-1}SEC^2$: CONTROL SURFACE SERVO TIME LAG $= T_I$ SECS.]
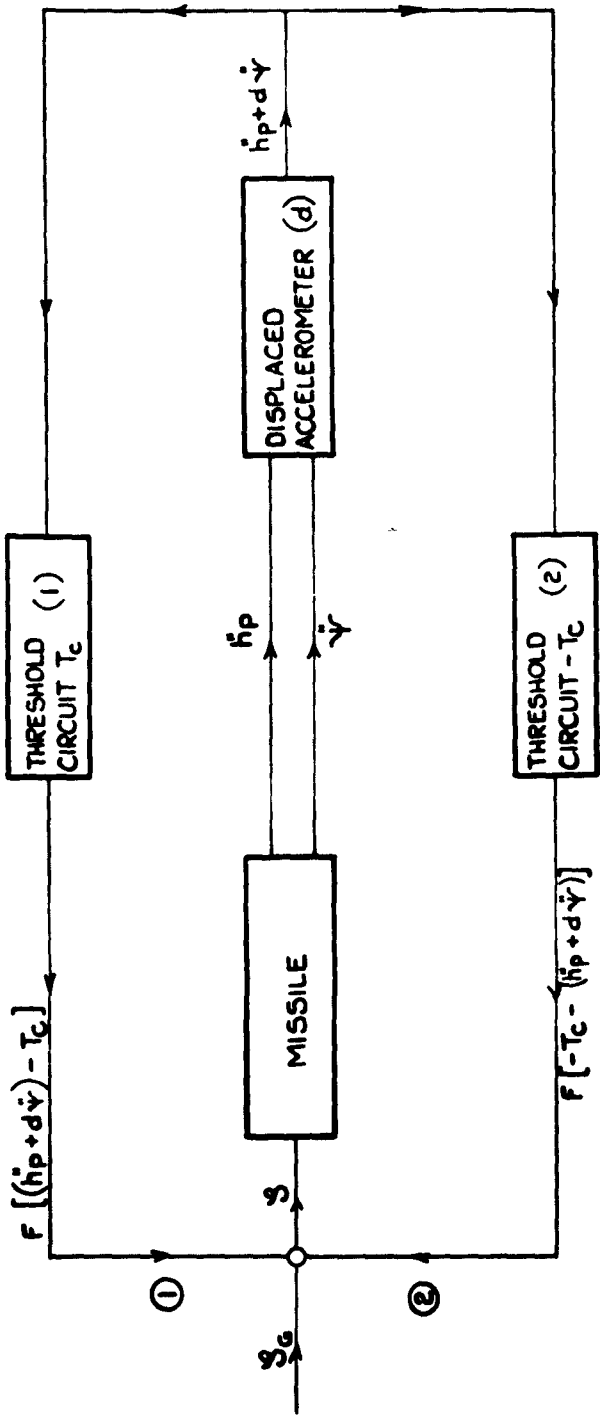
FIG. 9. BASIC DIAGRAM FOR THRESHOLD FEEDBACK FROM A
DISPLACED ACCELEROMETER.

β_W = WING INCIDENCE.
H_p = LATERAL ACCELERATION.
RATE-OF-YAW FEEDBACK, b = 0.09 sec.
DISPLACEMENT OF
ACCELEROMETER
d = $^{-14}/n_8$ = 4FT.
THRESHOLD LEVEL = 10g.

ACCELERATION FEEDBACK GAIN,
F, RAD. FT⁻¹ SEC²
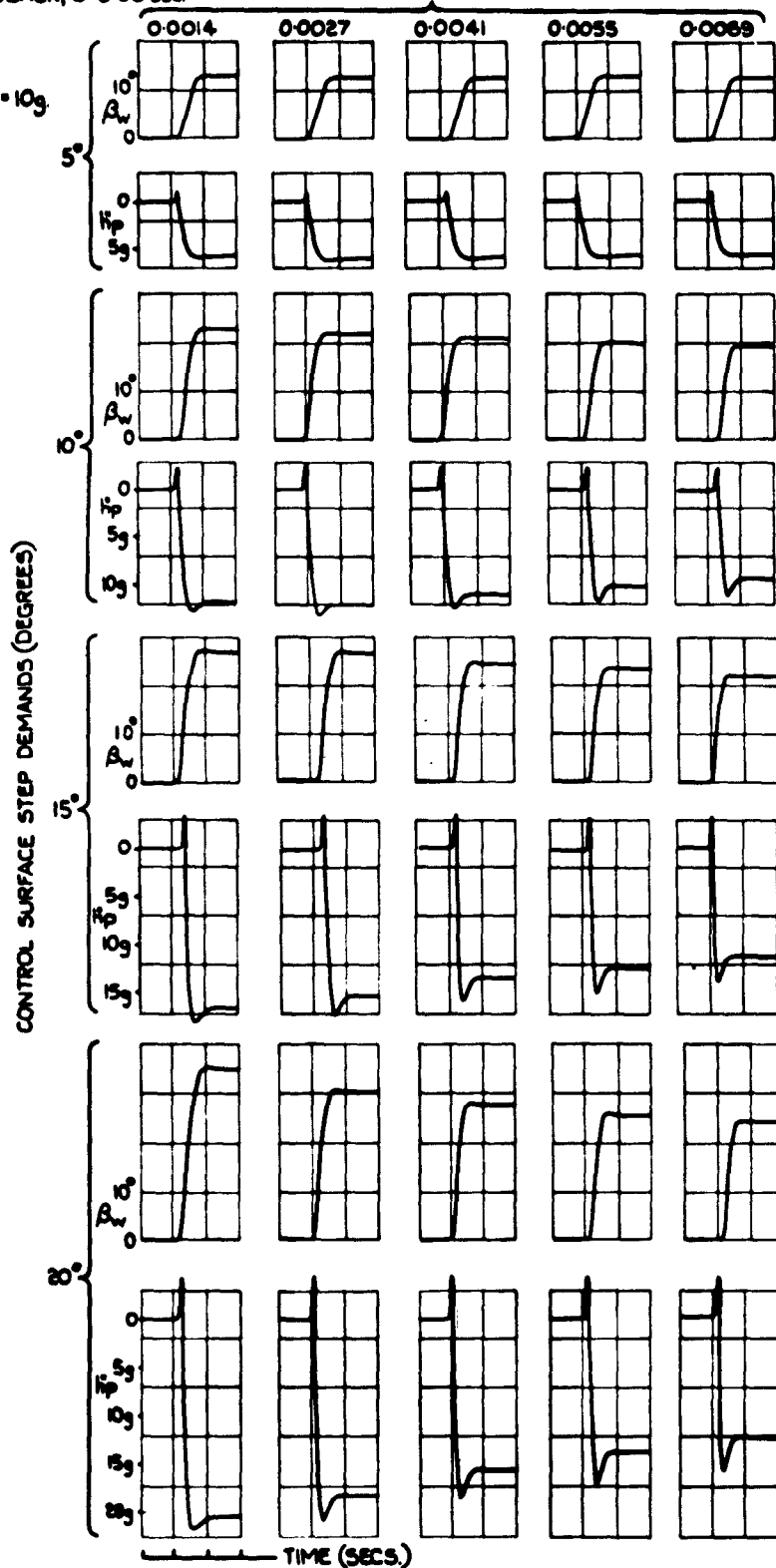
FIG.IO. RESPONSES TO CONTROL SURFACE STEP DEMANDS
OF THE TEST MISSILE WITH ACCELERATION FEEDBACK
FROM A DISPLACED ACCELEROMETER.
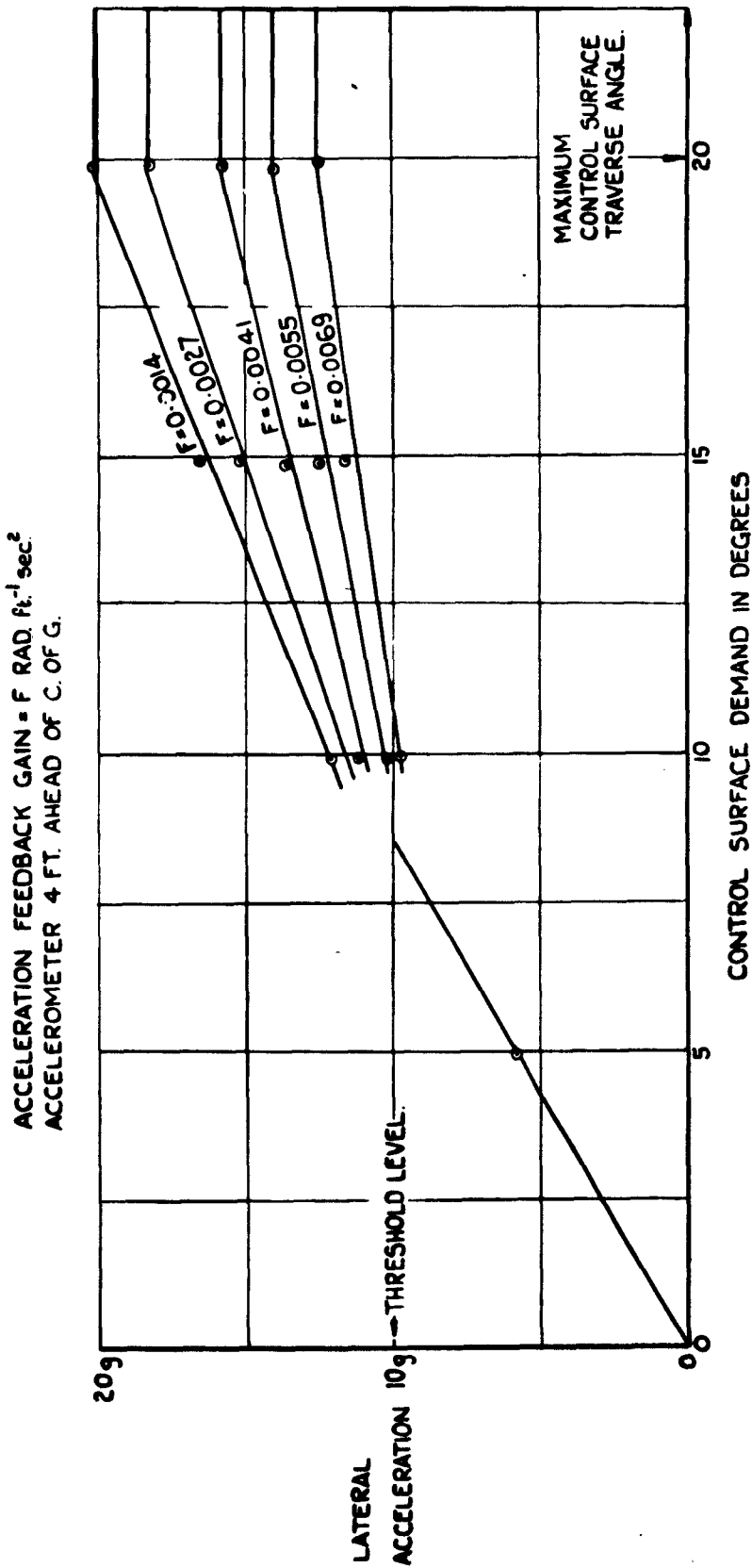
FIG. II. STEADY STATE ACCELERATION OF TEST MISSILE WITH THRESHOLD FEEDBACK FROM A DISPLACED ACCELEROMETER. (SIMULATOR RESULTS.)
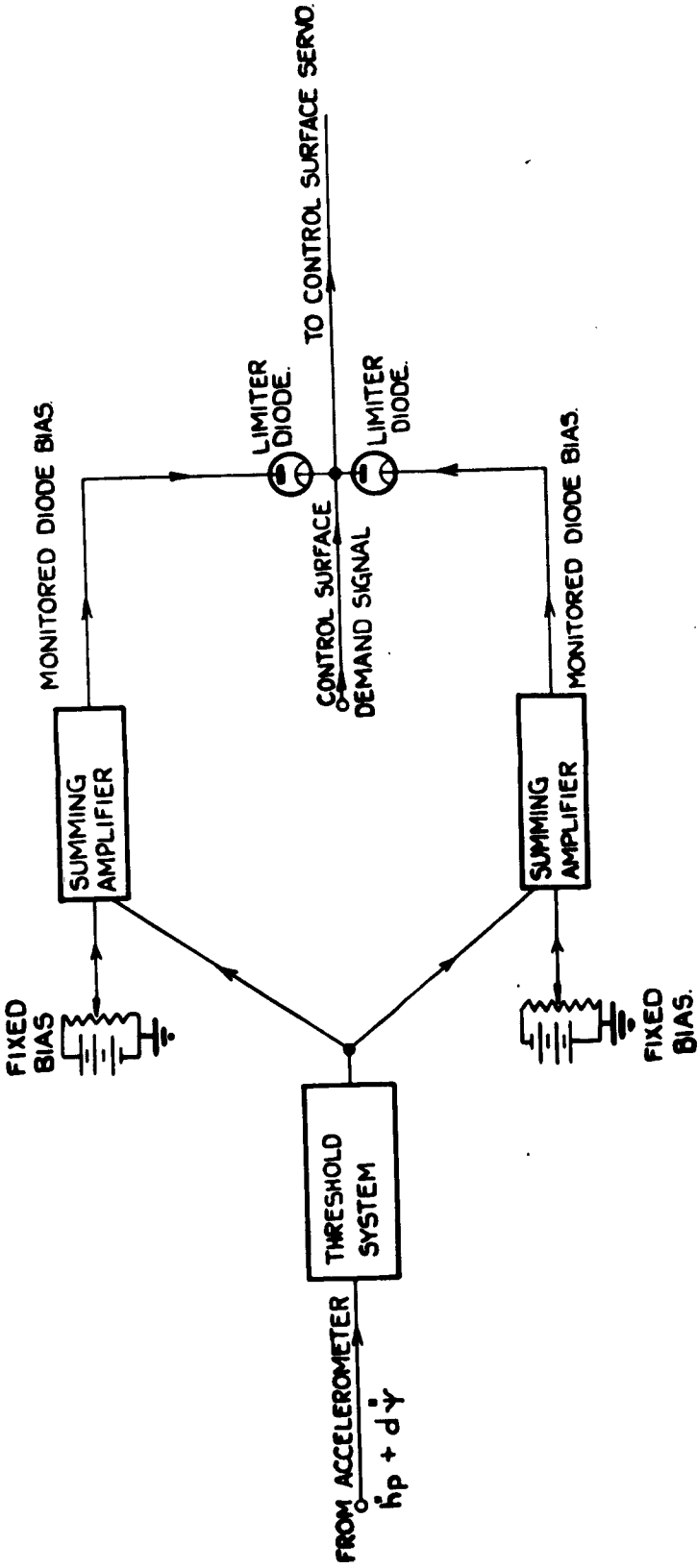
FIG. 12. SCHEMATIC DIAGRAM OF "MONITORED DIODE" ACCELERATION LIMITER.
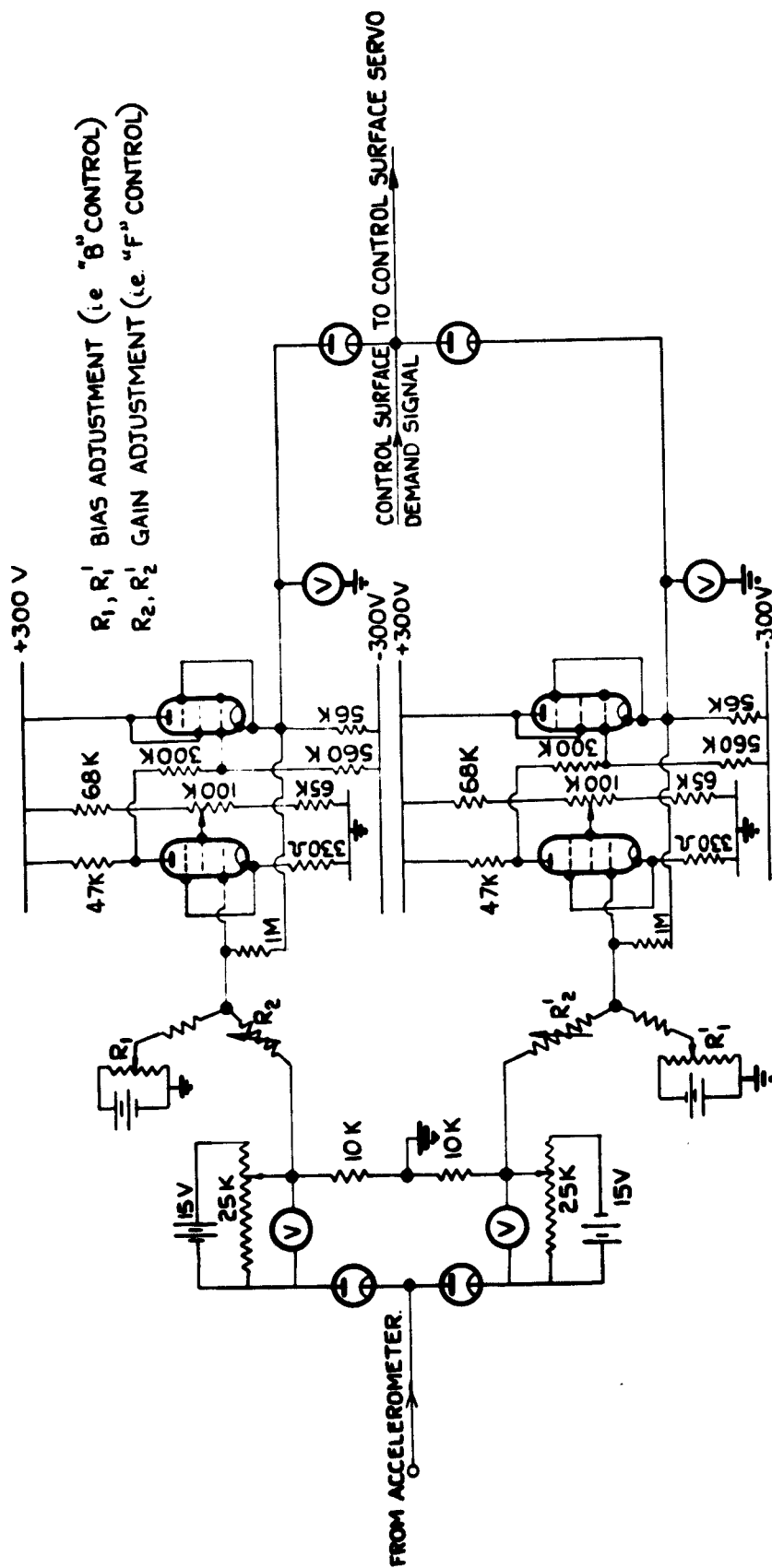
FIG. 13. CIRCUIT DIAGRAM OF SIMULATOR ARRANGEMENT FOR 'MONITORED DIODE' ACCELERATION LIMITER.
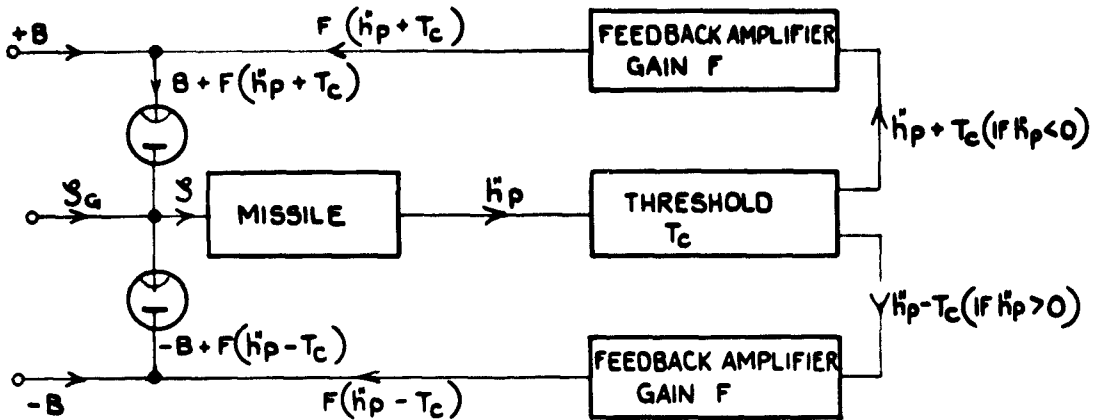
B, F AND T_c POSITIVE QUANTITIES; SYSTEM IN STEADY STATE.

(a) TWIN FEEDBACK SYSTEM.
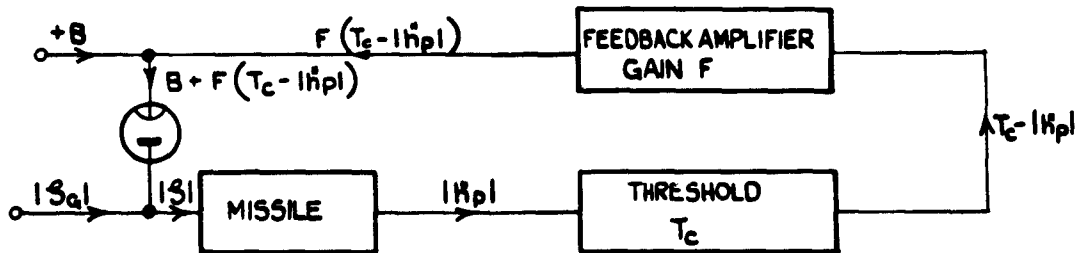
B, F AND T POSITIVE QUANTITIES; SYSTEM IN STEADY STATE.

(b) EQUIVALENT SINGLE LOOP SYSTEM.

FIG. 14.(a & b). DIAGRAMS FOR ANALYSIS OF MONITORED DIODE SYSTEM.

LATERAL ACCELERATION $(\ddot{h}_p)$ IN g's.

$B|\ell_h|$

FEEDBACK GAIN $F=0$ %g

$\dfrac{B+F_1 T_c}{F_1 + \frac{1}{|\ell_h|}}$

FEEDBACK GAIN $F = F_1$ %g

T_c

FEEDBACK GAIN $F = \infty$ %g

CONTROL SURFACE DEMAND SIGNAL (S_G) IN DEG.

$\dfrac{T_c}{|\ell_h|}$ $\dfrac{B+F_1 T_c}{1+F_1|\ell_h|}$ B
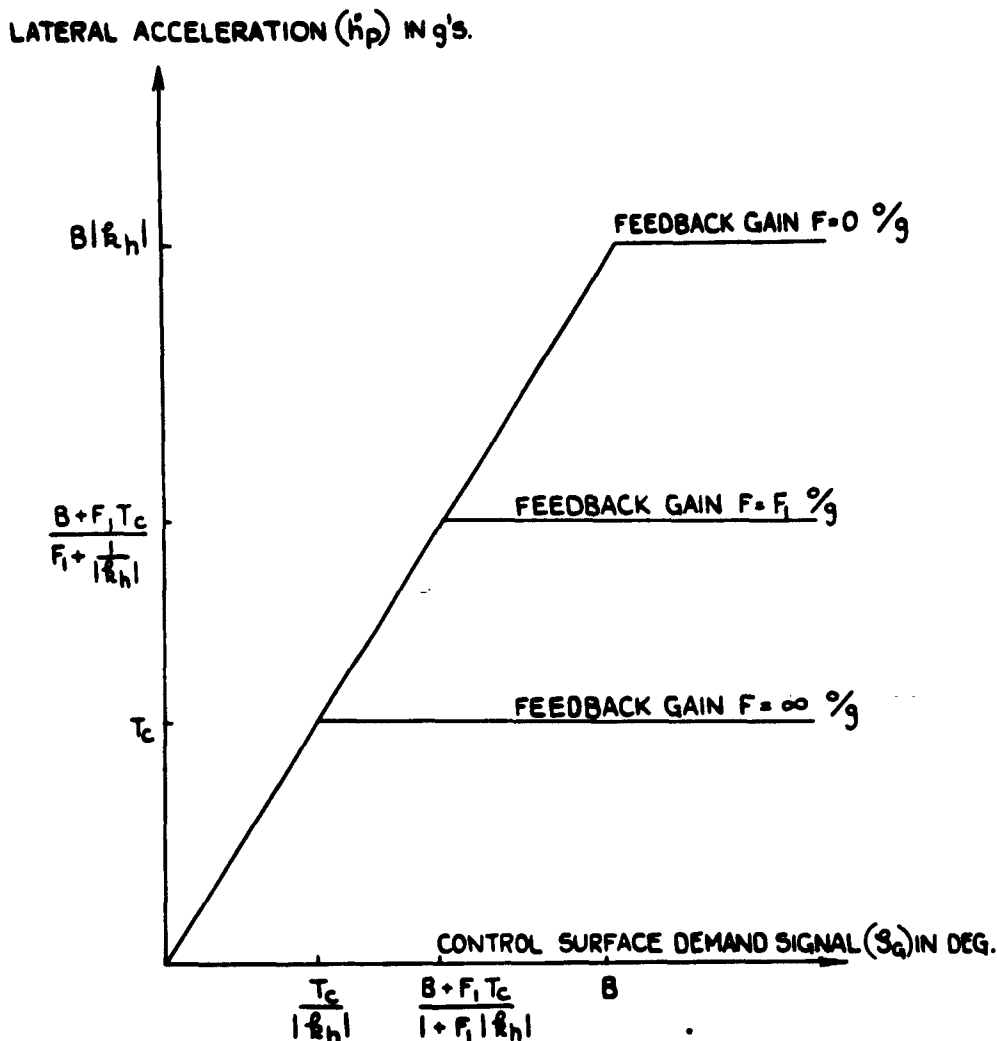
FIG. 15. STEADY STATE ACCELERATION AS A FUNCTION OF THE DEMAND (S_G) FOR THE MONITORED DIODE SYSTEM.
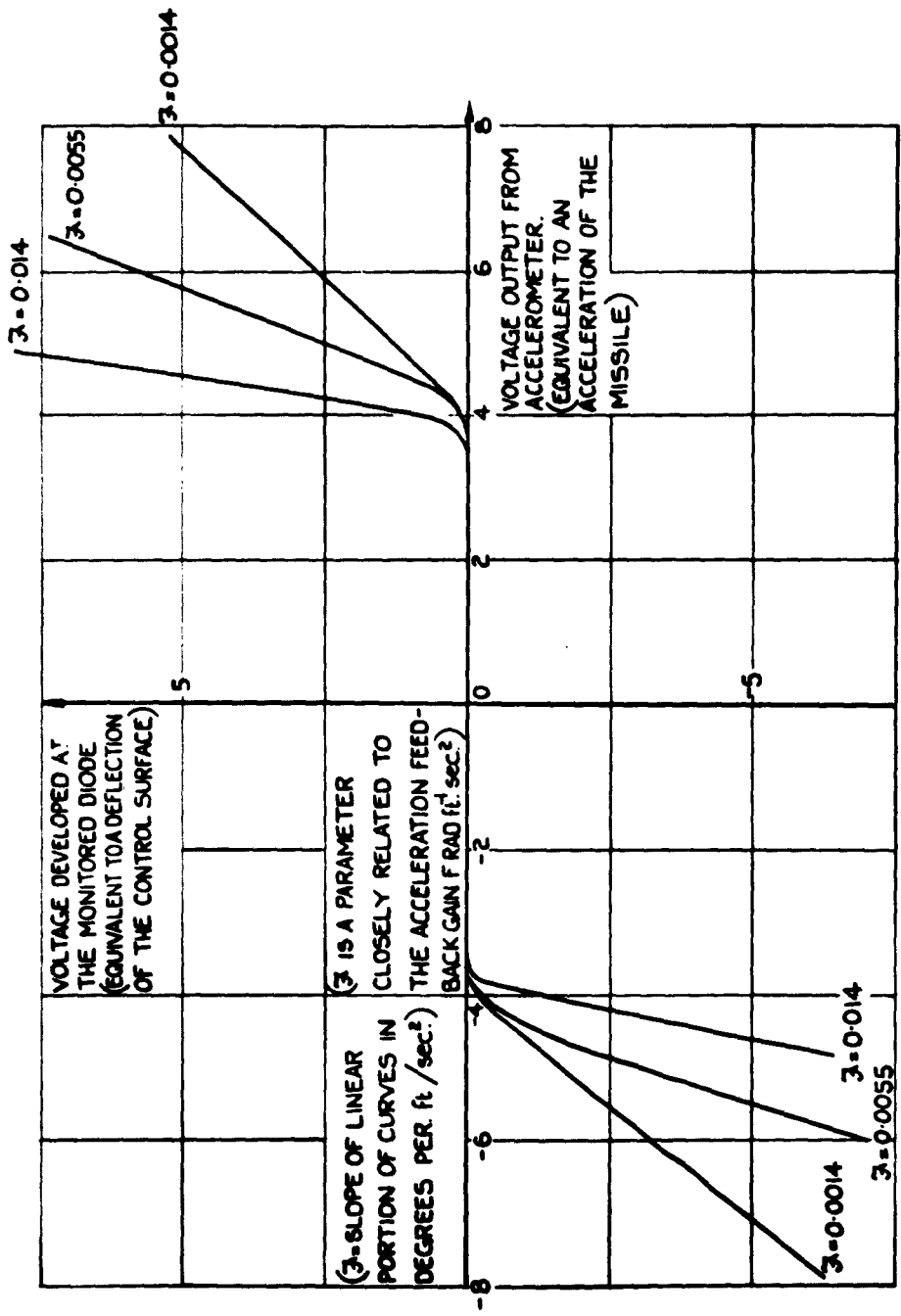
FIG. 16. CALIBRATION CURVES FOR THRESHOLD SYSTEM USED ON THE SIMULATOR.
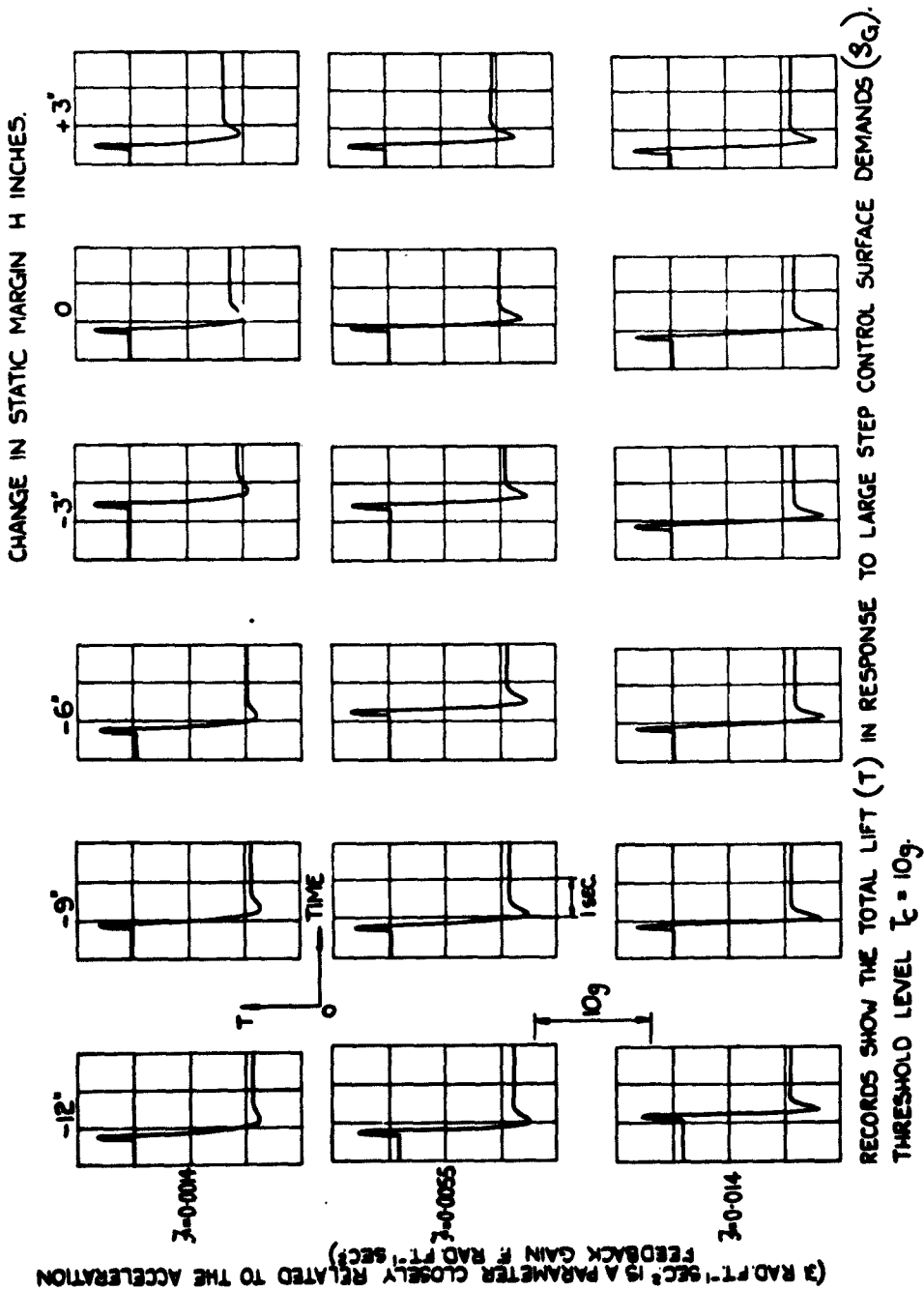
FIG.17. THE MONITORED DIODE LIMITING SYSTEM APPLIED TO THE TEST MISSILE. (TOTAL LIFT.)

CHANGE IN STATIC MARGIN H INCHES.

+12' +9' +6' +3' 0 -3' -6' -9' -12'

RECORDS SHOW THE TOTAL LIFT (T) IN RESPONSE TO LARGE STEP CONTROL SURFACE DEMANDS (δ_G).
THRESHOLD LEVEL T_c = 10g.

λ=0·0014

λ=0·0055

λ=0·014

(λ RAD. FT⁻¹ SEC² IS A PARAMETER CLOSELY RELATED TO THE ACCELERATION FEEDBACK GAIN F RAD. FT⁻¹ SEC²)

TIME

T

O

10g

1 SEC.

REPORT G.W.15.
FIG.18.

4299.

CHANGE IN STATIC MARGIN H INCHES.
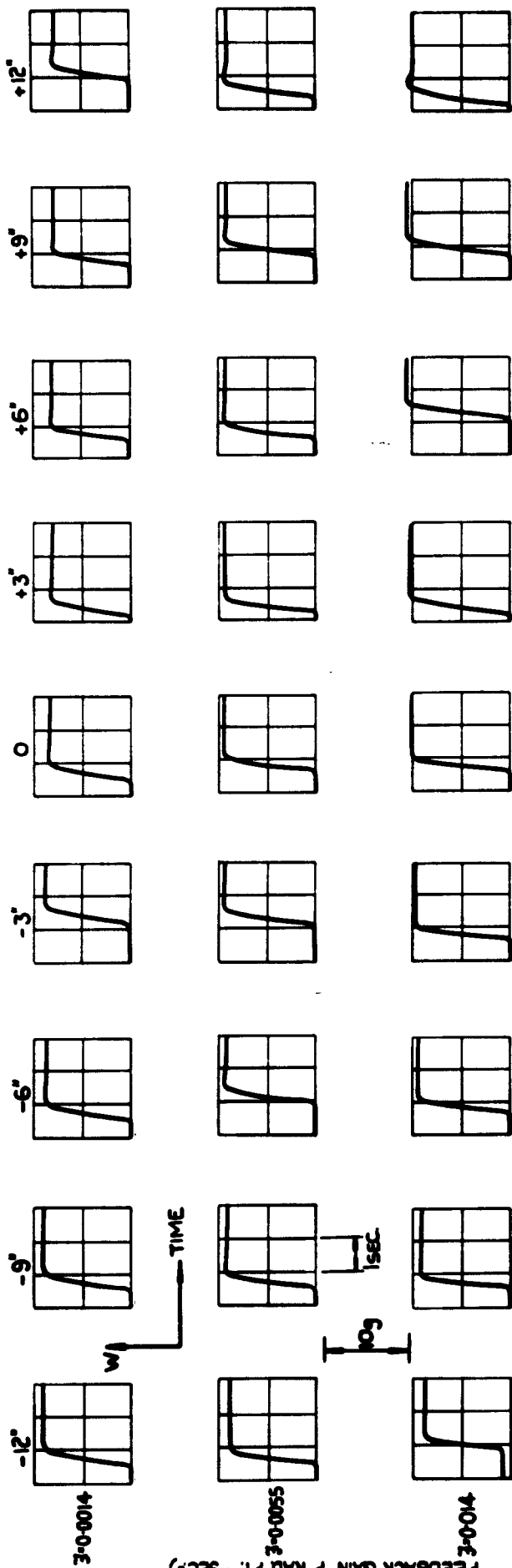
RECORDS SHOW THE WING LIFT (w) IN RESPONSE TO LARGE STEP CONTROL SURFACE DEMANDS (3_G)

THRESHOLD LEVEL $T_C = 10g$.

(3 RAD FT.$^{-1}$SEC^2 IS A PARAMETER CLOSELY RELATED TO THE ACCELERATION FEEDBACK GAIN F RAD FT.$^{-1}$ SEC.^{2})

FIG.18.THE MONITORED DIODE LIMITING SYSTEM APPLIED TO THE TEST MISSILE.
(WING LIFT)
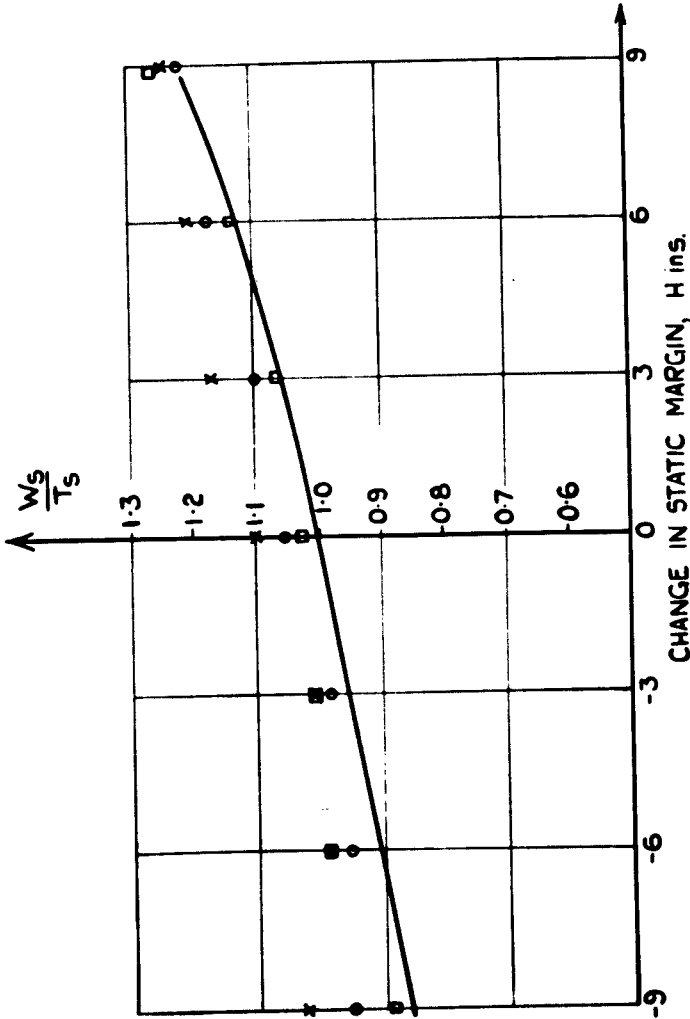
FIG. 19. STEADY STATE RATIO OF WING LIFT TO TOTAL LIFT AS A FUNCTION OF H.
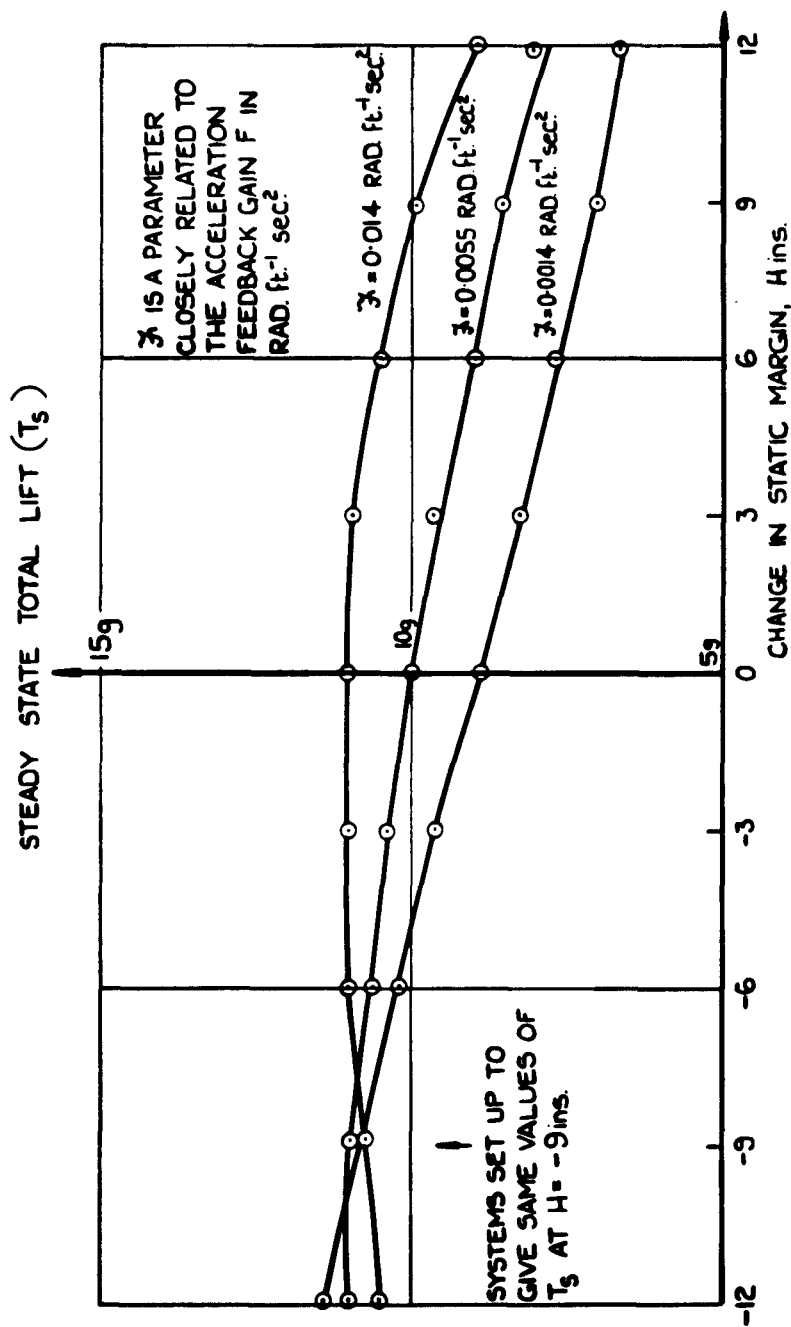
FIG.20. THE STEADY STATE TOTAL LIFT OF THE TEST MISSILE WITH THE MONITORED DIODE LIMITING SYSTEM. (SIMULATOR RESULTS).

STEADY STATE WING LIFT (W$_s$)

$\mathfrak{F}$ IS A PARAMETER CLOSELY RELATED TO THE ACCELERATION FEEDBACK GAIN F IN RAD. Ft⁻¹ sec²

$\mathfrak{F}$ = 0.014 RAD. Ft⁻¹ sec²

$\mathfrak{F}$ = 0.0055 RAD. Ft⁻¹ sec²

$\mathfrak{F}$ = 0.0014 RAD. Ft⁻¹ sec²

15g

10g

5g

SYSTEMS SET UP TO GIVE SAME VALUES OF W$_s$ AT H = -9 ins.

CHANGE IN STATIC MARGIN, H ins.

12   9   6   3   -3   -6   -9   -12
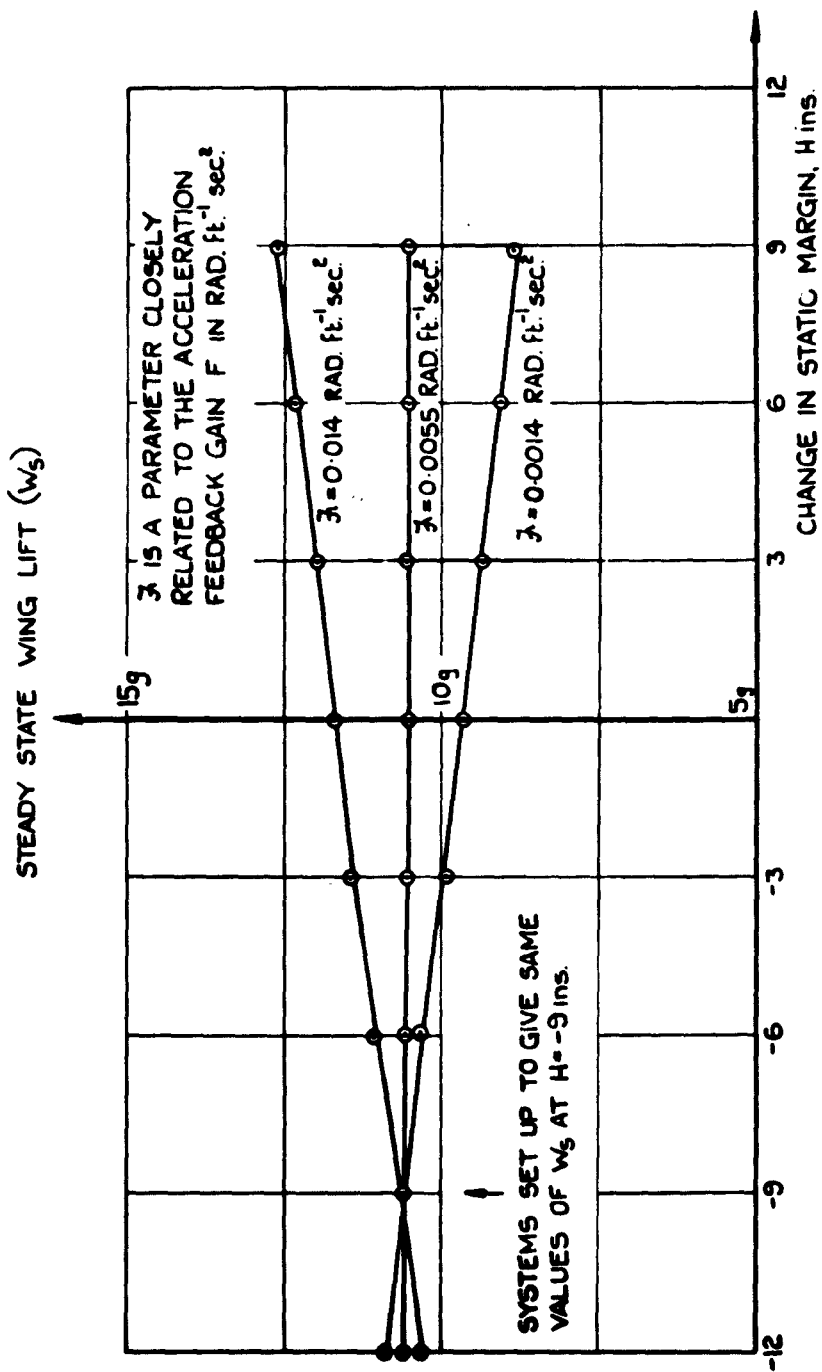
FIG. 21. THE STEADY STATE WING LIFT OF THE TEST MISSILE WITH THE MONITORED DIODE LIMITING SYSTEM. (SIMULATOR RESULTS).

STEADY STATE WING LIFT W_S

MONITORED DIODE SYSTEM SET TO GIVE NOMINAL 10g LIMIT FOR VARIOUS FEEDBACK GAINS.

10g

λ = MEASURE OF ACCELERATION FEEDBACK GAIN IN RAD. $ft.^{-1} sec^2$
- λ = 0·0014
- ○ λ = 0·0055
- × λ = 0·014.

5g

0   10   20   30

CONTROL SURFACE DEMAND SIGNAL (DEGREES)
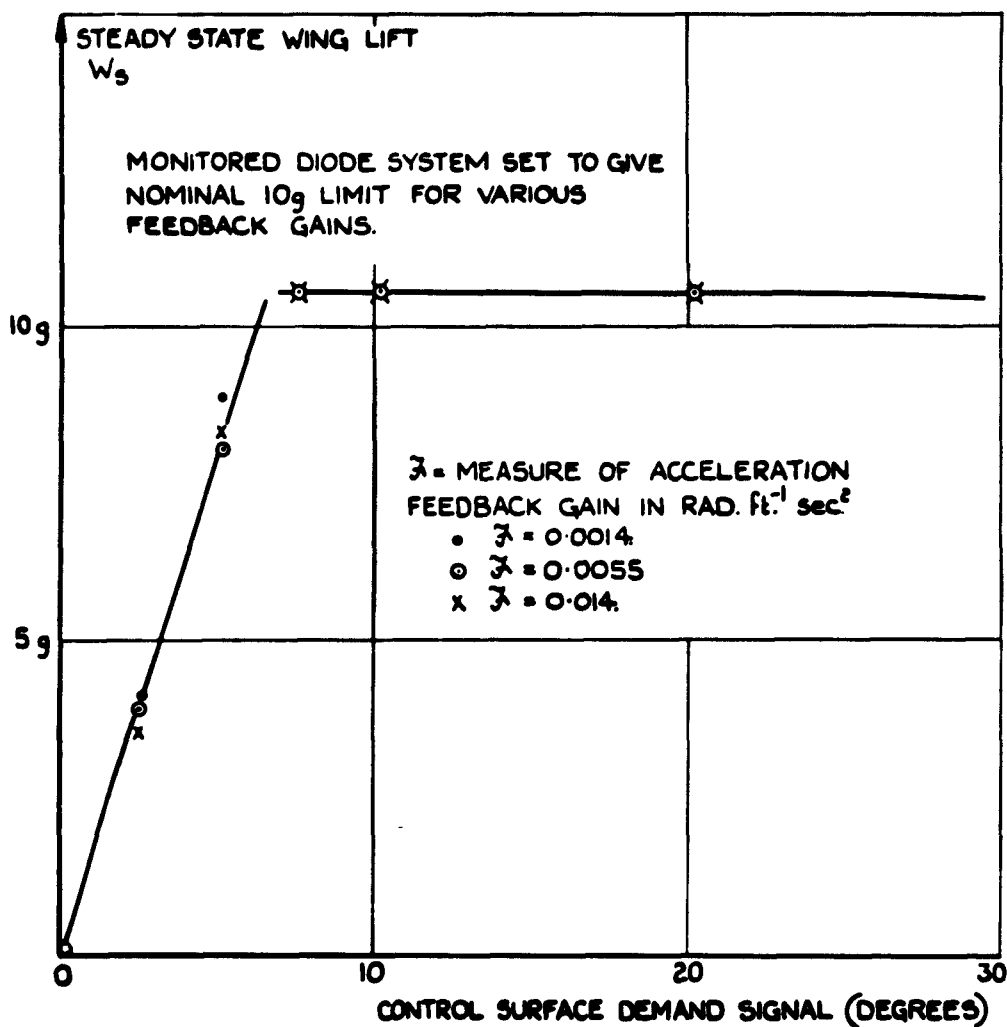
FIG.22. STEADY STATE WING LIFT vs. CONTROL SURFACE DEMAND SIGNAL FOR THE TEST MISSILE WITH THE MONITORED DIODE LIMITING SYSTEM.

(RECORDS ARE OF WING LIFT vs TIME FOR
THE TEST BEAM RIDER DURING RECOVERIES
FROM AN INITIAL BEAM RIDING ERROR.)
(ALL FEEDBACKS ARE FROM AN ACCELEROMETER
4 FT. AHEAD OF THE CENTRE-OF-GRAVITY.)

REPORT G.W. 15.
FIG.23.

(1) NO LIMITS
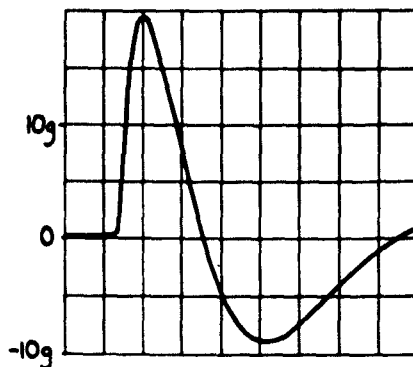
(2) MECHANICAL STOPS ON
CONTROL SURFACES AT 20.°
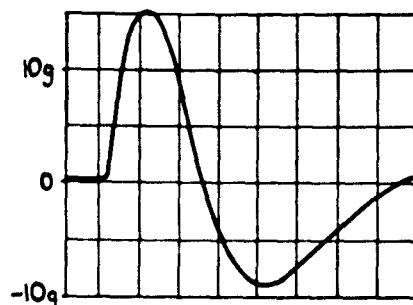
(3) MECHANICAL STOPS ON
CONTROL SURFACES PLUS
THRESHOLD ACCELERATION
FEEDBACK.
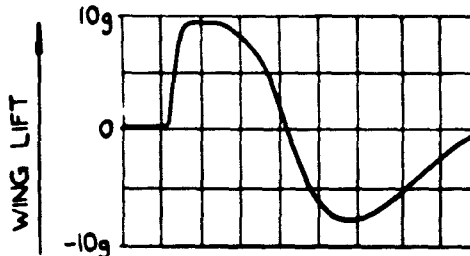
(4) THRESHOLD FEEDBACK OF
ACCELERATION ONLY.
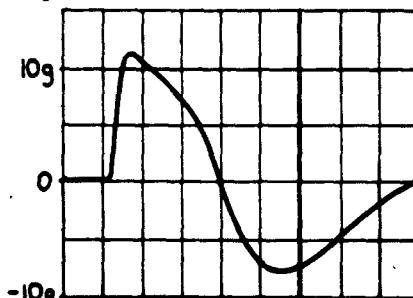
(5) THE MONITORED DIODE
LIMITING SYSTEM.
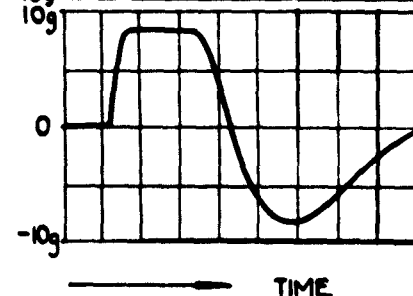
FIG.23. COMPARATIVE WING LIFT RESPONSES OF
THE TEST BEAM RIDER WITH
VARIOUS LIMITING SYSTEMS.

CURVE (a)
TYPICAL ACCELERATION
MANOEUVRE.
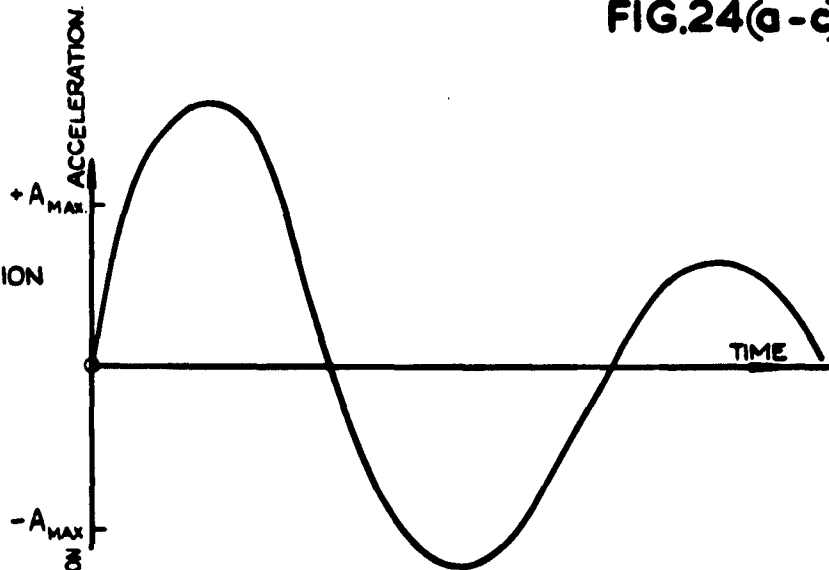
CURVE (b)
"ACCELERATION CLIPPING"
APPLIED TO TYPICAL
ACCELERATION MANOEUVRE.
LIMITING LEVEL = ± A_{MAX}
(EQUIVALENT TO CURVE (a)
BETWEEN ± A_{MAX}.)
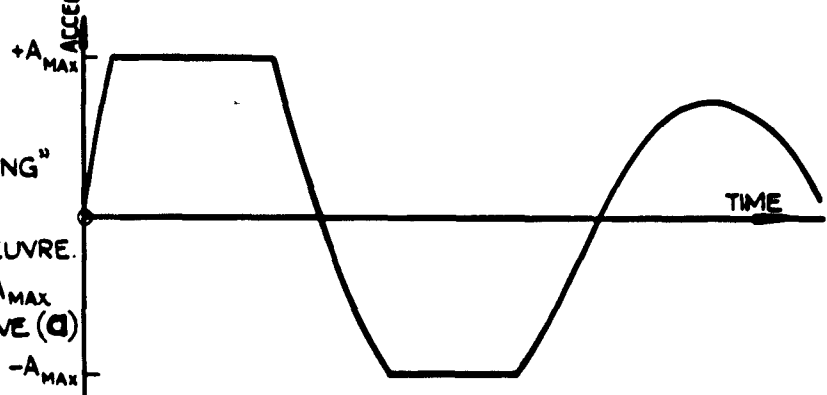
CURVE (c)
SIMPLE DIODE LIMITING OF
INPUT DEMAND SIGNALS AS
APPLIED TO TYPICAL
ACCELERATION MANOEUVRE.
LIMITING LEVEL = ± A_{MAX}.
MISSILE WEATHERCOCK
MOTION CRITICALLY
DAMPED GIVING CRITICALLY
DAMPED BUILD UP TO
± A_{MAX}. LEVELS.
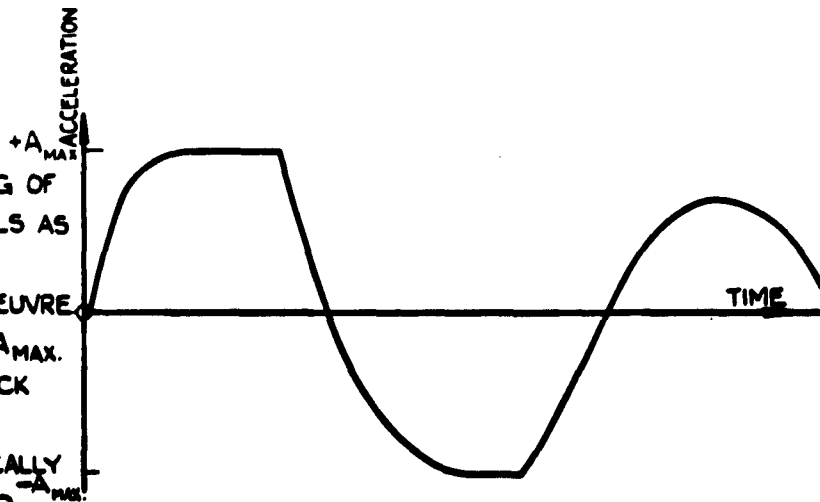
FIG.24(a-c)COMPARISON OF "ACCELERATION CLIPPING"
WITH SIMPLE DIODE LIMITING SYSTEM.

(a) NO LIMITING.

(b) ACCELERATION CLIPPING.

(c) CONTROL SURFACE DEMAND LIMITS. (RESET FOR EACH H)

(d) MONITORED DIODE LIMITING.

(e) THRESHOLD FEEDBACK OF ACCELERATION.

(f) THRESHOLD FEEDBACK OF ACCELERATION PLUS MECHANICAL STOPS.

R.M.S. WING LIFT (W)

CHANGE IN STATIC MARGIN H, ins.
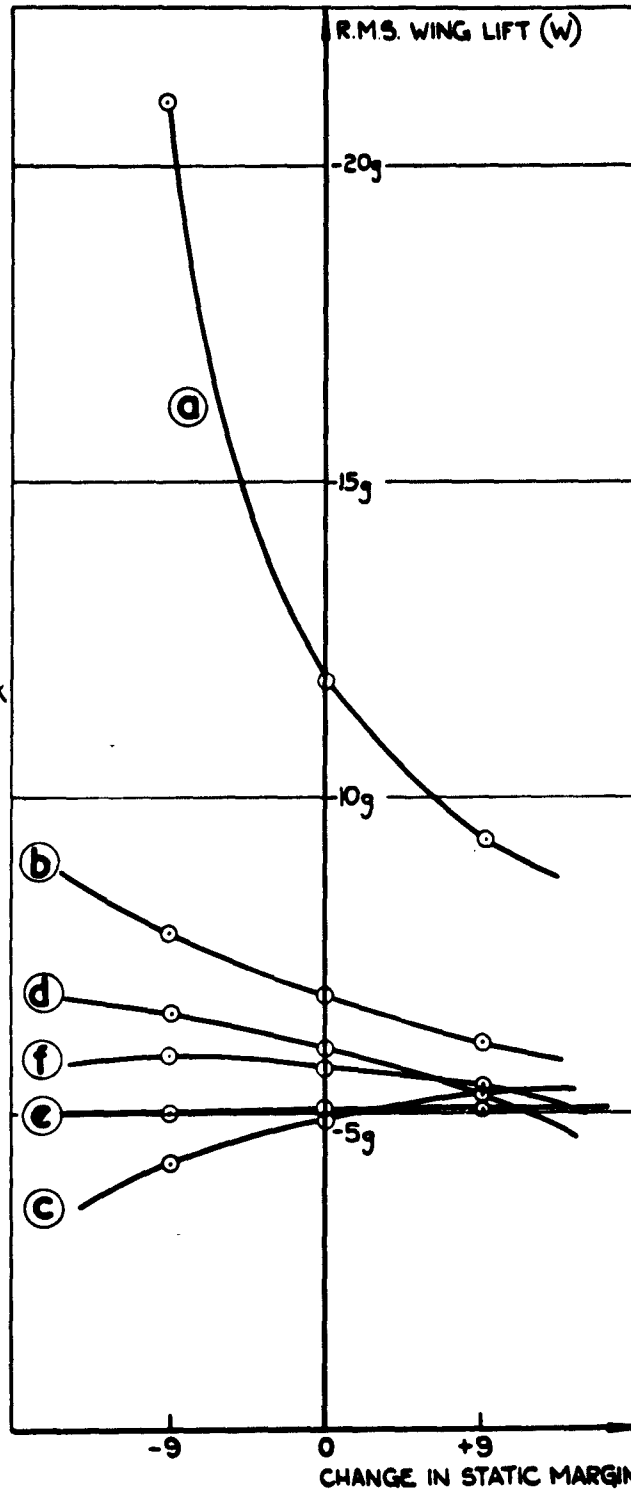
(THE TEST BEAM RIDER, LATERAL ACCELERATION LIMITS = 10g, R.M.S. BEAM JITTER = 60 FT.)

FIG.25. COMPARISON OF R.M.S. WING LIFTS FOR DIFFERENT LIMITING SYSTEMS AS APPLIED TO THE TEST BEAM RIDER IN THE PRESENCE OF RADAR BEAM JITTER.
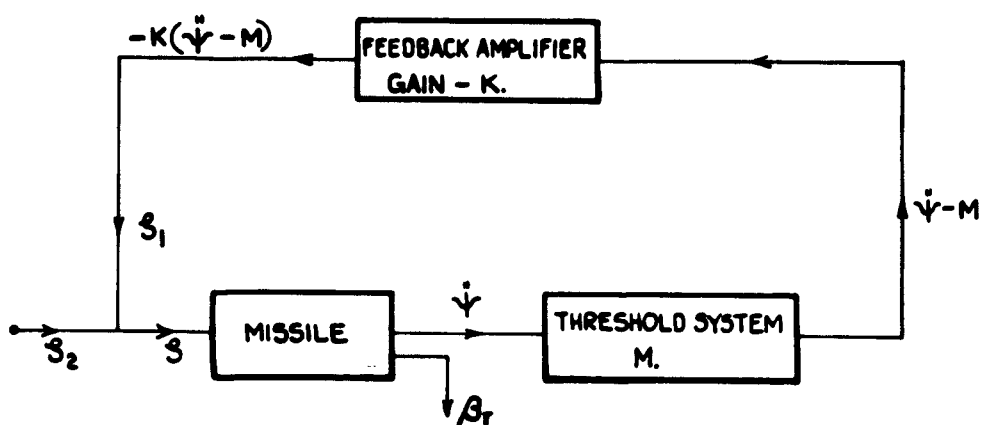
FIG. 26. BASIC SYSTEM FOR CONTROL SURFACE
LIFT LIMITING.

① ANGULAR ACCELERATION FEEDBACK APPLIED TO OTHERWISE UNMODIFIED MISSILE.
CHARACTERISTIC EQUATION OF WEATHERCOCK MODE. $(p^2 + 2u_k \omega_k p + \omega_k^2) = 0$.

② ANGULAR ACCELERATION FEEDBACK APPLIED TO MISSILE WHICH HAS LATERAL
ACCELERATION AND RATE-OF-YAW FEEDBACKS SUCH THAT WHEN K=0 THE
DAMPING RATIO IS UNITY AND THE UNDAMPED WEATHERCOCK ANGULAR
FREQUENCY IS 10 sec^{-1}
CHARACTERISTIC EQUATION OF WEATHERCOCK MODE. $(p^2 + 2u_{ki} \omega_{ki} p + \omega_{ki}^2) = 0$
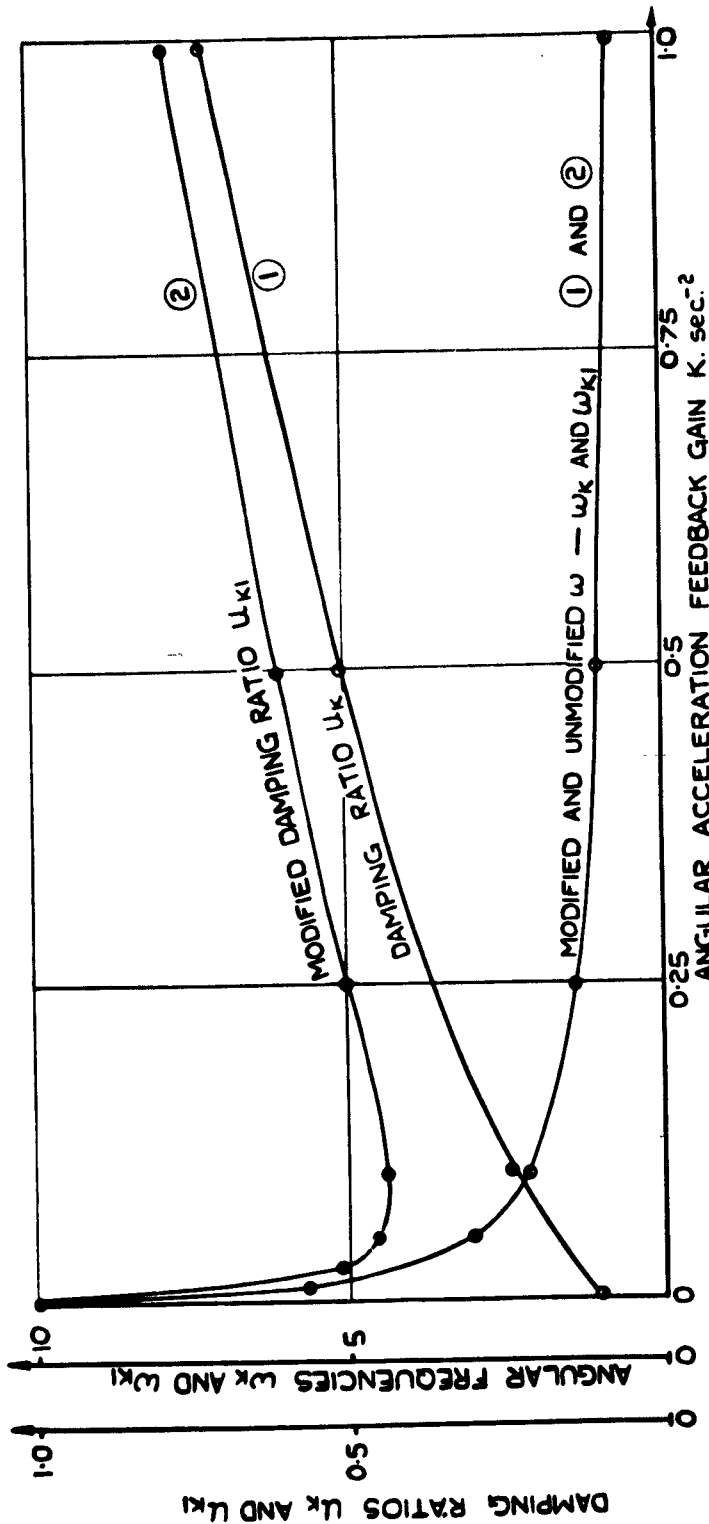
FIG. 27. THE EFFECT OF ANGULAR ACCELERATION FEEDBACK ON THE
WEATHERCOCK MODE OF THE TEST MISSILE.

FIG.28.

CONTROL SURFACE INCIDENCE (B_T DEGREES)

LATERAL ACCELERATION ($\ddot{h}_P$ IN g's)

CONTROL SURFACE ANGLE (S DEGREES)

K=0·021

K=0·084

K=0·21

ANGULAR ACCELERATION FEEDBACK GAIN K sec.$^{-1}$

[TEST MISSILE WITH y_s=O : CONTROL EQUATION $S = S_G + b\tau + f\dot{h}_P + K\ddot{\psi}$; b=0·09 SEC, f=-6·3 10^{-5} RAD. Ft.$^{-1}$ SEC.^{2}: DEMAND FOR S=10° STEP]
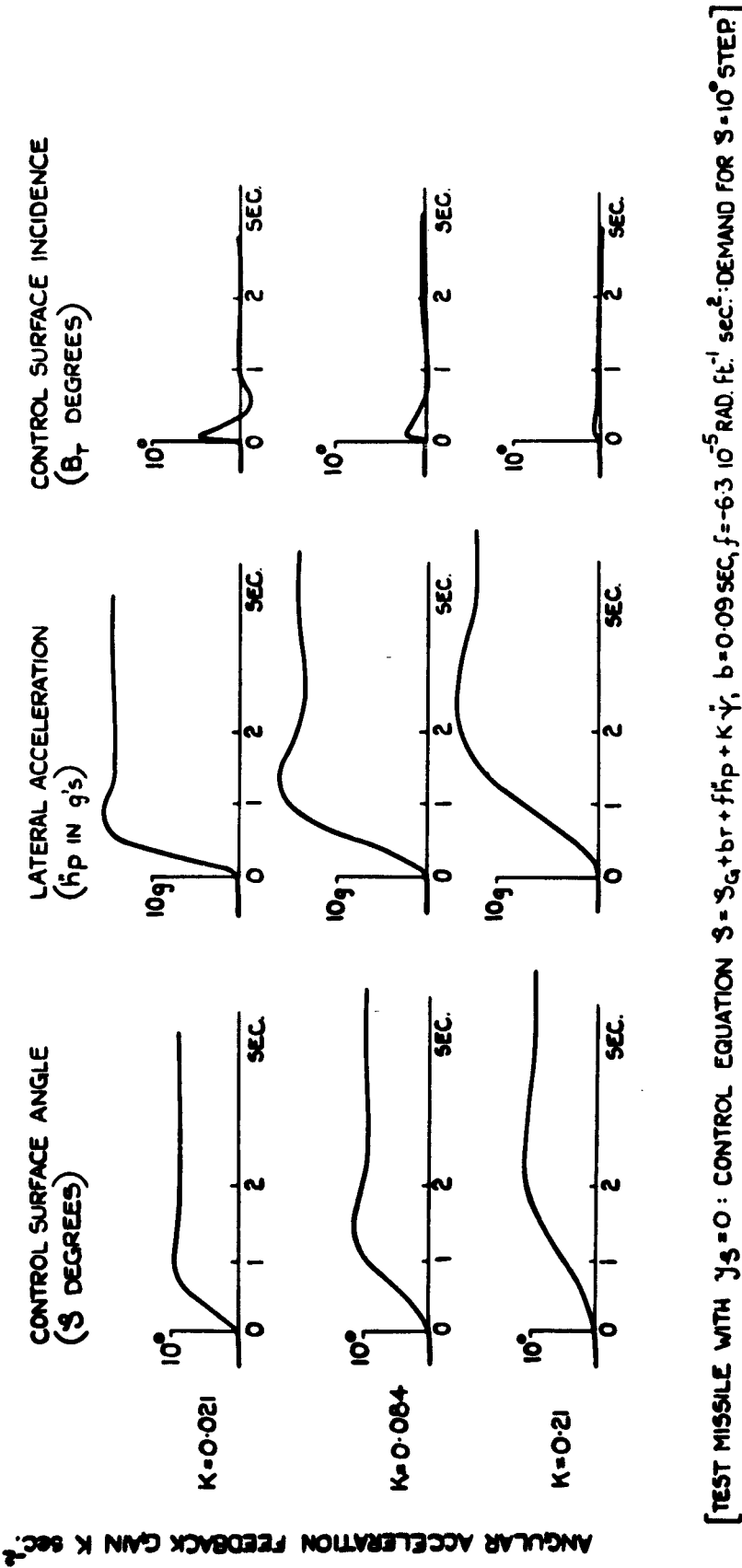
FIG.28. RESPONSE OF TEST MISSILE (WITH y_s=O) TO STEP CONTROL SURFACE DEMANDS IN THE PRESENCE OF ANGULAR ACCELERATION FEEDBACK.

CHARACTERISTIC EXPRESSION FOR THE WEATHERCOCK MOTION:-

$$Q_c = (1 - f_{y_5} - Kn_5) \left[p^2 + 2u_{KI} \omega_{KI} p + \omega_{KI}^2 \right]$$

——— THEORETICAL.

⊚ ⊙ SIMULATOR.

DAMPING RATIO u_{KI}

UNDAMPED ANGULAR FREQUENCY ω_{KI}

ANGULAR ACCELERATION FEEDBACK GAIN. K sec.$^{-2}$
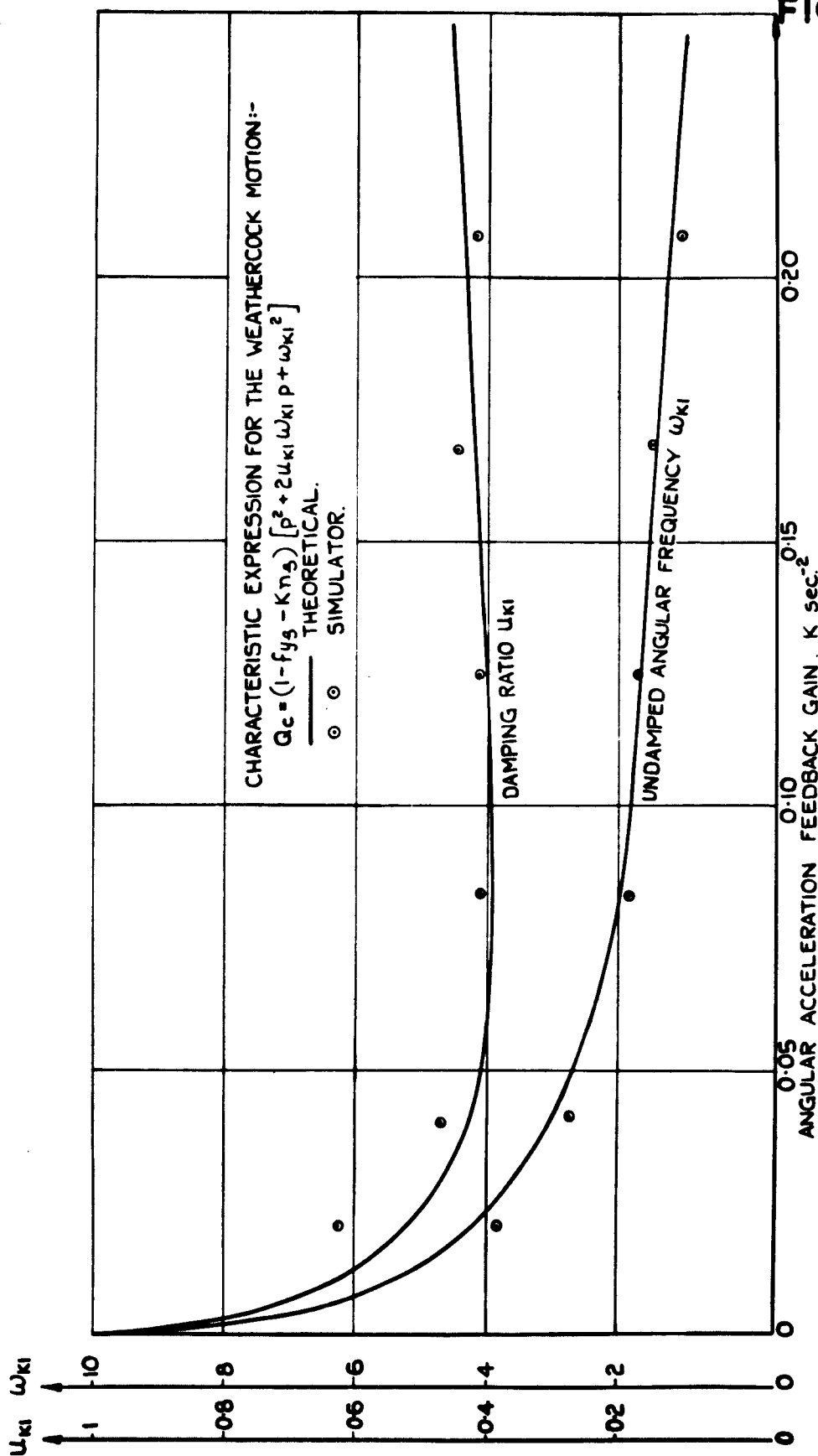
FIG. 29. A COMPARISON OF THE THEORETICAL AND THE SIMULATED WEATHERCOCK FREQUENCY AND DAMPING AS FUNCTIONS OF THE ANGULAR ACCELERATION FEEDBACK GAIN.

CHARACTERISTIC EQUATION FOR MOTION OF BEAM RIDER:-

$$(p+\alpha)(p^2+2u_w\omega_w p+\omega_w^2)(p^2+2u_c\omega_c p+\omega_c^2)=0$$

WEATHERCOCK-LIKE MODE.   WEAVE OR CONTROL MODE.

● ● SIMULATOR RESULTS FOR THE DOMINANT MODE.

ω_w

ω_c

sec⁻¹

ω_w AND ω_c

0·01   0·02   0·03   0·04   0·05

ANGULAR ACCELERATION FEEDBACK GAIN K sec⁻²

u_c

u_w

u_w AND u_c

0·01   0·02   0·03   0·04   0·05

ANGULAR ACCELERATION FEEDBACK GAIN K sec.²
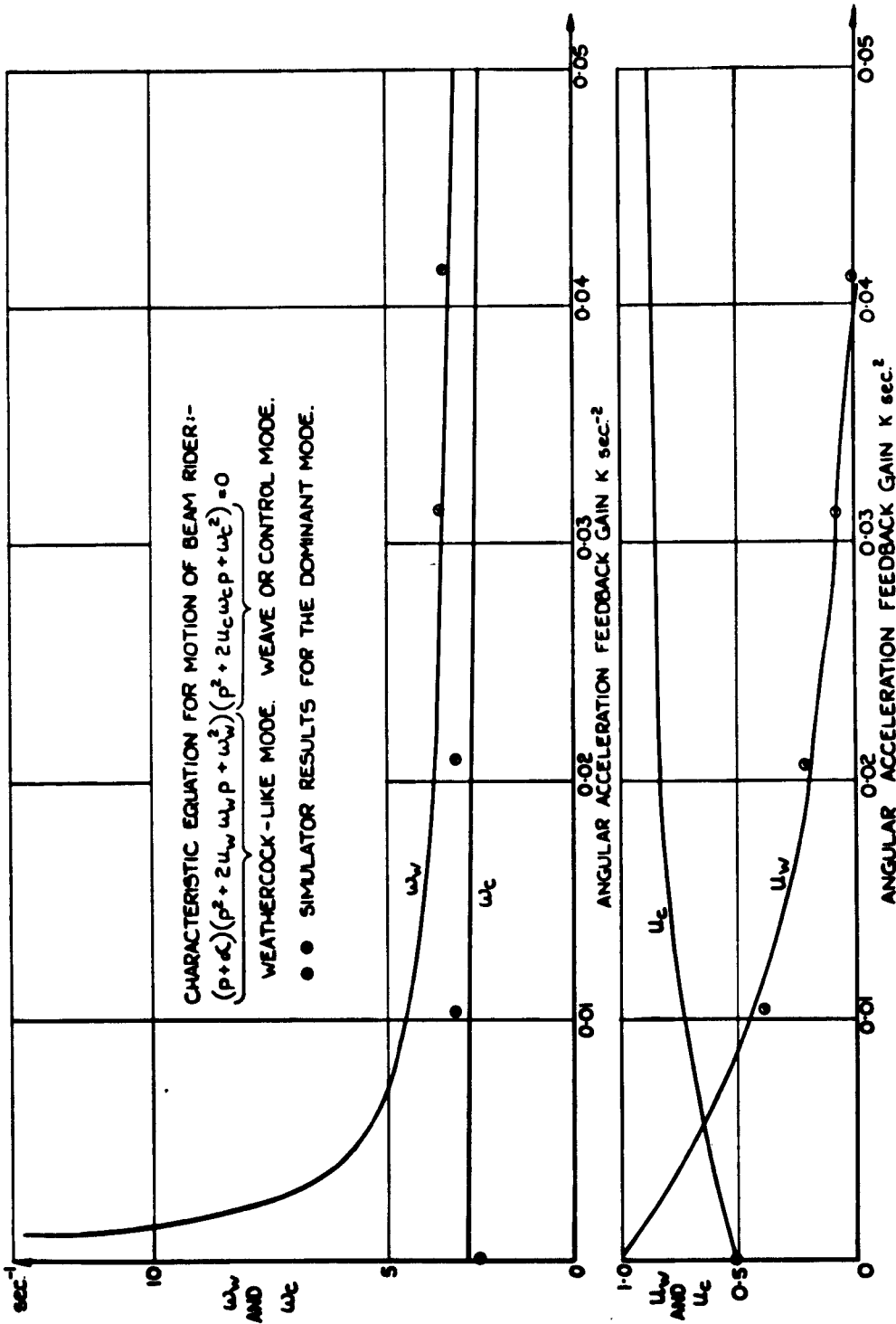
FIG. 30. THE EFFECTS OF ANGULAR ACCELERATION FEEDBACK ON THE MODES OF MOTION OF A BEAM RIDER.

LATERAL ACCELERATION ($\ddot{y}p$ IN g's)

ANGULAR ACCELERATION FEEDBACK GAIN K sec.$^{-2}$

K=0

K=0.021

K=0.031

K=0.041

10g

10g

10g

10g

0

0

0

0

TIME (SECS.)
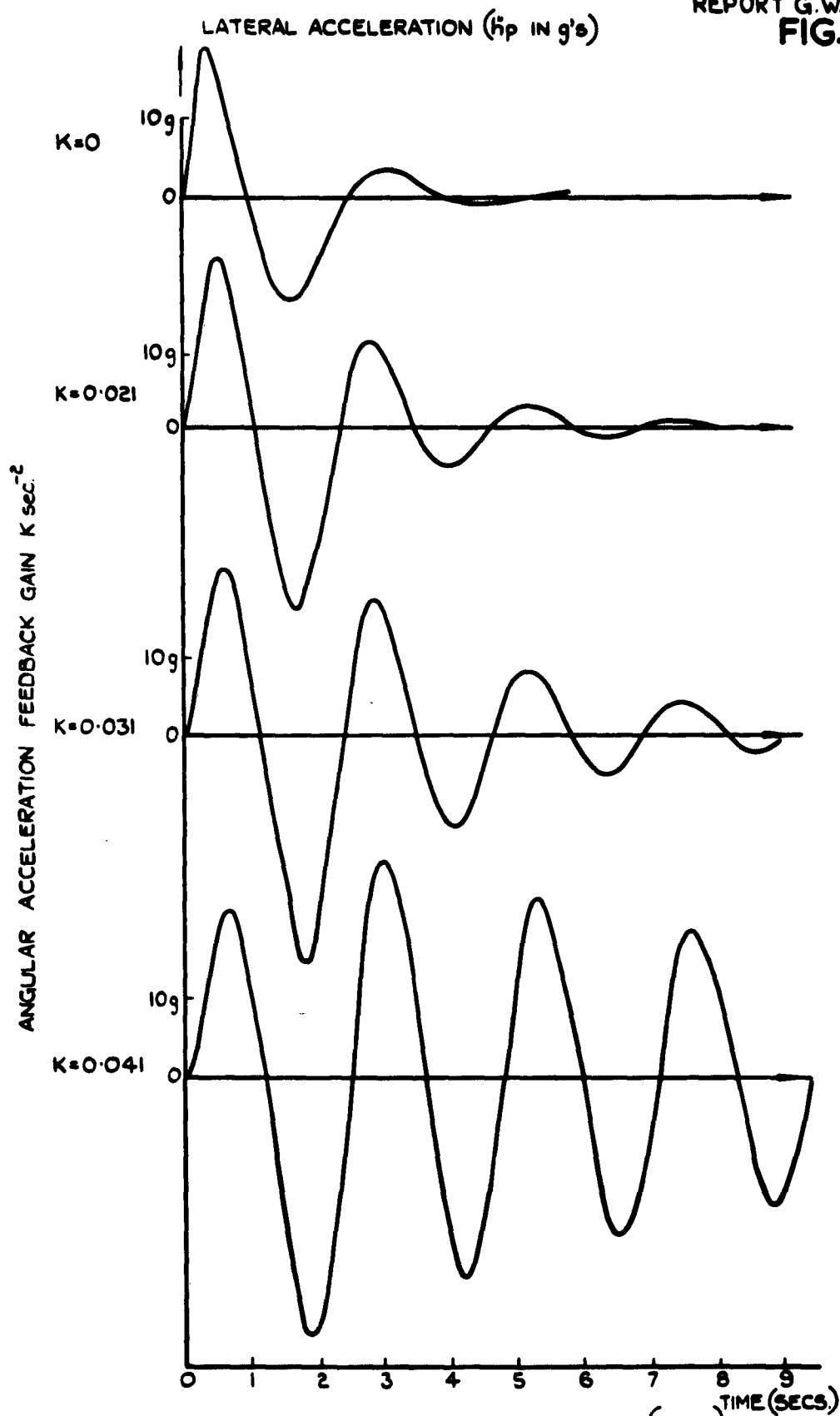
(RECORDS SHOW THE RESPONSES OF THE TEST BEAM RIDER ($y_3 = 0$)
TO A STEP DISPLACEMENT OF THE RADAR BEAM OF 375 ft.)

FIG.31. THE "BEAT EFFECT" PRODUCED IN THE
RESPONSE OF THE TEST BEAM RIDER
BY ANGULAR ACCELERATION FEEDBACK.

LATERAL DISPLACEMENT (hp ft)

375 ft.

LATERAL ACCELERATION (ḧp IN g's)

10g

10g

CONTROL SURFACE ANGLE (𝜗°)

CONTROL SURFACE RATE (𝜗̇ %sec)

CONTROL SURFACE INCIDENCE (β_T°)

ANGULAR ACCELERATION (ψ̈ %sec²)

ANGULAR VELOCITY (ψ̇ %sec.)

SIDESLIP VELOCITY (υ ft/sec.)

TIME (SECS.)
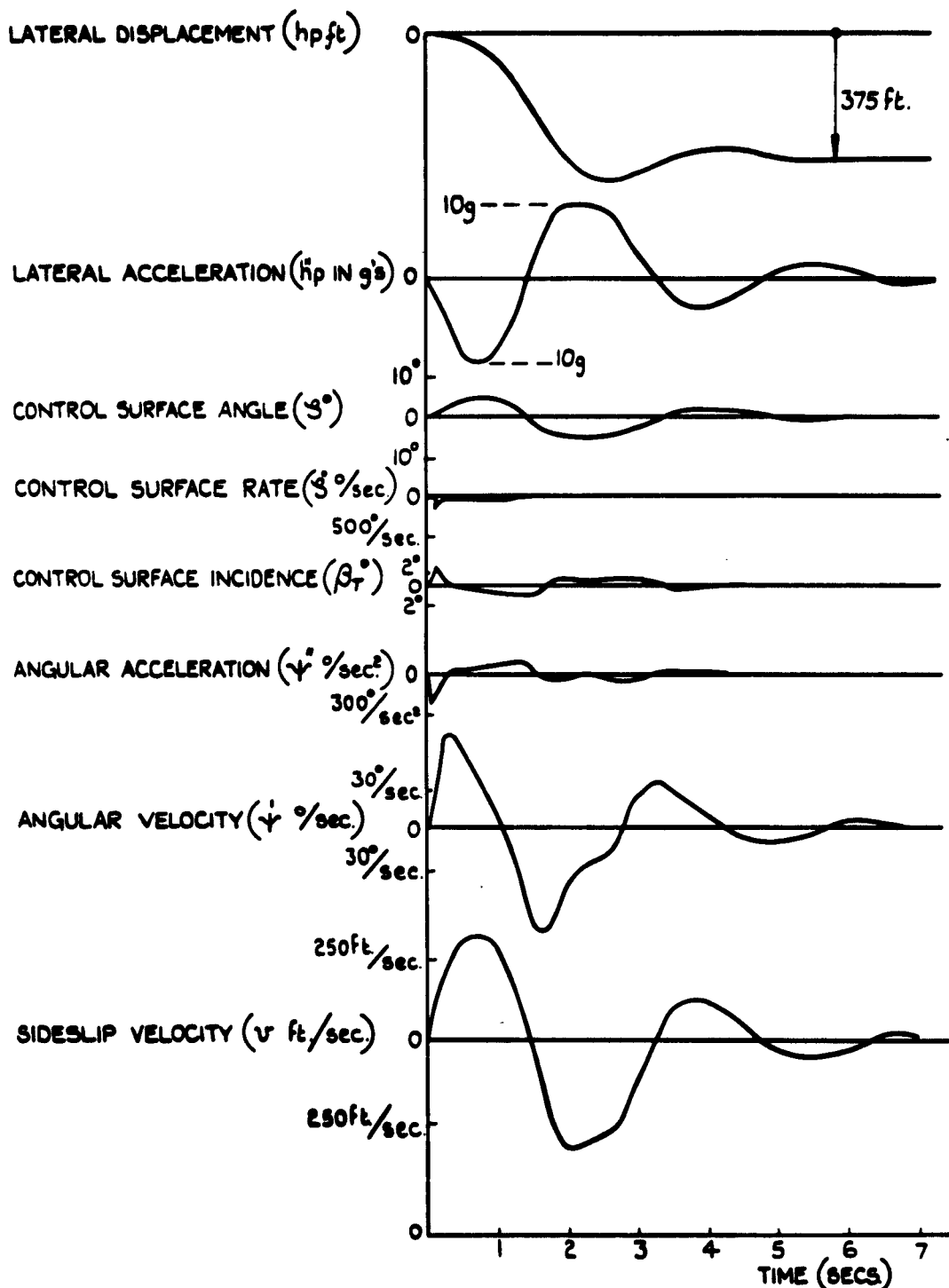
[TEST BEAM RIDER WITH ANGULAR ACCELERATION FEEDBACK K = 0·021 sec.⁻²
AND LATERAL ACCELERATION LIMITS OF ±10g.]

FIG. 32. COMPLETE RESPONSE OF TEST BEAM
RIDER TO A STEP BEAM DISPLACEMENT OF
375 FT. WHEN ANGULAR ACCELERATION
FEEDBACK IS APPLIED TO THE MISSILE.

FIG. 33.

THEORETICAL CURVES.

□, ⊙, x, SIMULATOR MEASUREMENTS OF PEAK CONTROL SURFACE INCIDENCE FOR THRESHOLDS 1,2,4.

◆, △, ✝, SIMULATOR MEASUREMENTS OF PEAK ANGULAR ACCELERATION FOR THRESHOLDS 1,2,4.

THRESHOLDS.(1) ±1200°/SEC² OF ANGULAR ACCELERATION,
OR ± 6° OF CONTROL SURFACE INCIDENCE.
(2)± 600°/SEC² OF ANGULAR ACCELERATION,
OR ± 3° OF CONTROL SURFACE INCIDENCE.
(3)±300°/SEC² OF ANGULAR ACCELERATION,
OR ± 1·5° OF CONTROL SURFACE INCIDENCE.
(4) 0°/SEC² OF ANGULAR ACCELERATION,
0° OF CONTROL SURFACE INCIDENCE.

THRESHOLDS

ANGULAR ACCELERATION FEEDBACK GAIN K. SEC⁻²

PEAK CONTROL SURFACE INCIDENCE (β₀) DEGREES

PEAK ANGULAR ACCELERATION (ϕ̈) DEGREES/SEC²

FIG. 33. PEAK VALUES OF CONTROL SURFACE INCIDENCE AND ANGULAR ACCELERATION IN RESPONSE TO CONTROL SURFACE DEMANDS FOR 10 DEGREES, IN THE PRESENCE OF THRESHOLD FEEDBACK OF ANGULAR ACCELERATION.

CONTROL SURFACE INCIDENCE   CONTROL SURFACE INCIDENCE

β_r β_r

ANGULAR ACCELERATION FEEDBACK GAIN K sec.$^{-2}$

K=0

K=0.021

K=0.042

K=0.084

K=0.125

K=0.167

K=0.21

(ANGULAR ACCELERATION THRESHOLD = ± 600°/sec.^{2})
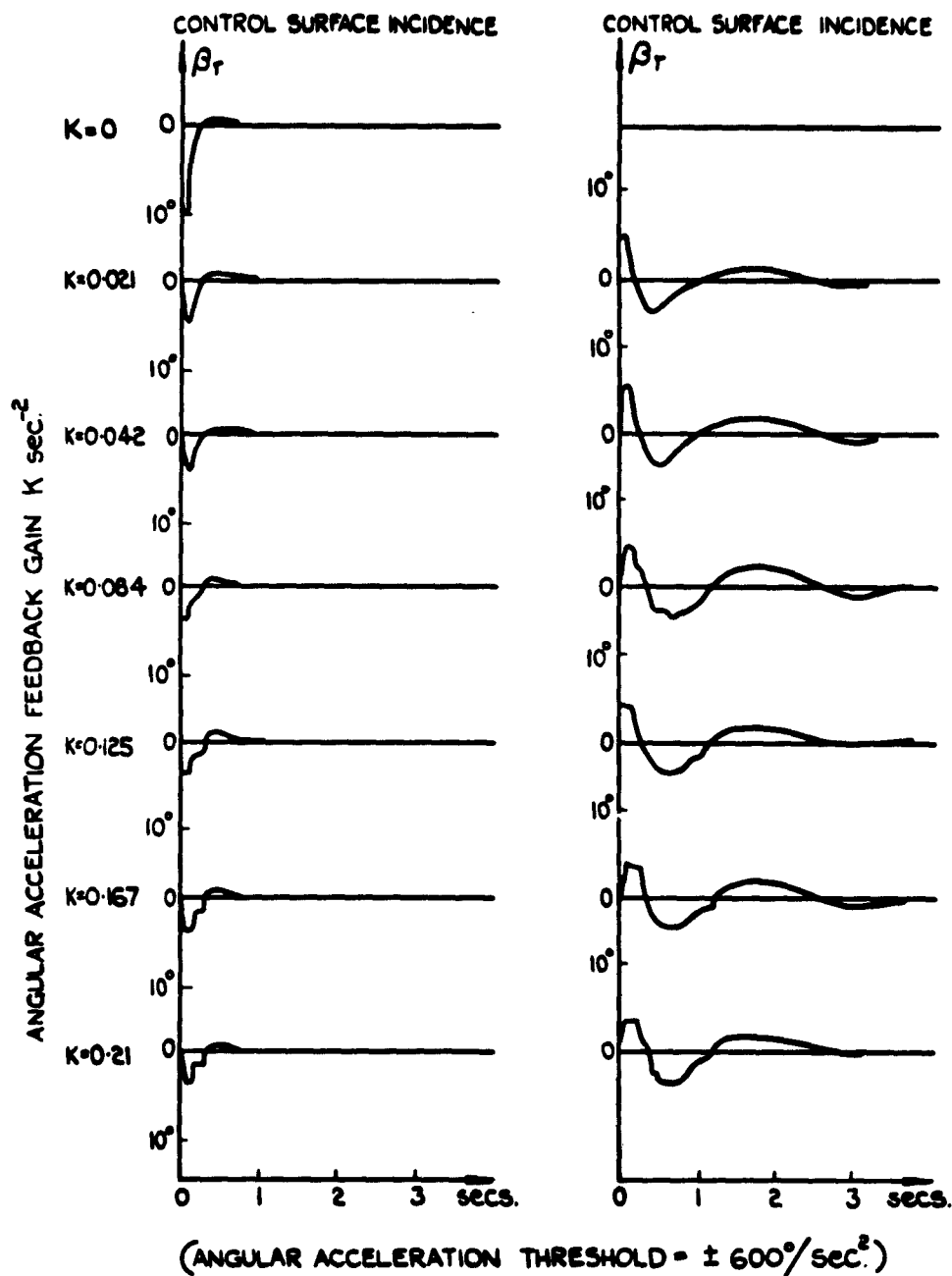
① RESPONSES OF TEST MISSILE TO
DEMANDS FOR 10° OF CONTROL
SURFACE DEFLECTION.

② RESPONSES OF TEST BEAM RIDER
TO 375 ft. LATERAL DISPLACEMENT
OF THE RADAR BEAM.

FIG.34. EXAMPLES OF CONTROL SURFACE
LIFT LIMITING.
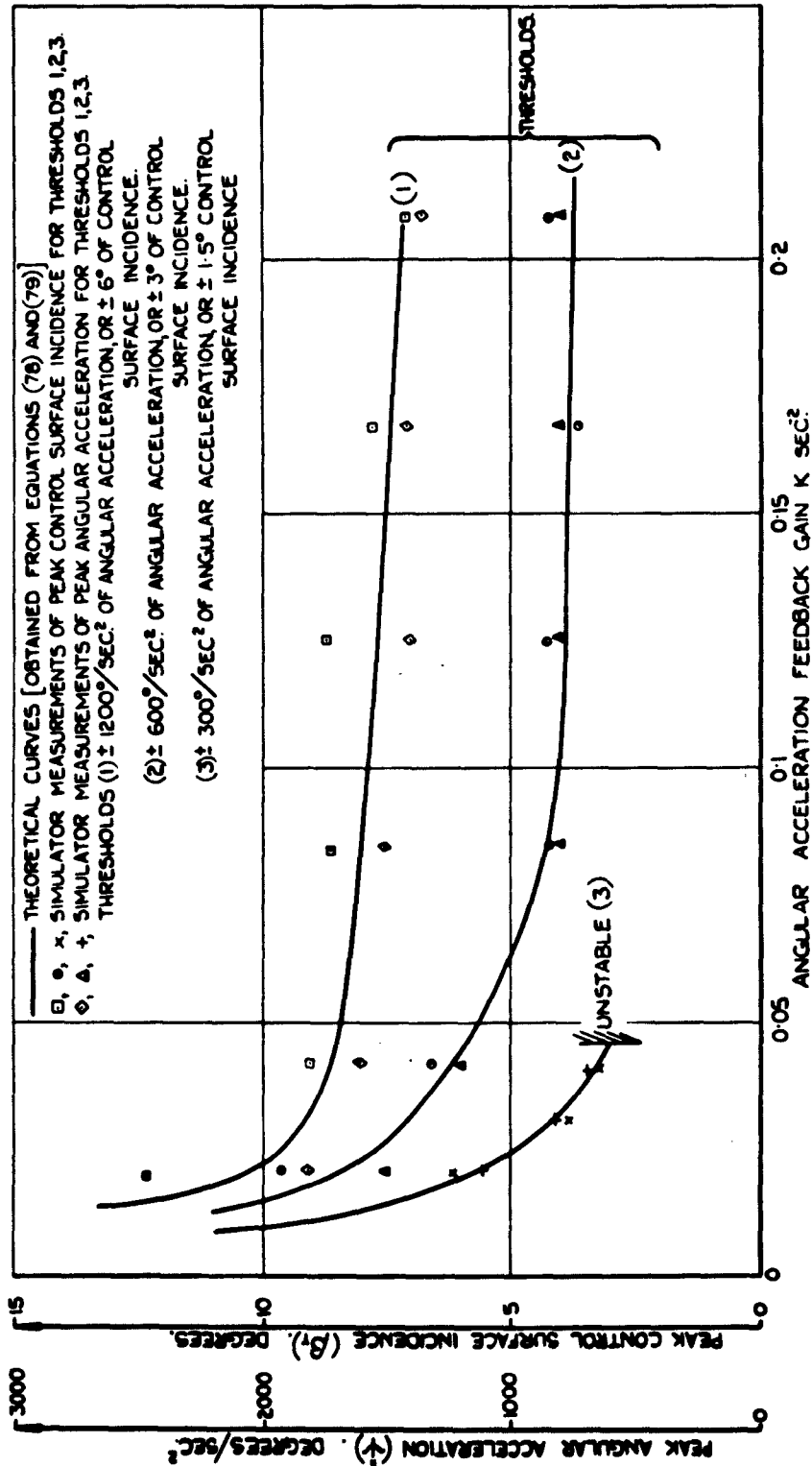
FIG.35. PEAK VALUES OF CONTROL SURFACE INCIDENCE & ANGULAR ACCELERATION,
IN RESPONSE TO A 375 FT. STEP DISPLACEMENT OF THE RADAR BEAM,
IN THE PRESENCE OF THRESHOLD FEEDBACK OF ANGULAR ACCELERATION.

FIG. 36.

ANGULAR ACCELERATION THRESHOLD LEVELS,

① 90°/SEC.²
② 60°/SEC.²
③ 30°/SEC.²
④ 0°/SEC.²

AREA ABOVE CURVE REPRESENTS UNSTABLE ZONE.

AREA BELOW CURVE REPRESENTS STABLE ZONE.

ANGULAR ACCELERATION FEEDBACK GAIN K SEC²

0.3   0.2   0.1   0

0   10g   20g   30g   40g   50g
LATERAL ACCELERATION LIMITS
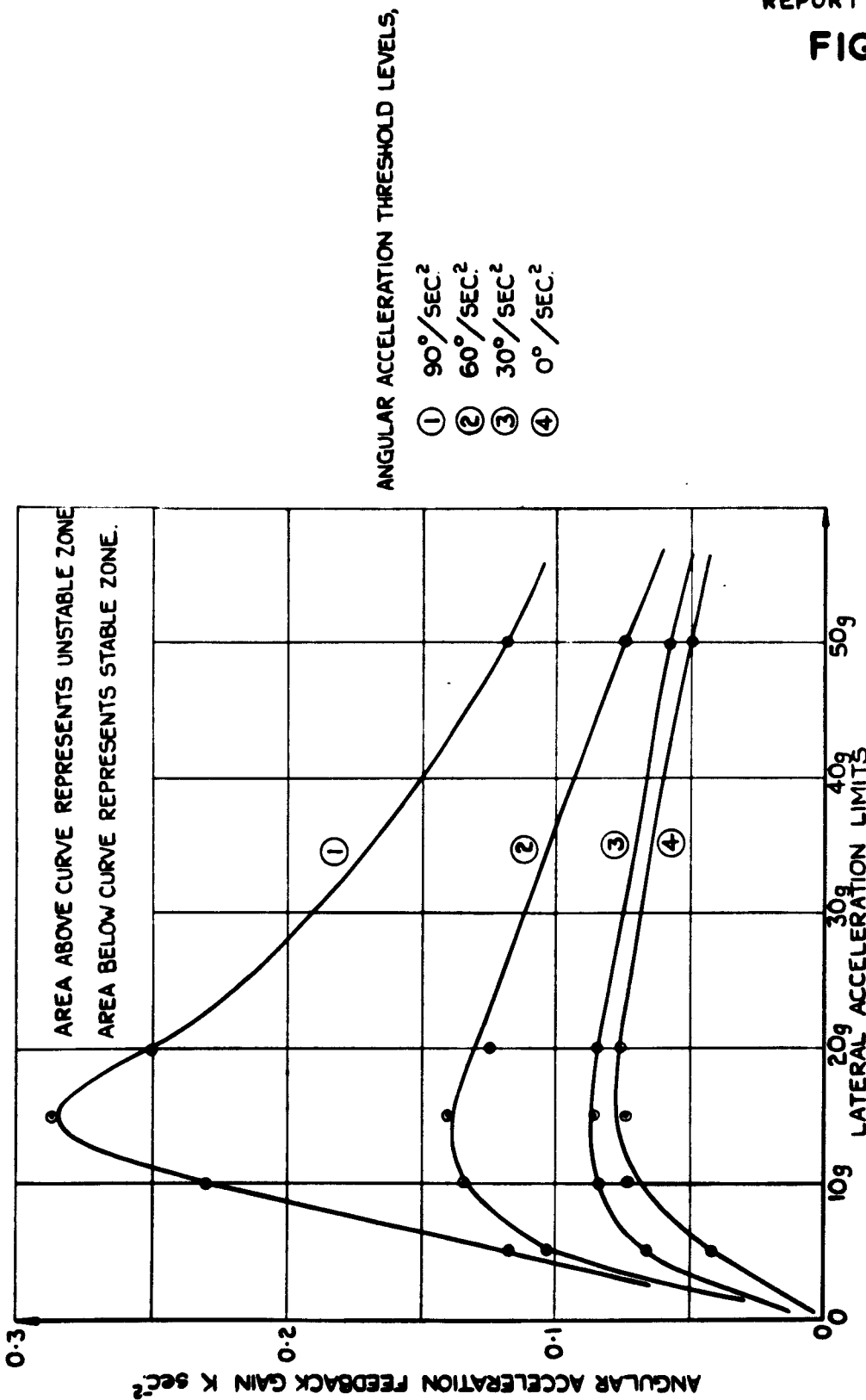
(TEST BEAM RIDER. STABILITY BOUNDARIES DETERMINED USING A 300 ft. LATERAL STEP DISPLACEMENT OF THE RADAR BEAM.)

FIG. 36. THE ANGULAR ACCELERATION FEEDBACK GAIN REQUIRED TO PRODUCE INSTABILITY IN THE TEST BEAM RIDER. (SIMULATOR RESULTS.)
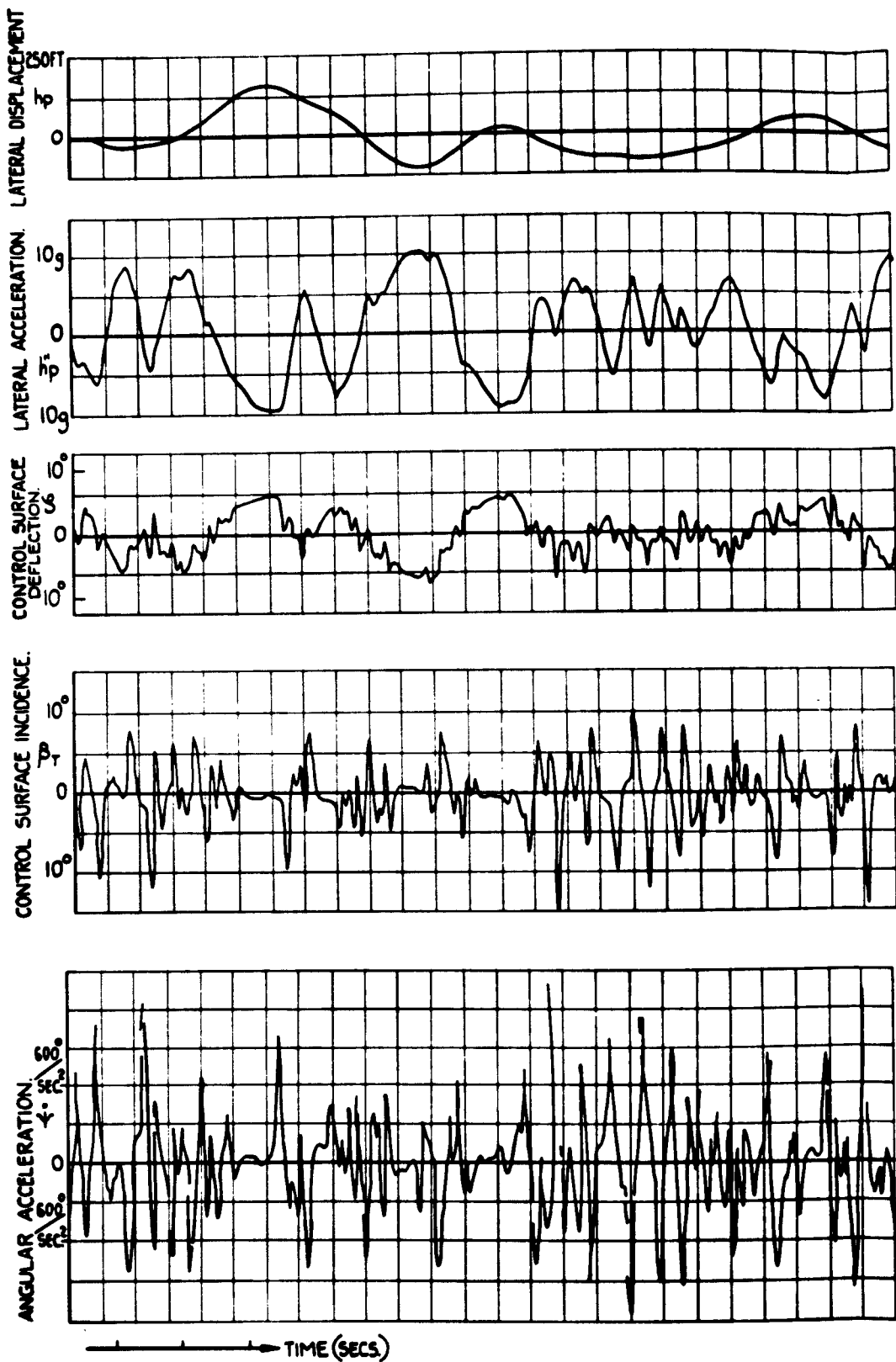
(a) NO CONTROL SURFACE LIFT LIMITING.

(TEST BEAM RIDER. LATERAL ACCELE

FIG.37(a & b) RESPONSE OF TEST BEA
(WITH AND WITHOUT CONT
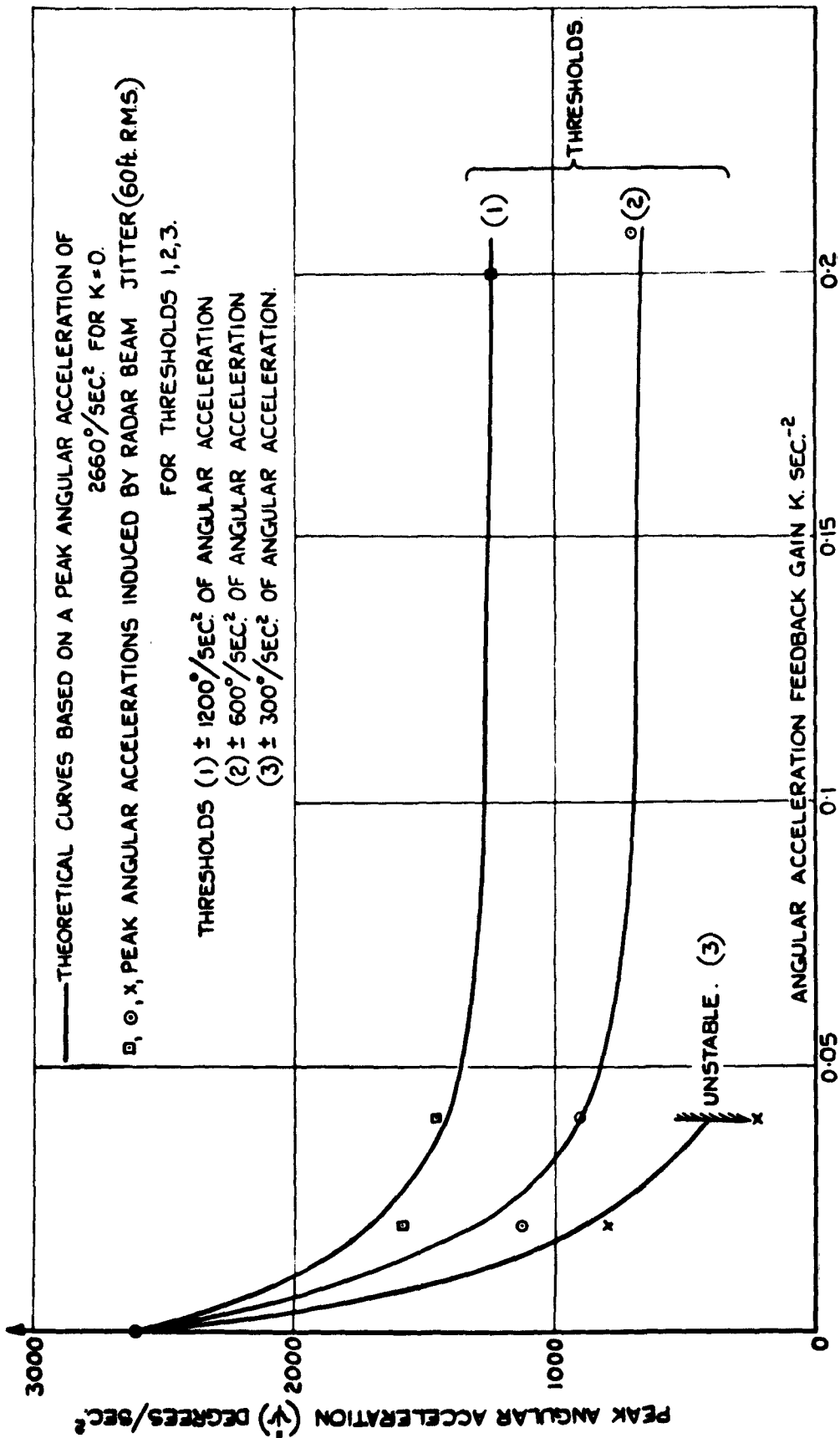
FIG. 38. PEAK ANGULAR ACCELERATION INDUCED BY RADAR BEAM JITTER, IN THE PRESENCE OF THRESHOLD FEEDBACK OF ANGULAR ACCELERATION. (SIMULATOR RESULTS).

ANGULAR ACCELEROMETER LAG.

$$\frac{-K}{1+pT_a}$$

S_f

S_d S_d-S_f $\dfrac{1}{1+pT_x}$ S $f_a(P)$ $\dot\psi$

CONTROL SURFACE
LAG.

MISSILE RESPONSE

(a) THE CLOSED LOOP SYSTEM.

$K=0$

$\dot\psi_o = n_S S_D$

$T_R=0$ $\begin{cases} T_a=0 \\ \\ T_a \neq 0 \end{cases}$

$\dot\psi_o = \dfrac{n_S}{1-Kn_S} S_D$

$\dot\psi_o = n_S S_D$

$K \neq 0$

$T_R \neq 0$ $\begin{cases} T_a=0 \\ \\ T_a \neq 0 \end{cases}$

$\dot\psi_o = 0$

$\dot\psi_o = 0$
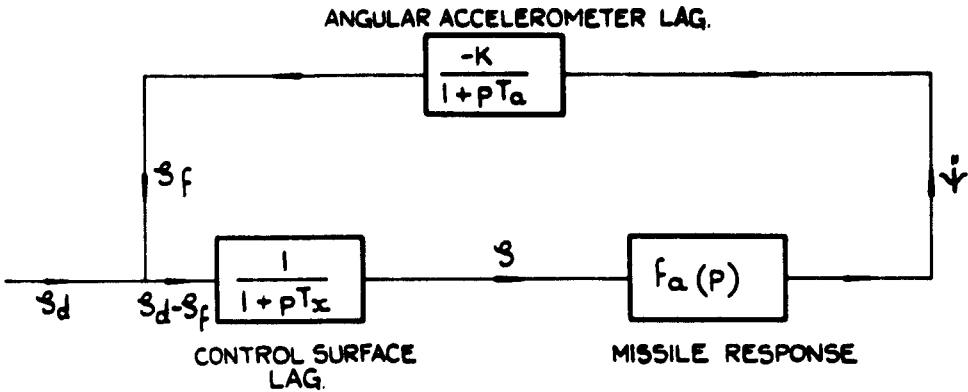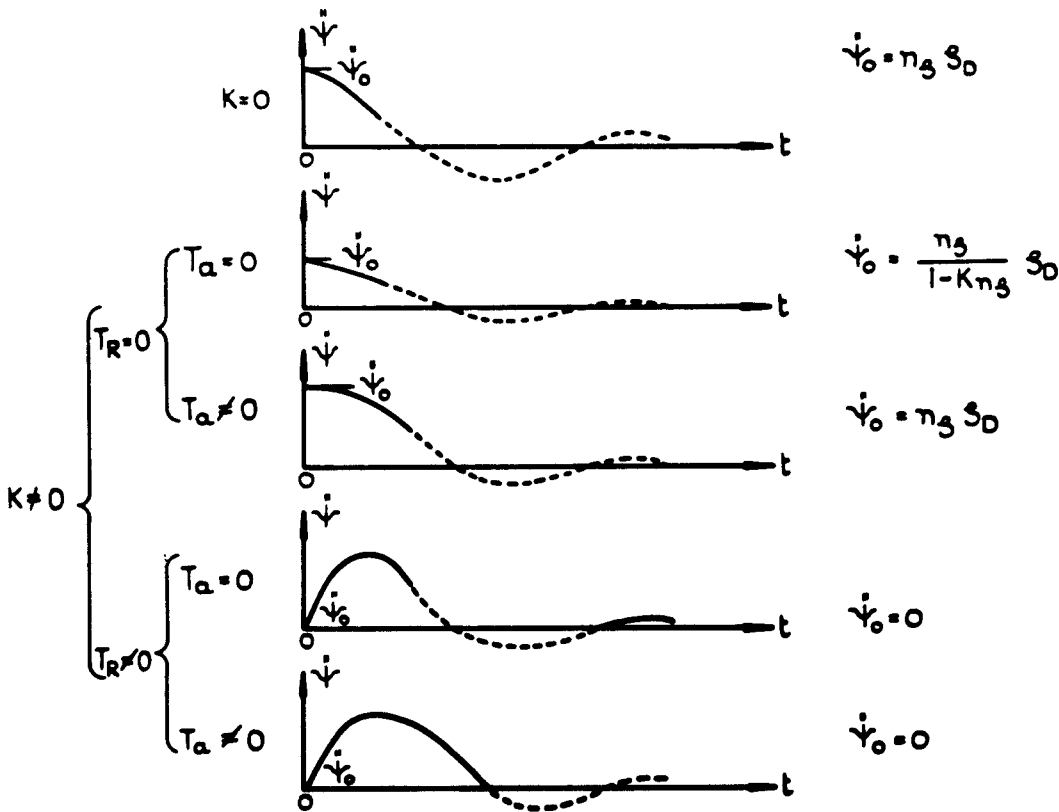
(b) ANGULAR ACCELERATION RESPONSES TO A STEP IN
CONTROL SURFACE DEMAND S_D.

FIG.39(a&b) ANGULAR ACCELERATION FEEDBACK IN
THE PRESENCE OF TIME LAGS.
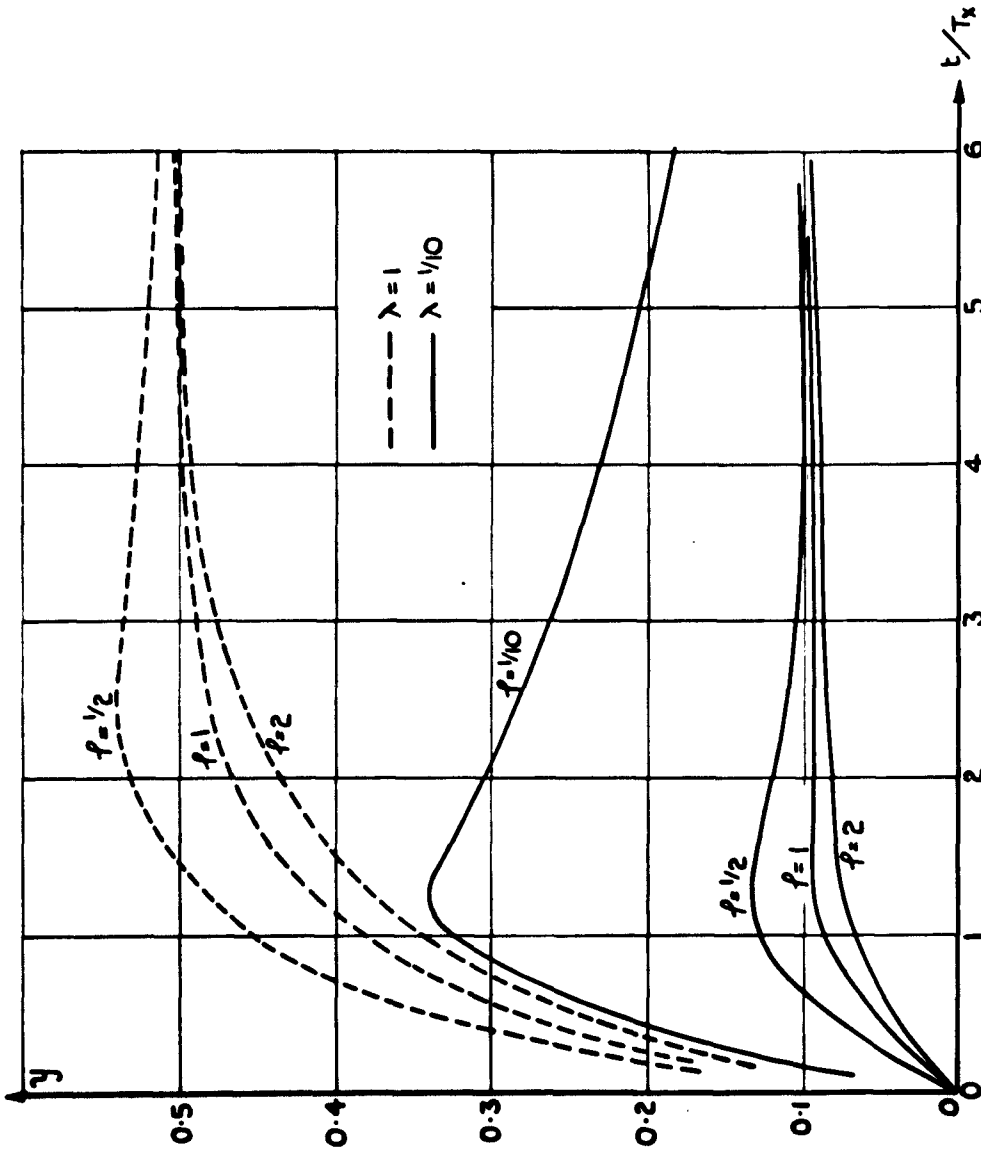
FIG. 40. PLOTS OF $y = \dfrac{1 - e^{-t/T_x}}{1 + \lambda(1 - e^{-\gamma t/T_x})}$

CONTROL SURFACE DEFLECTION.
$\mathcal{S}$

$+\mathcal{S}_L$

0 — — — — — — — — — — — — — — — — — — — TIME

$-\mathcal{S}_L$

CASE (a)   CASE (b)   CASE (c)
H < O   H = O   H > O

CONTROL SURFACE INCIDENCE.
β_T

$+\beta_T'$

$+\beta_T'$

$+\beta_T'$

— — — — — — — — — — — — — — — — — — — TIME

$-\beta_T'$

$-\beta_T'$

$-\beta_T'$

$-\beta_T'$

CASE (a)   CASE (b)   CASE (c)
H < O   H = O   H > O
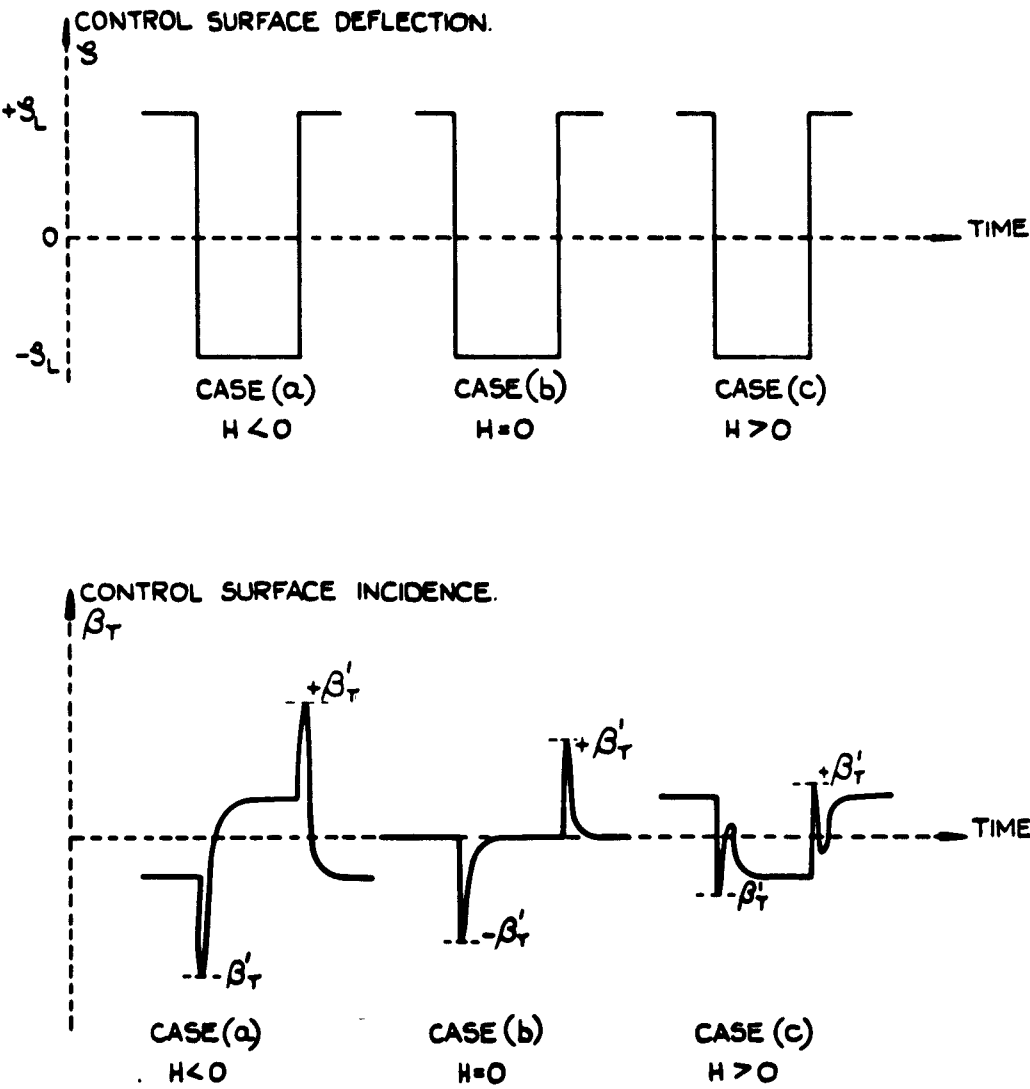
FIG.41. CONTROL SURFACE INCIDENCE IN
RESPONSE TO A LOW FREQUENCY SQUARE WAVE
MOTION OF THE CONTROL SURFACE DEFLECTION.

CONTROL SURFACE INCIDENCE

FIG. 42. PEAK CONTROL SURFACE
INCIDENCE CHART.
(UNLIMITED CONTROL SURFACE INCIDENCE.)
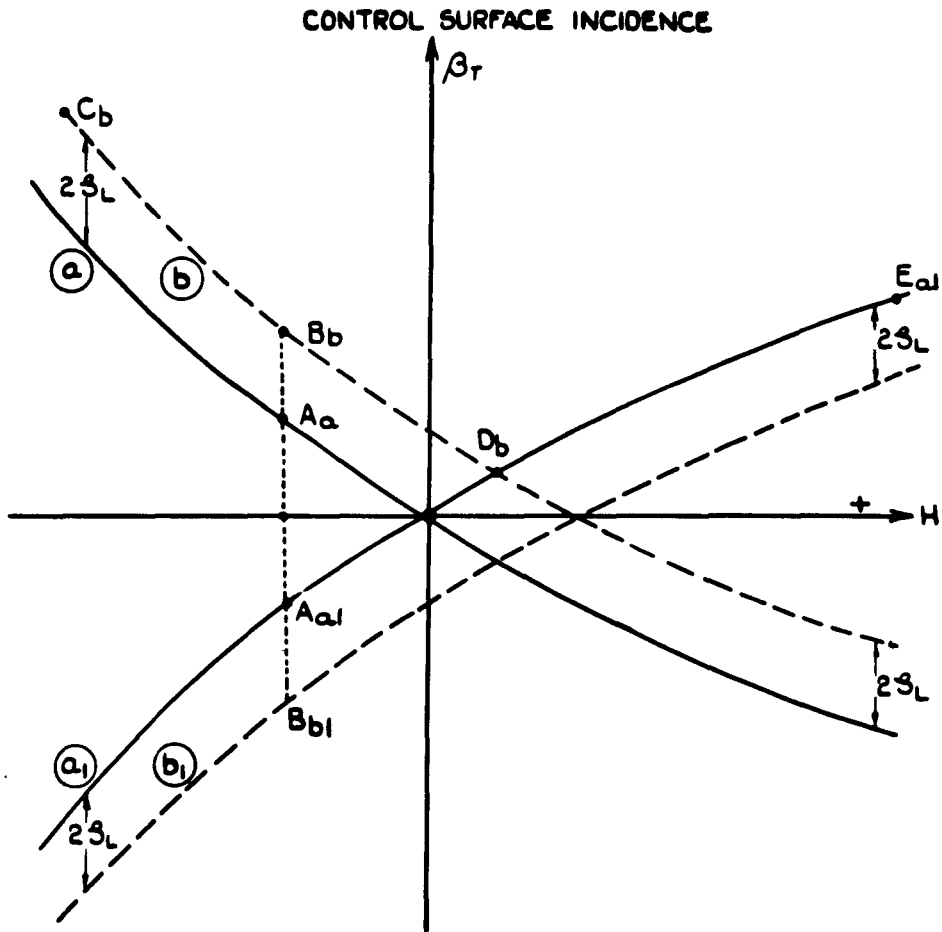
(a) AND (a₁) ARE THE STEADY STATE CURVES FOR β_T AS A FUNCTION OF H,
ASSUMING A STEADY STATE CONTROL SURFACE DEFLECTION OF $\pm S_L$
(b) AND (b₁) ARE CURVES (a) AND (a₁) DISPLACED BY 2 S_L UNITS.

CONTROL SURFACE INCIDENCE.

β_T

(a)
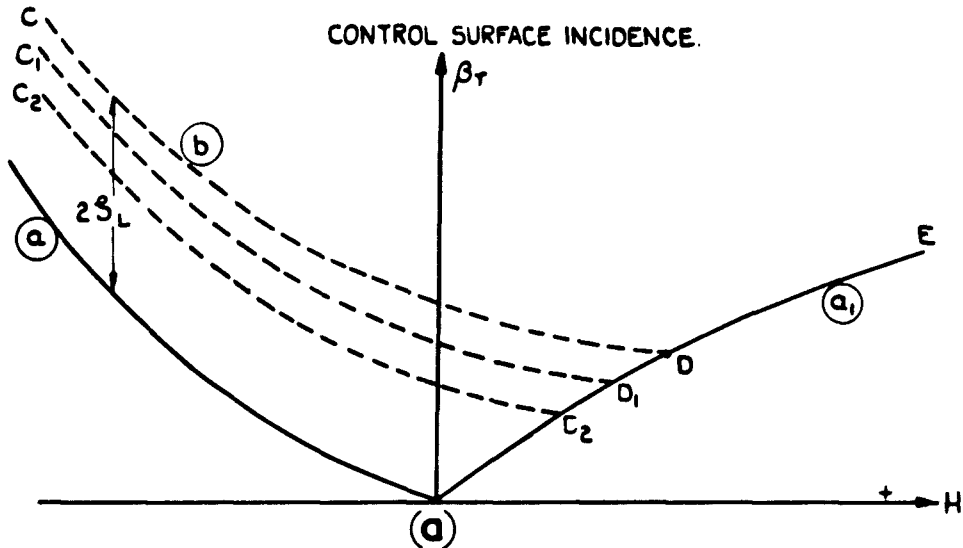
CURVES (a), (a₁) AND (b) ARE AS ON FIG. 42.

THE FAMILY OF CURVES $C_1 D_1$, $C_2 D_2$, ETC. ARE OBTAINED BY DISPLACING (b) TOWARDS (a) i.e. BY REDUCING THE SEPARATION $(2 S_L)$ BY LIMITING ACTION.

CONTROL SURFACE INCIDENCE

β_T

(b)
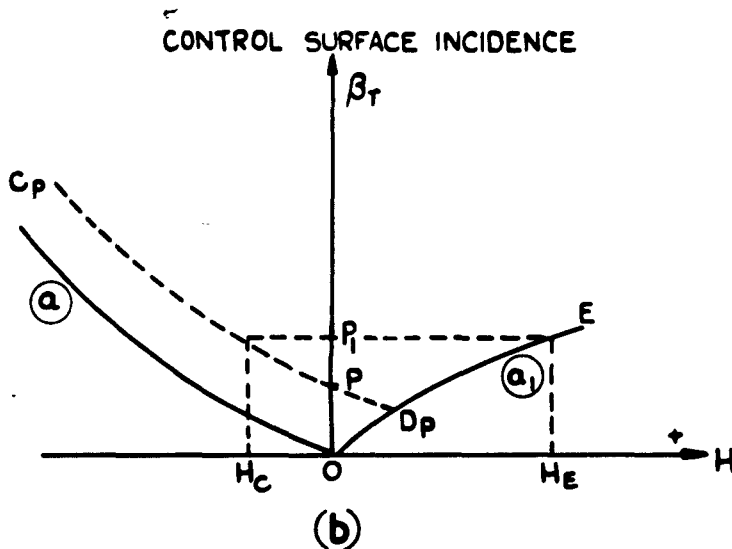
FIG. 43 (a & b). PEAK CONTROL SURFACES
INCIDENCE CHARTS.
(LIMITED CONTROL SURFACE INCIDENCES)

FIG. 44. PEAK CONTROL SURFACE INCIDENCE CHART (TEST MISSILE.)
(CASE A.)
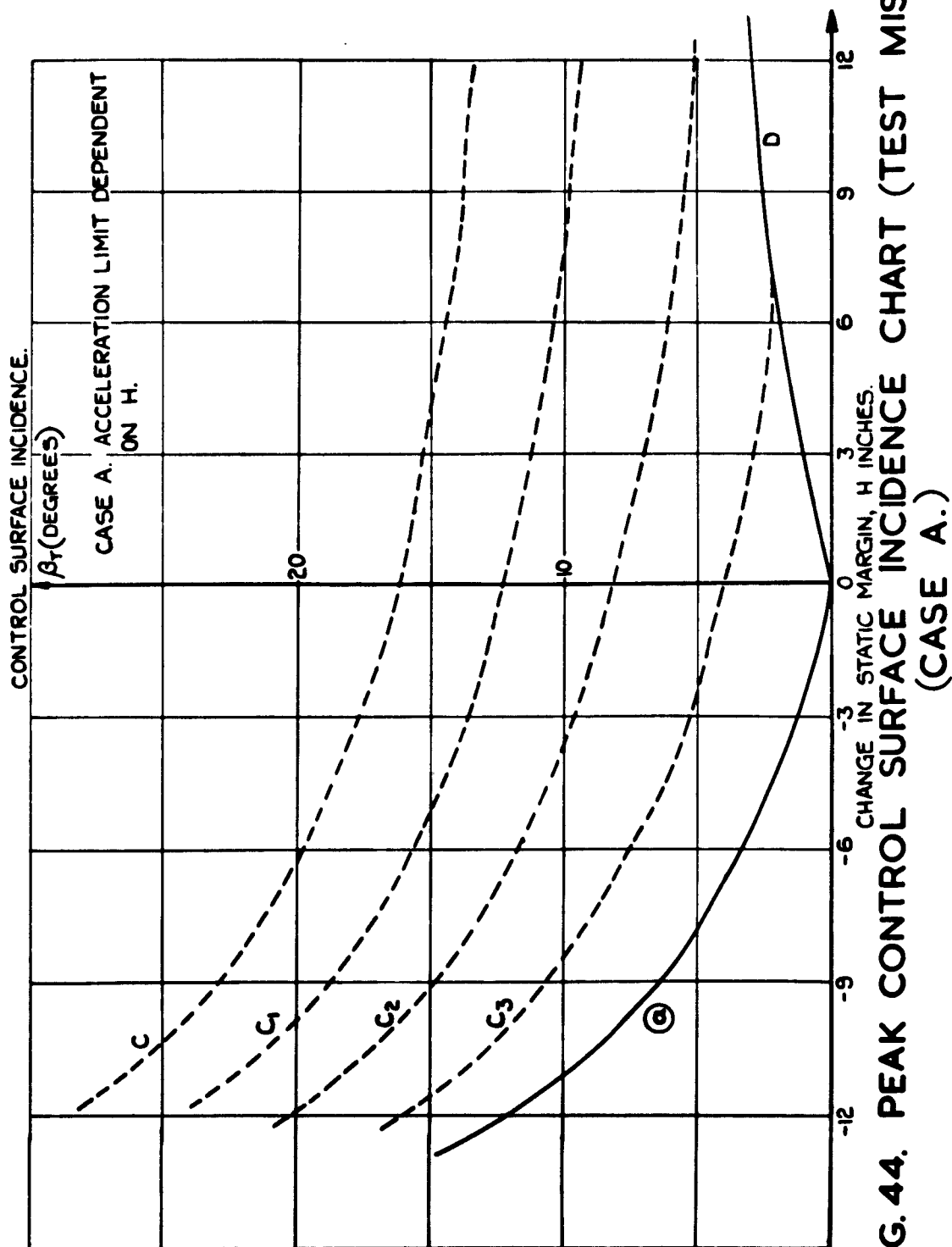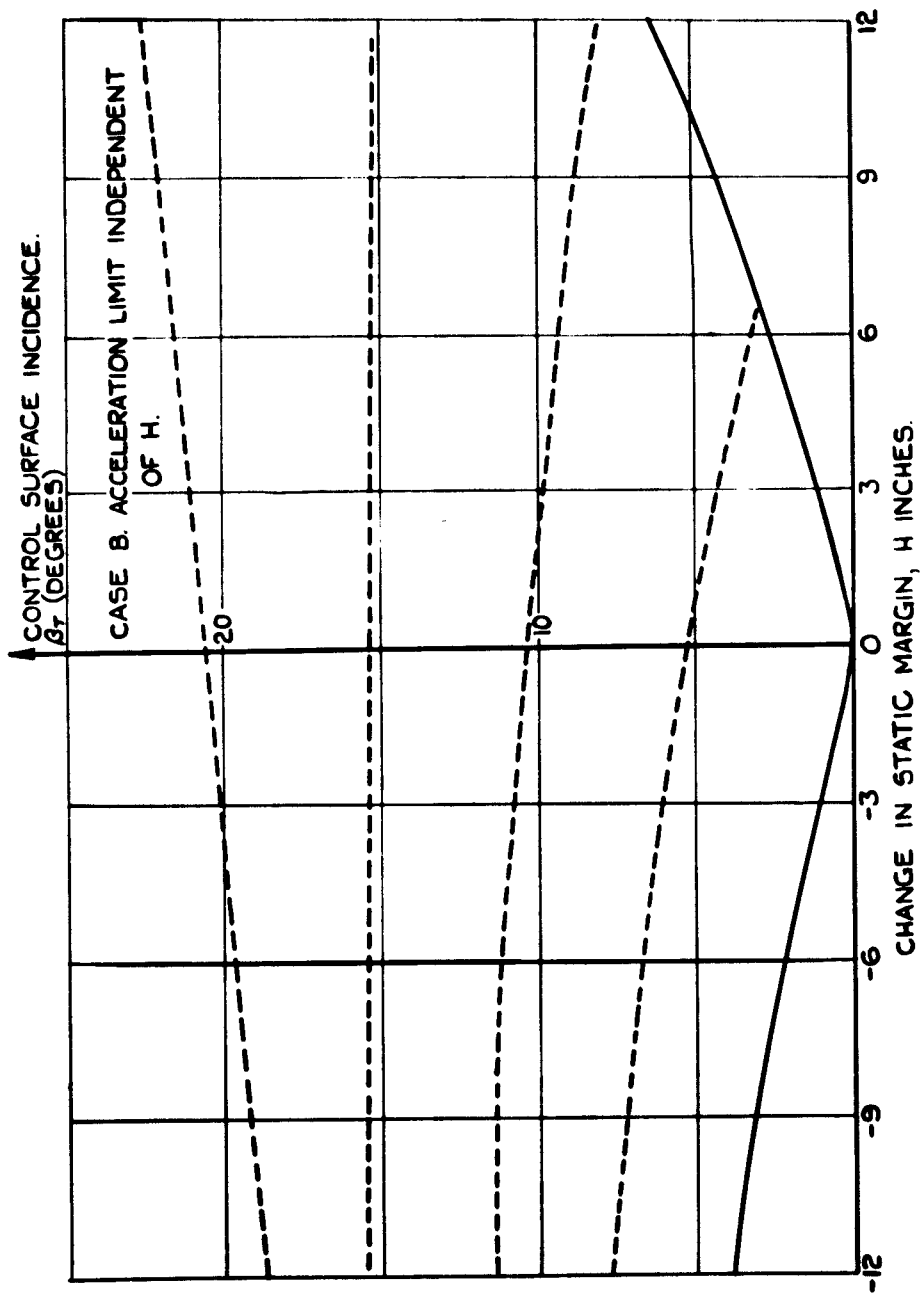
FIG. 45. PEAK CONTROL SURFACE INCIDENCE CHART. (TEST MISSILE).
(CASE B).

FIG.46. COMBINED TOTAL LIFT & CONTROL SURFACE LIFT LIMITING AS APPLIED TO THE TEST MISSILE. N°1.
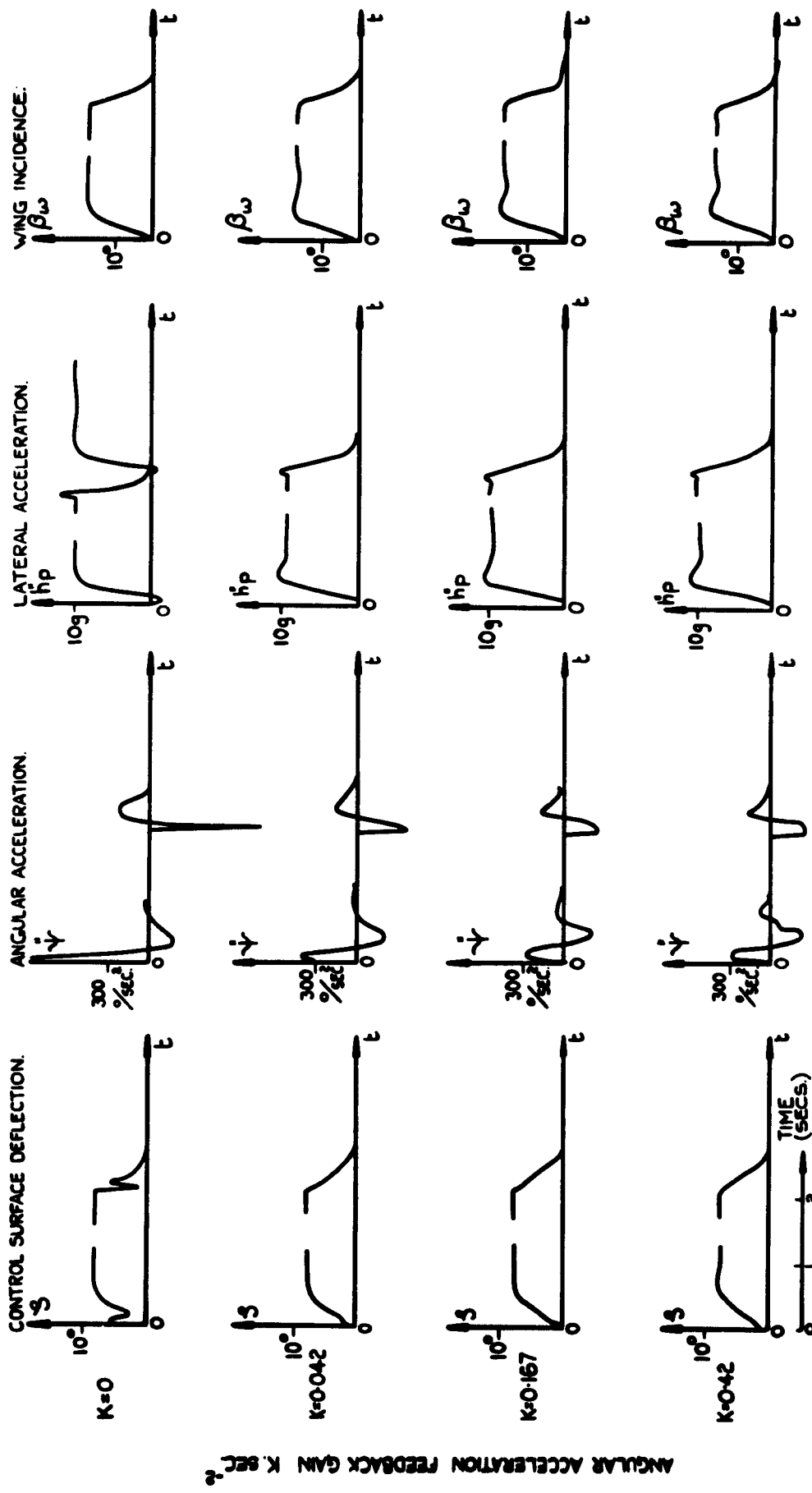
(RESPONSES OF THE TEST MISSILE TO ON AND OFF 10° STEPS OF THE CONTROL SURFACE DEMAND SIGNAL. ANGULAR ACCELERATION THRESHOLD = 300°/SEC² MONITORED DIODE ACCELERATION LIMIT = 10g.)

ANGULAR ACCELERATION FEEDBACK GAIN K.SEC²

FIG.47. COMBINED TOTAL LIFT & CONTROL SURFACE LIFT LIMITING AS APPLIED TO THE TEST MISSILE. Nº 2.
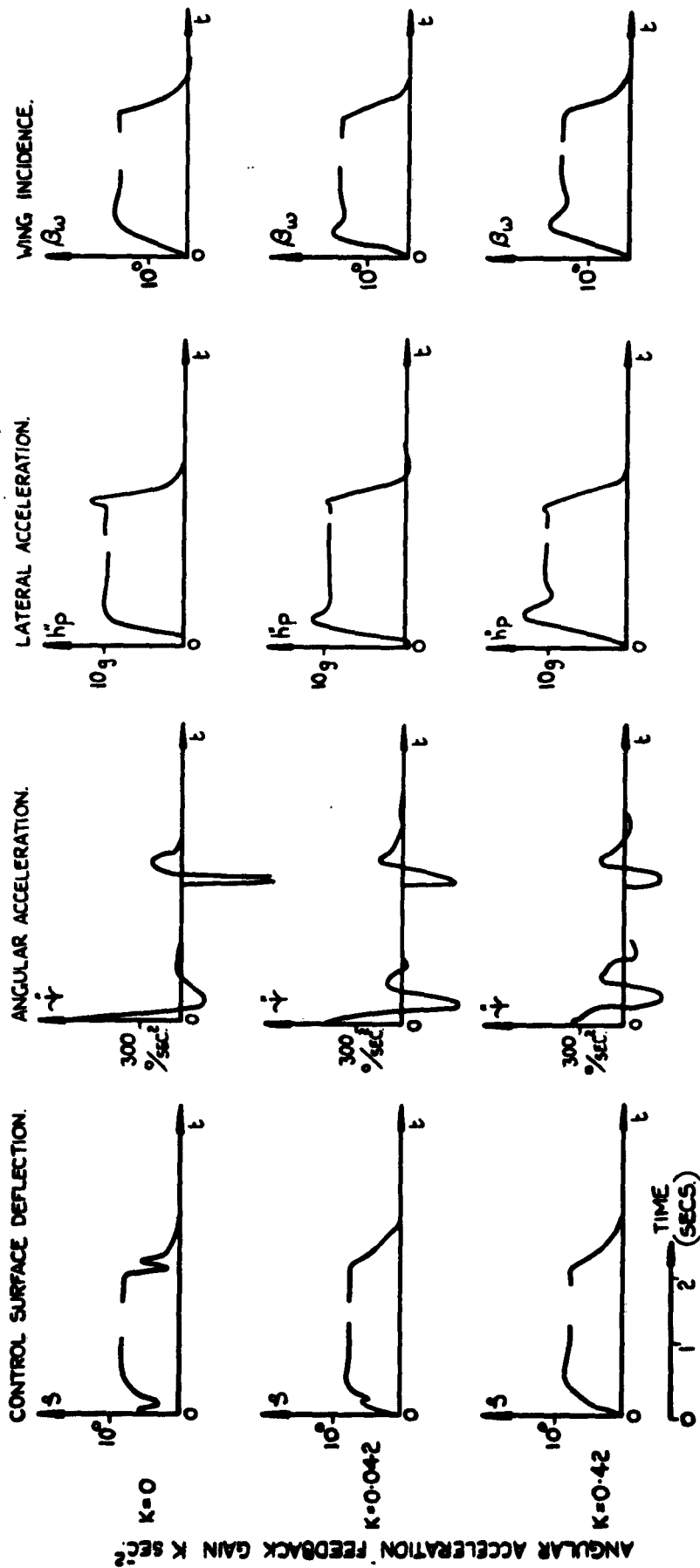
(RESPONSES OF THE TEST MISSILE TO ON AND OFF 20° STEPS OF THE CONTROL SURFACE DEMAND SIGNAL. ANGULAR ACCELERATION THRESHOLD = 300°/SEC.² MONITORED DIODE ACCELERATION LIMIT = 10g.)

FIG. 48.
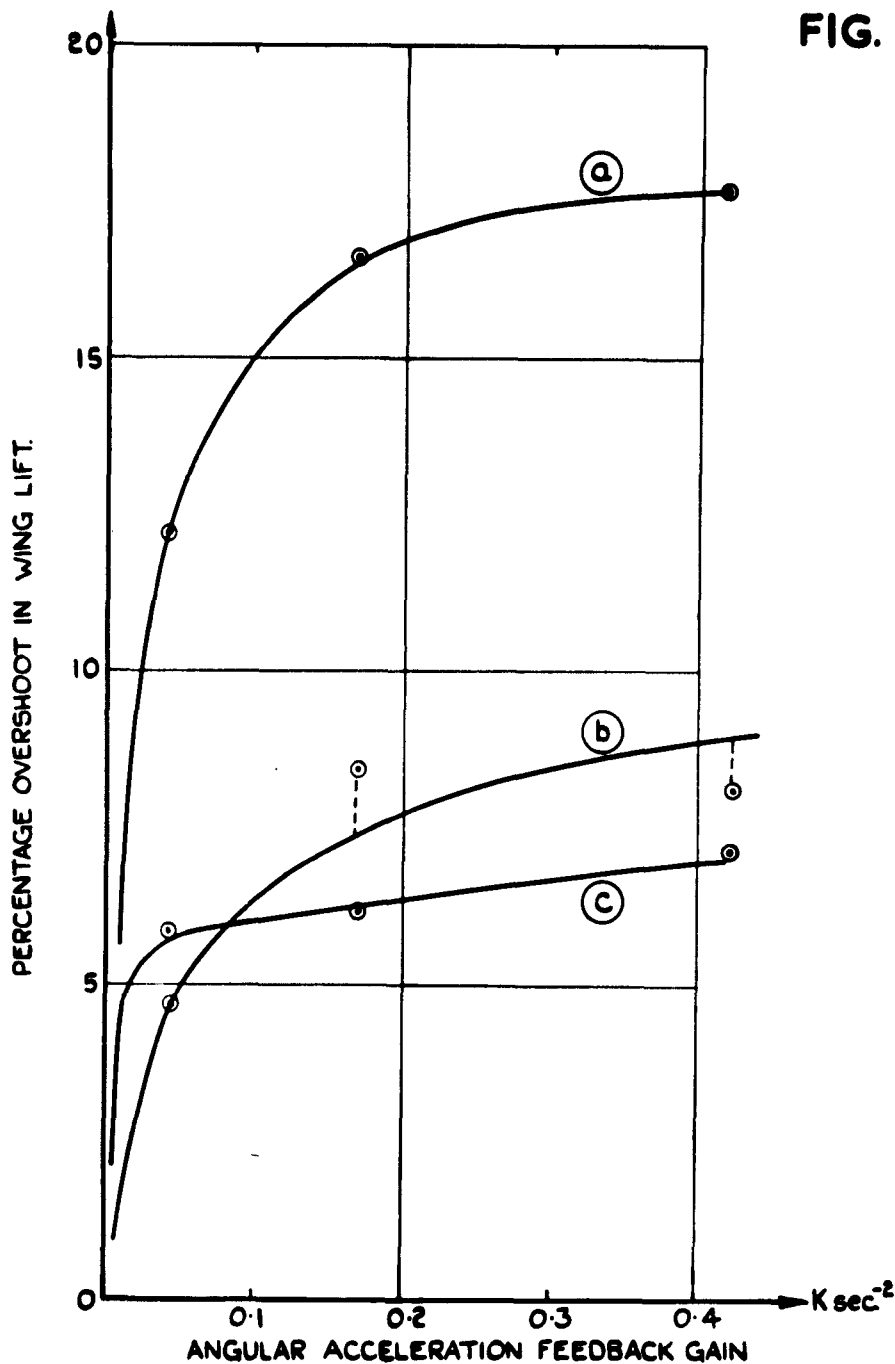
@ 20° CONTROL SURFACE DEMAND. THRESHOLD:-300°/SEC² OF ANGULAR ACCELERATION.

ⓑ 20° CONTROL SURFACE DEMAND. THRESHOLD:-600°/SEC² OF ANGULAR ACCELERATION.

ⓒ 10° CONTROL SURFACE DEMAND. THRESHOLD:-300°/SEC² OF ANGULAR ACCELERATION.

FIG. 48. OVERSHOOT IN WING LIFT WITH COMBINED TOTAL LIFT AND CONTROL SURFACE LIFT LIMITS.

FIG.49. COMBINED TOTAL LIFT & CONTROL SURFACE LIFT LIMITING AS APPLIED TO THE TEST BEAM RIDER. N°1.
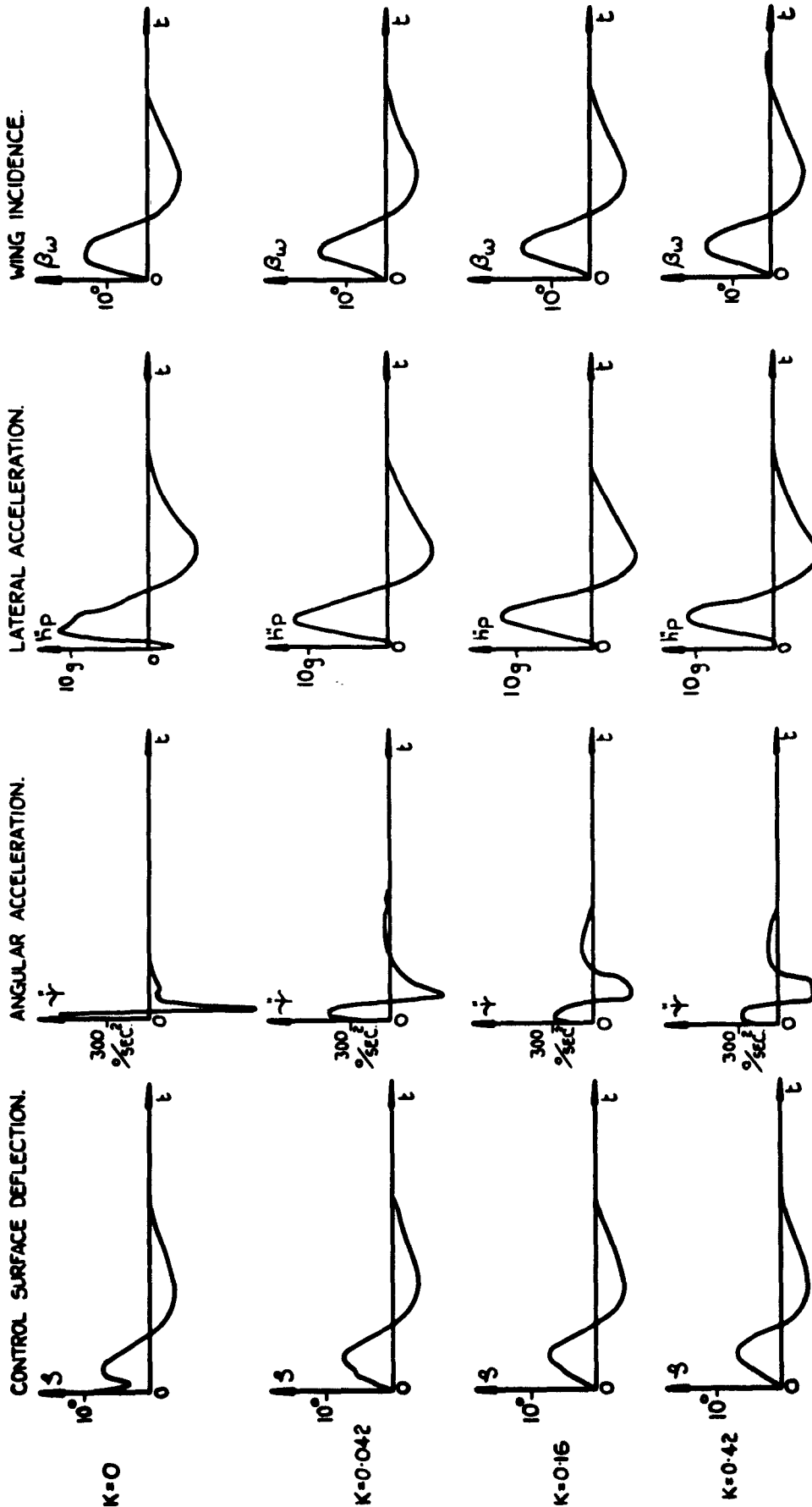
(RESPONSES OF TEST BEAM RIDER TO 250 FT RADAR BEAM DISPLACEMENT. ANGULAR ACCELERATION THRESHOLD = 300°/sec². MONITORED DIODE ACCELERATION LIMITS = 10g.)

FIG.50. COMBINED TOTAL LIFT & CONTROL SURFACE LIFT LIMITING AS APPLIED TO THE TEST BEAM RIDER. N°2.
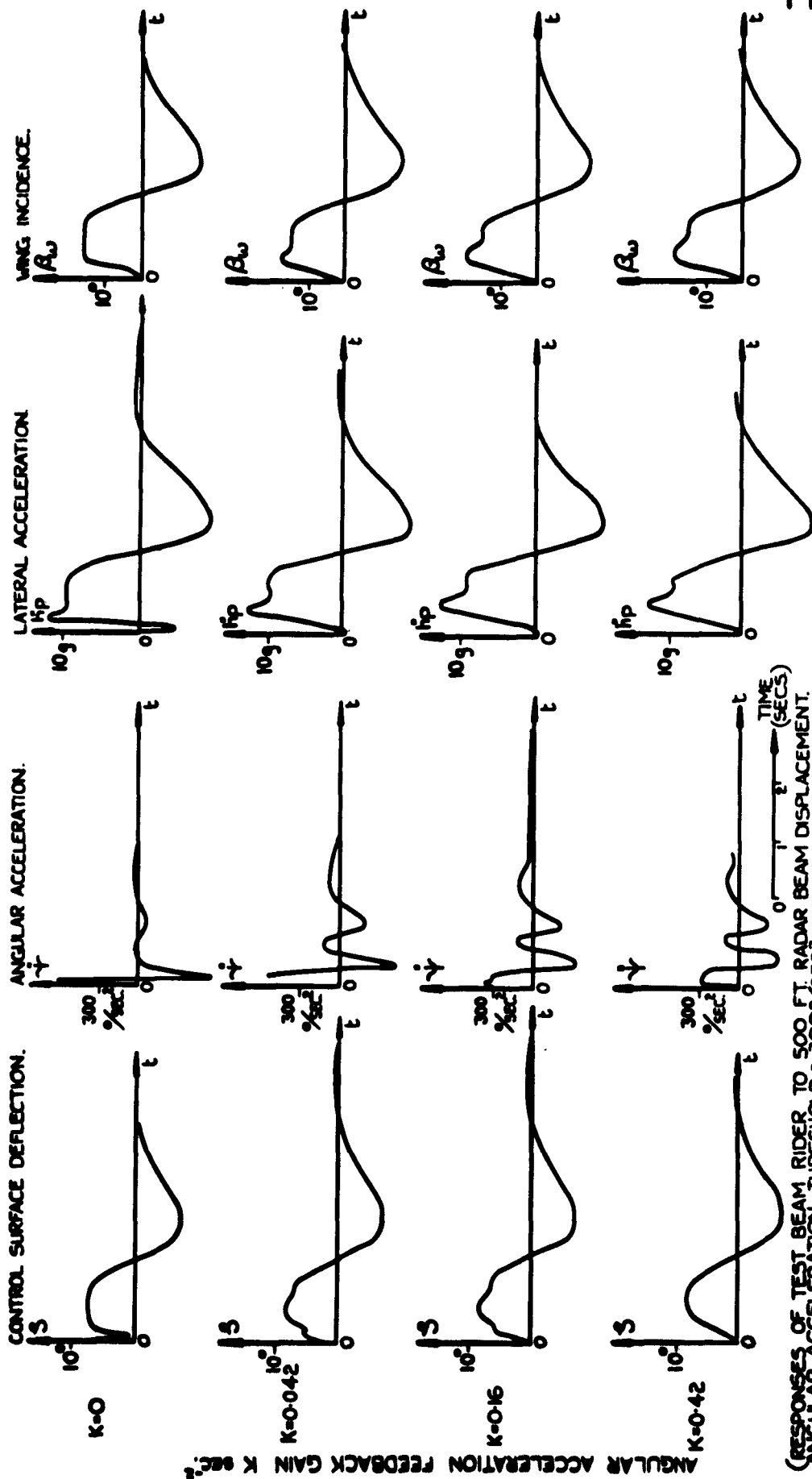
(RESPONSES OF TEST BEAM RIDER TO 500 FT. RADAR BEAM DISPLACEMENT.
ANGULAR ACCELERATION THRESHOLD = 300°/sec²
MONITORED DIODE ACCELERATION LIMIT 5 = 10g.)

MISSILE DESIGN NUMBER.	CONTROL SURFACE SIZE RELATIVE TO DATUM DESIGN.	ACCELERATION RESPONSE TO A STEP INPUT DEMAND FOR 15g LATERAL ACCELERATION (kp)	CONTROL SURFACE INCIDENCE
I (DATUM DESIGN)	1	CURVE (a) ————	UNLIMITED
II	½	CURVE (b) – – – –	UNLIMITED
II	½	CURVE (c) ··········	LIMITED TO 12·5°
II	½	CURVE (d) –·–·–	LIMITED TO 6°
III	¼	CURVE (e) ———	LIMITED TO 12·5°

FIG.51. THEORETICAL ACCELERATION RESPONSES FOR DIFFERENT MISSILE DESIGNS.

These abstract cards are inserted in R.A.E. Reports and Technical Notes for the convenience of Librarians and others who need to maintain an Information Index.

Detached cards are subject to the same Security Regulations as the parent document, and a record of their location should be made on the inside of the back cover of the parent document.

SECRET

Royal Aircraft Est. Report No. G.W.15
1953.3
Gait, J.J. and Allen, D.W.

623.451-519:
621-526:
533.6+1.15:
533.6.013.13

THE PREVENTION OF EXCESSIVE LIFT FORCES ON GUIDED MISSILES

In order to prevent the development of destructive or excessive lift forces during the flight of a guided missile it is generally necessary to limit the total lift on the missile by some form of automatic control action. It may also be necessary or advantageous similarly to limit the control surface lifts of the missile.

Methods of obtaining overriding limiting actions which, within bounds, function independently of missile altitude, velocity and static margin.

SECRET
P.T.O.

SECRET

Royal Aircraft Est. Report No. G.W.15
1953.3
Gait, J.J. and Allen, D.W.

623.451-519:
621-526:
533.6+1.15:
533.6.013.13

THE PREVENTION OF EXCESSIVE LIFT FORCES ON GUIDED MISSILES

In order to prevent the development of destructive or excessive lift forces during the flight of a guided missile it is generally necessary to limit the total lift on the missile by some form of automatic control action. It may also be necessary or advantageous similarly to limit the control surface lifts of the missile.

Methods of obtaining overriding limiting actions which, within bounds, function independently of missile altitude, velocity and static margin.

SECRET
P.T.O.

are proposed and critically examined. These methods depend on feedback to the control surfaces, via suitable threshold circuits, of the outputs of lateral and angular accelerometers suitably situated within the missile.

It is concluded that such an approach to the limiting problem gives a technique whereby the control surface lift force and the total lift force on the missile may be separately or jointly constrained within the given design limits for these forces.

dstl

Information Centre
Knowledge Services
[dstl] *Porton Down,*
Salisbury
Wilts
SP4 0JQ
22060-6218
Tel: 01980-613753
Fax 01980-613970

Defense Technical Information Center (DTIC)
8725 John J. Kingman Road, Suit 0944
Fort Belvoir, VA   22060-6218
U.S.A.

AD#: AD011585

Date of Search: 31 July 2008

Record Summary: AVIA 6/19385
        Title: Prevention of excessive lift forces on guided missiles
        Availability Open Document, Open Description, Normal Closure before FOI Act: 30 years
        Former reference (Department) REPORT GW 15
        Held by The National Archives, Kew

This document is now available at the National Archives, Kew, Surrey, United Kingdom.

DTIC has checked the National Archives Catalogue website (http://www.nationalarchives.gov.uk) and found the document is available and releasable to the public.

Access to UK public records is governed by statute, namely the Public Records Act, 1958, and the Public Records Act, 1967.
The document has been released under the 30 year rule.
(The vast majority of records selected for permanent preservation are made available to the public when they are 30 years old. This is commonly referred to as the 30 year rule and was established by the Public Records Act of 1967).

This document may be treated as <u>UNLIMITED</u>.